Supplementary Information

A new class of ligand derived from the reactions of bis(dialkylphosphino)amines and 9-diazofluorene: preparation, structure and reactivity†

Authors: Matthew J. J. Laprade,[a,b] Katherine N. Robertson,[a] Jason A. C. Clyburne*[a] and Christopher M. Kozak*[b]

Affiliations:

[a] Department of Chemistry, Saint Mary's University Halifax, Nova Scotia, B3H 3C3, Canada.

[b] Department of Chemistry, Memorial University of Newfoundland, St. John's, Newfoundland, A1C 5S7, Canada

* Corresponding authors jason.clyburne@smu.ca; ckozak@mun.ca

Contents

X-ray Crystallography 3
Compound 1a 12
Compound 1b 14
Compound 2a 18
Compound 2b 22
Compound 3 26
Compound 4 30
Compound 5 32
Compound 6 36
Characterization Data of 1a 40
Characterization Data of 1b 45
NMR Data before and after heating 1b in DMSO solution 53
Characterization Data of 2b 59
Characterization Data of 3 65
Characterization Data of 4 72
Characterization Data of 5 79
Characterization Data of 6 86
Characterization Data of Polymers 92
References 108

X-ray Crystallography

System One – used for complexes 1a, 1b, 2a, 2b and 3

The crystal chosen was attached to the tip of a 400 μm MicroLoop with paratone-N oil. Measurements were made on a Bruker APEXII CCD equipped diffractometer (30 mA, 50 kV) using monochromated Mo Kα radiation (λ = 0.71073 Å) at 125 K.[6] The initial orientation and unit cell were indexed using a least-squares analysis of a random set of reflections collected from three series of 0.5° ω-scans, 10 seconds per frame and 12 frames per series, that were well distributed in reciprocal space. For data collection, four ω-scan frame series were collected with 0.5° wide scans, **x** second frames and 366 frames per series at varying φ angles (φ = 0°, 90°, 180°, 270°). The crystal to detector distance was set to 6 cm and a complete sphere of data was collected. The data were collected with frame times appropriate for the crystal available (10 to 90 seconds per frame). Cell refinement and data reduction were performed with the Bruker SAINT software,[7] which corrects for beam inhomogeneity, possible crystal decay, and Lorentz and polarisation effects. A multi-scan absorption correction was applied (SADABS[8]). The structures were solved using SHELXT-2014[9] and were refined using a full-matrix least-squares method on F^2 with SHELXL-2019[9]. The refinements were all unremarkable. The non-hydrogen atoms were refined anisotropically. Hydrogen atoms bonded to carbon were included at geometrically idealized positions and allowed to ride on the position of the parent carbon atom. The isotropic thermal parameters of the hydrogen atoms were fixed at $1.2U_{\mathrm{eq}}$ of the parent carbon atom or $1.5U_{\mathrm{eq}}$ for methyl hydrogens. The position(s) of the hydrogen atom(s) bonded to nitrogen was located in a near final difference Fourier map. It was included in the final cycle of refinement and allowed to refine isotropically. Where needed, U_{iso} H(N) was set to $1.5U_{\mathrm{eq}}$ N and/or the N-H bond length was restrained to 0.90 (0.02) Å.

Compound 1a

The structure was found to contain one complete molecule and to be solvated with one half of a molecule of hexane in the asymmetric unit. The hexane molecule lies across an inversion center with it located at the midpoint of the central C-C bond. Thus, only half of the atoms in the hexane molecule are unique.

The crystals in this sample were very fine, small needles. In addition, there are no strongly diffracting heavy atoms in the structure. Thus, very long frame times were used (90 seconds per frame) and a complete sphere of data out to 6 cm was collected. Still the quality of the data set obtained was not optimal. This resulted in a number of checkcif alerts remaining once the refinement had been completed, even though the refinement itself was quite routine. One Level B alert could not be removed: the value of $\sin(\theta_{\max})/\lambda$ is less than 0.575 – the calculated $\sin(\theta_{\max})/\lambda = 0.5715$. In addition, a number of Level C alerts also remained due to the poor quality of the data, including (1) the value of Rint is greater than 0.12 - Rint given is 0.137, (2) the ratio of Observed / Unique Reflections (too) Low - 45%, and (3) missing FCF Refl Between Thmin & STh/L= 0.572 – 18. The somewhat low data quality also results in low bond precision but does not detract from the determined connectivity in the structure. To improve this, enhanced rigid body restraints (RIGU) were placed over all of the atoms in the structure.

Compound 1b

The structure was found to contain one complete molecule and to be solvated with one molecule of dichloromethane in the asymmetric unit. The dichloromethane molecule was disordered. It was split over three different positions, with each of the three parts restrained to have similar geometries using SAME instructions during the Shelxl refinement. All of the chlorine atoms were restrained to have similar anisotropic displacement parameters. The occupancies of each part of the disorder were refined but constrained to total one using a SUMP instruction. The occupancies came out to final values of 53.4(3), 32.7(3) and 13.9(3) % for Parts A, B and C, respectively.

Compound 2a

The isopropyl groups of the cation (two unique groups) were found to be disordered. The atoms in each group were split over two positions with occupancies of 50% for each. The C-C bond lengths were restrained to 1.53(0.015) Å, while the P-C bonds were restrained to be similar using a SADI instruction. The thermal parameters of the carbon atoms in the isopropyl groups were also restrained to be similar using a SIMU instruction in the Shelxl refinement. Finally, enhanced rigid body restraints (RIGU) were placed over all of the atoms in the structure.

The structure crystallized in the non-centrosymmetric space group *Fdd*2. The central nitrogen atom of the cation sits on a C_2 rotation axis in the unit cell and only one half of the atoms in the cation are unique. The chloride anion also lies on the same rotation axis. The Shelxl calculated Flack and Parson's parameters were 0.0(1) and 0.08(6), respectively. This result is supported by values calculated for the Hooft and Parson's parameters using the program Platon.[10] These values came out to 0.06(6) and 0.09(7), respectively. All of this suggests that the correct absolute configuration has been chosen.

Compound 2b

The structure crystallizes in the centrosymmetric space group *C*2/*c*. The central nitrogen atom of the cation sits on a C_2 rotation axis in the unit cell. Thus, only one half of the atoms in the cation are unique. The chloride anion also lies on the same rotation axis. For each cation/anion pair there are two molecules of acetonitrile solvating the structure; only one of these is uniquely defined in the asymmetric unit.

Compound 3

Three reflections were removed from the final refinement because of poor agreements between F^2_{obs} and F^2_{calc}. These were 4 6 3, 1 -5 10 and -1 5 8. An extinction parameter was also refined to give a final value of 0.0112(3).

The data was found to be twinned using the TwinRotMax routine in Platon.[10] The same program was used to write an HKLF5 data file that was then used in the final refinement. The two-component twin BASF value refined to a fraction of 0.374(3).

The crystals in this sample were very thin plates. Thus, long frame times were used (50 seconds per frame) and a complete sphere of data out to 6 cm was collected. Still the quality of the data set obtained was not optimal. This resulted in several checkcif Level C alerts remaining once the refinement had been completed, even though the refinement itself was quite routine.

System Two – used for complexes 4, 5 and 6

Single-crystal X-ray diffraction data was collected at 173(2) K on a XtaLAB Synergy-S, Dualflex, HyPix-6000HE diffractometer using Cu Kα radiation (λ = 1.5406 Å). The crystal was mounted on a nylon CryoLoop with Paratone-N oil. The data were collected, reduced and processed within CrysAlisPro.[11] A multi-scan absorption correction was applied to the collected reflections. The structure was solved with the ShelXT[9] structure solution program using Intrinsic Phasing. and refined using the ShelXL[9] refinement package using Least Squares minimisation. All non-hydrogen atoms were refined anisotropically. The organic hydrogen atoms were generated geometrically.

Compound 4

Data was collected and integrated to a maximum resolution of 0.78 Å (θ_{max} = 80.464°). Six reflections were removed from the final refinement because of poor agreement between F_{obs}^2 and F_{calc}^2.

The crystal used for data collection proved to be a two-component twin. DC PROFFITRRPTWIN in CrysAlisPro[11] was employed to process the twinned data. An empirical absorption correction using spherical harmonics (ABSPACK in CrysAlisPro[11]) was applied to the collected reflections. Common scales were applied for all twin components. An HKLF5 reflection file was generated and used for the final refinement. The data was merged using the crystal class with statistical intensity for the merging weights; Friedel pairs were not merged. BASF refined to a value of 0.376(1), giving the contribution of the second twin domain.

Compound 5

Data was collected and integrated to a maximum resolution of 0.78 Å (θ_{max} = 79.343°). Seventeen reflections were removed from the final refinement because of poor agreement between F_{obs}^2 and F_{calc}^2. This could be indicative of the presence of a second small twin domain that was not accounted for during data processing. It was too small to be detected using the process TwinRotMat as implemented in the program Platon.[10]

The compound was found to crystallize in the centrosymmetric Monoclinic space group $P2_1/n$ with two molecules in the asymmetric unit. In addition, one complete molecule of tetrahydrofuran (THF) solvent and one partially occupied molecule of THF solvent was also included in the asymmetric unit. There is slight disorder in the structure, introduced by the partially occupied molecule of THF. All of the atoms in this molecule are present in the independent unit but have only half occupancies. A related molecule, also of half occupancy is generated by inversion across the center of the solvent ring.

Because of the large number of carbon atoms in the structure, the atom list for refinement was divided into four residues (RESI 1 Molecule 1; RESI 2 Molecule 2; RESI 3 Solvent 1; RESI 4 Solvent 2). The carbon atoms in residues 1 and 2 (molecules 1 and 2) were given the same numbering scheme so that the carbon labels did not exceed 100. The labels for the carbon atoms in the non-solvent molecules must specify the residue (i.e., C1_1 and C1_2 refer to C1 in molecules 1 and 2, respectively).

Compound 6

Data was collected and integrated to a maximum resolution of 0.78 Å (θ_{max} = 79.677°). One reflection (-3 4 21) was removed from the final refinement because of poor agreement between F_{obs}^2 and F_{calc}^2.

The compound was found to crystallize in the centrosymmetric Triclinic space group *P*-1 with one molecule in the asymmetric unit. The main molecule was found to have two molecules of tetrahydrofuran (THF) coordinated to the sodium atom. In addition, one molecule of THF solvent was also included in the asymmetric unit. There was considerable disorder in the structure; one of the coordinated THF molecules, the solvent THF and one of the coordinated diazofluorene ligands were all disordered. In the case of the ligand, it could coordinate to the phosphorus centre with either face of the ring system facing up/down in related forms. All three regions of disorder were described using two-part models. The geometries of each part of the same disorder were restrained to be similar. The atoms involved in the disorder were restrained to have similar anisotropic displacement parameters. The occupancies of each part were assigned a different free variable, and their sum was then restrained to total one. Where appropriate, the bond lengths from the disordered to the ordered part of the molecule were also restrained to be similar. Finally, a rigid bond restraint was placed over all of the heavy atoms in the solvent. The final occupancies of the disordered solvent refined to 95.1(3) and 4.9%, for parts A and B, respectively. For the coordinated THF solvent, the corresponding values refined to 88.6(4) and 11.4%, respectively. Finally, for the ligand, the occupancies refined to 95.0(2) and 5.0% for parts A and B of the disorder, respectively.

The final checkcif file contained a number of Level G alerts pertaining to the close contacts formed between part B (the minor component) of the free THF solvent with the main molecule. The position of the THF was examined closely but by all criteria examined, it was placed correctly. This position for the free THF is only present 5 % of the time. When in this location, it must come into close proximity (and some conflict) with the main molecule.

All diagrams were prepared using the program Mercury CSD 4.3.[12] The crystallographic data has been deposited with the Cambridge Crystallographic Data Centre. CCDC 2352790-2352797 contain the supplementary crystallographic data for this paper. The individual number for each structure is given in Table S1. The data can be obtained free of charge via www.ccdc.cam.ac.uk/data_request/cif, or by emailing data_request@ccdc.cam.ac.uk, or by contacting The Cambridge Crystallographic Data Centre, 12 Union Road, Cambridge CB2 1EZ, UK; fax: +44 1223 336033.

Table S1. Crystal data and structural refinement details (Part 1).

Identification code	**Compound 1a**	**Compound 1b**	**Compound 2a**	**Compound 2b**
CCDC deposit number	2352790	2352791	2352792	2352793
Empirical formula	$C_{41}H_{52}N_5P_2$	$C_{51}H_{39}Cl_2N_5P_2$	$C_{38}H_{46}ClN_5P_2$	$C_{54}H_{44}ClN_7P_2$
Formula weight	676.81	854.71	670.19	888.35
Crystal system	Triclinic	Triclinic	Orthorhombic	Monoclinic
Space group	*P*-1	*P*-1	*Fdd*2	*C*2/*c*
Unit cell dimensions (Å and °)	*a* = 9.675(3)	10.4341(10)	44.675(8)	31.166(3)
	b = 13.444(5)	11.7915(12)	12.046(2)	9.0650(10)
	c = 15.414(5)	18.6856(18)	13.484(2)	20.185(2)
	α = 69.680(4)	96.9450(10)	90	90
	β = 86.860(4)	91.3780(10)	90	126.5420(10)
	γ = 88.453(4)	111.0640(10)	90	90
Volume ($Å^3$)	1877.2(11)	2123.9(4)	7256(2)	4581.6(9)
Z	2	2	8	4
Density (calculated, Mg/m^3)	1.197	1.336	1.227	1.288
Absorption coefficient (mm^{-1})	0.151	0.272	0.227	0.199
F(000)	726	888	2848	1856
Crystal size (mm^3)	0.320x0.070x0.040	0.400x0.300x0.100	0.300x0.175x0.175	0.475x0.300x0.210
Theta range for data collection (°)	1.410 - 23.967	1.101 - 28.885	1.823 - 27.151	1.627 - 28.951
Index ranges (*h*,*k*,*l*)	-11/11, -15/15, -17/17	-14/14, -15/15, -24/24	56/57, -15/15, -17/17	-40/42, -12/12, -26/27
Reflections collected	16666	25945	20166	27173
Independent reflections [R(int)]	5850 [0.1367]	10242 [0.0300]	4020 [0.0936]	5740 [0.0300]
Completeness to theta = 25.242°	99.7 %**	99.8 %	100.0 %	100.0 %
Max. and min. transmission	0.7450 and 0.5890	0.7458 and 0.6997	0.7455 and 0.6544	0.7458 and 0.6993
Data / restraints / parameters	5850 / 366 / 446	10242 / 46 / 602	4020 / 369 / 274	5740 / 1 / 294
Goodness-of-fit on F^2	0.937	1.016	1.062	1.029
Final R indices [I>2sigma(I)]	R1 = 0.0678	0.0430	0.0541	0.0363
	wR2 = 0.1225	0.0953	0.0940	0.0895
R indices (all data)	R1 = 0.1830	0.0666	0.0820	0.0475
	wR2 = 0.1617	0.1066	0.1029	0.0963
Extinction coefficient	n.a.	n.a.	n.a.	n.a.
Largest diff. peak and hole ($e.Å^{-3}$)	0.290/-0.356	0.493/-0.424	0.234/-0.221	0.435/-0.343

**Completeness to theta = 23.967°

Table S1. Crystal data and structural refinement details (Part 2).

Identification code	**Compound 3**	**Compound 4**	**Compound 5**	**Compound 6**
CCDC deposit number	2352794	2352795	2352796	2352797
Empirical formula	$C_{37}H_{29}N_3OP_2$	$C_{54}H_{41}N_5P_2Zn$	$C_{110}H_{96}Al_2N_{10}O_{1.50}P_4$	$C_{62}H_{60}N_5NaO_3P_2$
Formula weight 593.57	863.21	1759.80	1008.08	
Crystal system	Triclinic	Monoclinic	Monoclinic	Triclinic
Space group	P-1	$P2_1/n$	$P2_1/n$	P-1
Unit cell dimensions (Å and °)	a = 8.812(3)	9.86347(8)	20.57390(10)	10.72595(14)
	b = 12.958(5)	20.78128(19)	19.10680(10)	12.93932(18)
	c = 13.777(5)	20.82638(17)	24.38480(10)	12.93932(18)
	α = 87.987(5)	90	90	106.1755(12)
	β = 79.194(5)	92.0003(7)	105.5230(10)	102.1874(11)
	γ = 71.304(5)	90	90	94.7288(11)
Volume (Å^3)	1463.1(9)	4266.30(6)	9236.04(9)	2623.56(6)
Z	2	4	4	2
Density (calculated, Mg/m^3)	1.347	1.344	1.266	1.276
Absorption coefficient (mm^{-1})	0.185	1.839	1.390	1.242
F(000)	620	1792	3696	1064
Crystal size (mm^3)	0.450x0.250x0.075	0.309x0.150x0.099	0.261x0.200x0.132	0.340x0.080x0.056
Theta range for data collection (°)	1.505 - 25.372	3.005 - 80.464	2.502 - 79.343	2.329 - 79.677
Index ranges (h,k,l)	-10/10, -15/15, -6/16	-12/12, -26/26, -26/26	-25/26, -23/23, -30/31	-13/13, -16/16, -25/22
Reflections collected	14263	106835	113925	63375
Independent reflections [R(int)]	5322 [0.1009]	17417 [0.0783]	19699 [0.0588]	11225 [0.0639]
Completeness to theta = 25.242°	99.4 %	99.9 %	100.0 %	100.0 %
Max. and min. transmission	0.7452 and 0.6558	1.00000 and 0.55445	1.00000 and 0.81291	1.00000 and 0.44974
Data / restraints / parameters	5322 / 1 / 393	17417 / 0 / 543	19699 / 0 / 1175	11225 / 1714 / 886
Goodness-of-fit on F^2	1.021	1.201	1.026	1.054
Final R indices [I>2sigma(I)]	R1 = 0.0804	0.0580	0.0480	0.0430
	wR2 = 0.1914	0.1964	0.1165	0.1163
R indices (all data)	R1 = 0.1497	0.0611	0.0569	0.0502
	wR2 = 0.2258	0.1996	0.1260	0.1235
Extinction coefficient	0.011(3)	n.a.	n.a.	n.a.
Largest diff. peak and hole (e.Å^{-3})	0.480/-0.440	0.418/-0.876	0.617/-0.525	0.486/-0.482

Table S2. Hydrogen bonds in the compounds studied [Å and °].

D-H...A	d(D-H)	d(H...A)	d(D...A)	<(DHA)
Compound **1a**				
N2-H2N...N4	0.89(5)	2.16(5)	2.954(6)	148(4)
Compound **1b**				
N2-H2N...N5	0.91(2)	2.39(2)	3.154(2)	142.3(18)
Compound **2a**				
N2-H2N...Cl1	0.91(6)	2.30(6)	3.147(5)	154(5)
Compound **2b**				
N2-H2N...Cl1	0.872(14)	2.417(14)	3.1968(12)	149.1(15)
Compound **3**				
N2-H2N...O1	0.89(2)	2.12(4)	2.852(6)	139(5)

Compound 1a

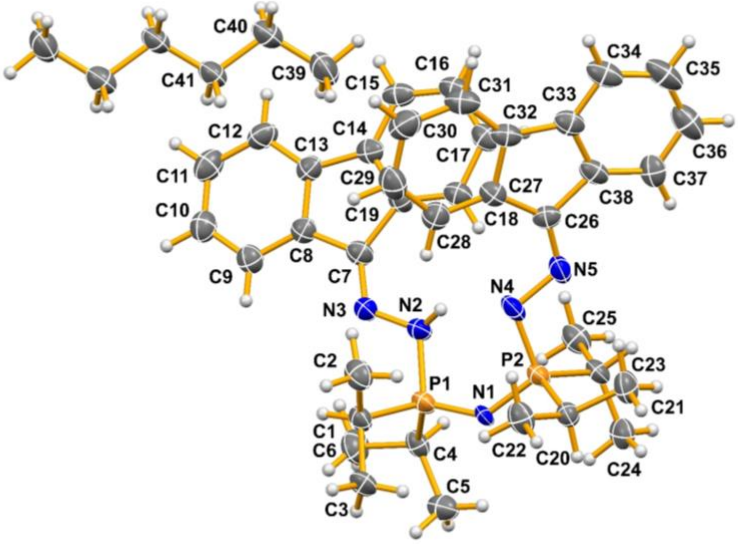

Figure S1: Structure of Compound **1a** with the unique atoms of the asymmetric unit labelled. Thermal ellipsoids have been drawn at the 50% probability level. Hydrogen atoms are included but have not been labelled.

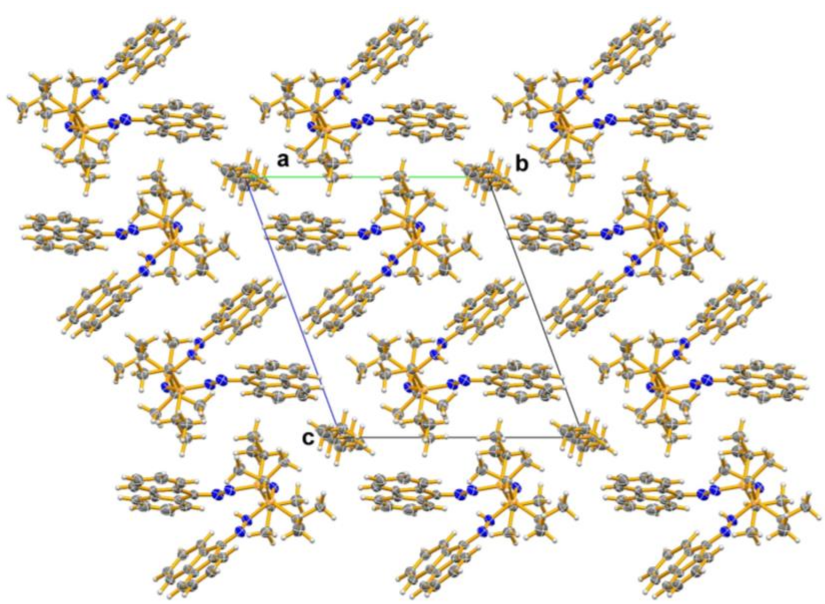

Figure *S*2: Packing diagram of Compound **1a** viewed down the A-axis. There are no stacking contacts in the structure below the 4 Å limit.

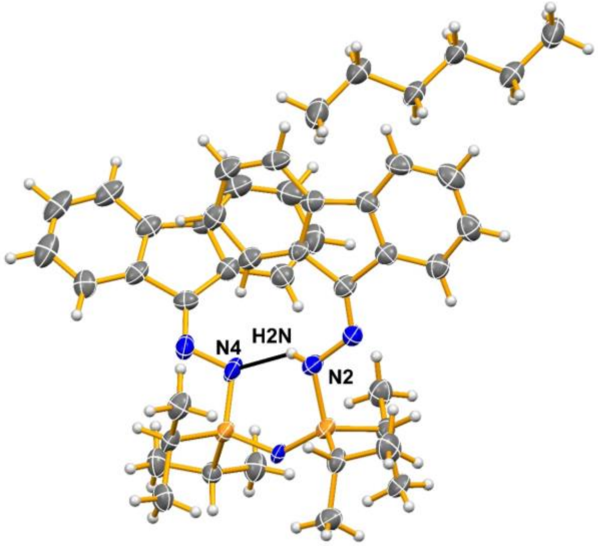

Figure *S*3: The intramolecular N-H…N hydrogen bond formed by compound **1a**. Thermal ellipsoids have been drawn with 50% probability. Only the atoms involved in the hydrogen bond have been labelled.

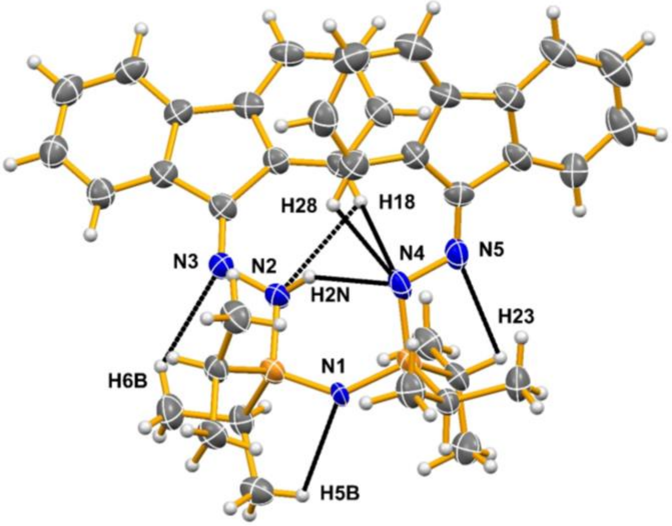

Figure *S*4: Intramolecular contacts accepted by nitrogen (dotted lines) in Compound **1a**. Contacts shown are to the limit of the sum of the van der Waals radii and H…H contacts have been omitted. Thermal ellipsoids have been drawn at the 50% probability level. Only the atoms involved in the interactions have been labelled.

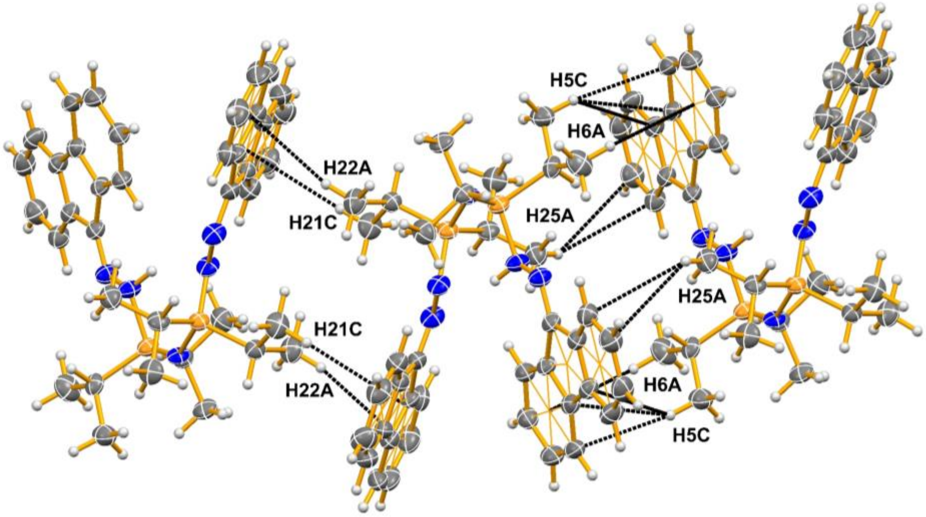

Figure *S5*: Intermolecular C-H contacts (dotted lines) in Compound **1a** drawn from the perspective of one central molecule. The solvent molecule does not participate in any such contacts. Contacts shown are to the limit of the sum of the van der Waals radii + 0.2 Å and H…H contacts have been omitted. Thermal ellipsoids have been drawn at the 50% probability level. Only selected atoms have been labelled.

Compound 1b

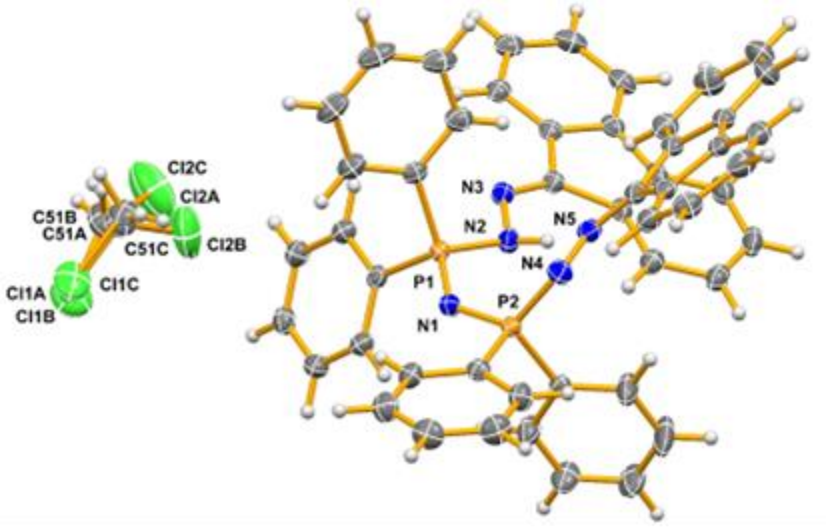

Figure S6: Structure of Compound **1b** with the atoms of the disordered solvent molecule clearly labelled. Only the non-carbon atoms of the main molecule have been labelled. Thermal ellipsoids have been drawn at the 50% probability level. Hydrogen atoms are included but have not been labelled.

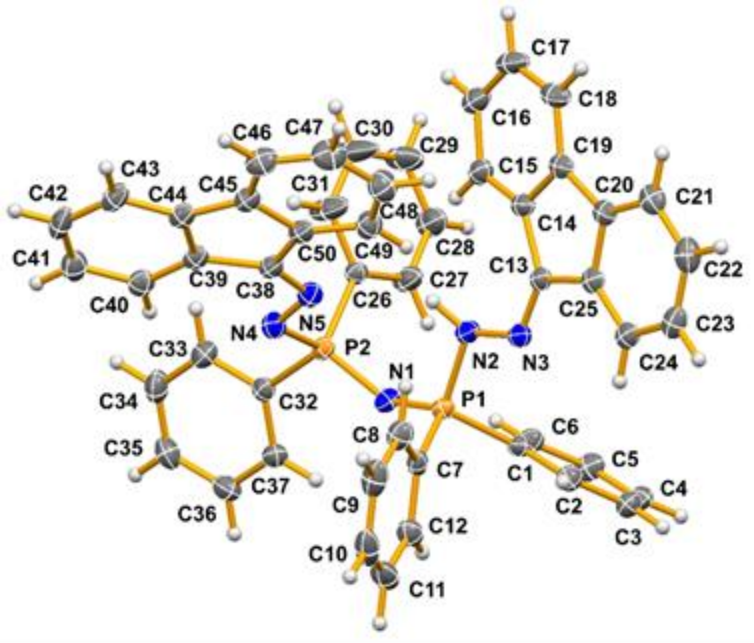

Figure *S*7: Structure of Compound **1b** with the atoms of the main molecule labelled. The disordered solvent molecule has been removed for clarity. Thermal ellipsoids have been drawn at the 50% probability level. Hydrogen atoms are included but have not been labelled

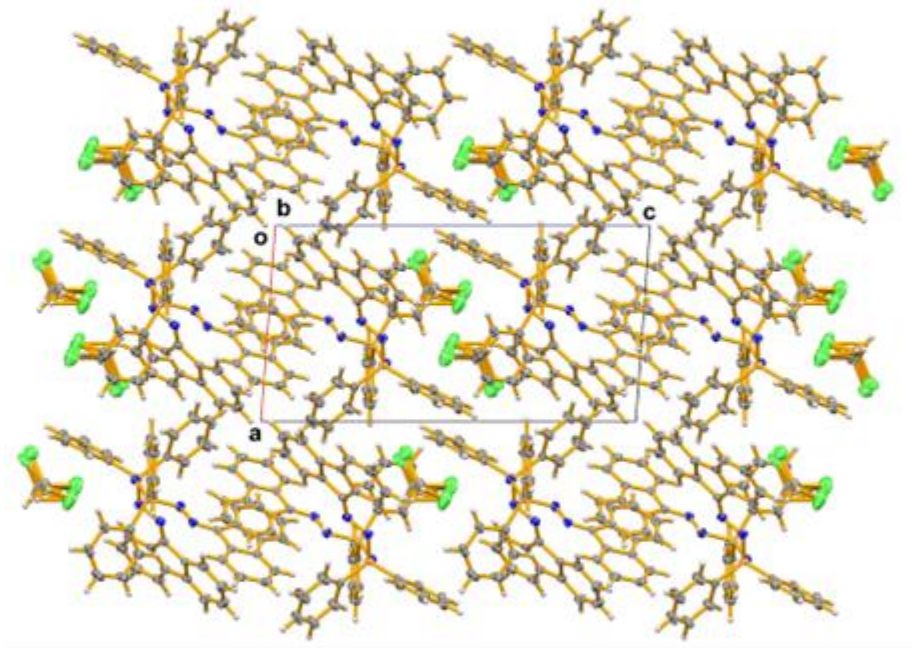

Figure *S*8: Packing diagram of Compound **1b** viewed down the B-axis.

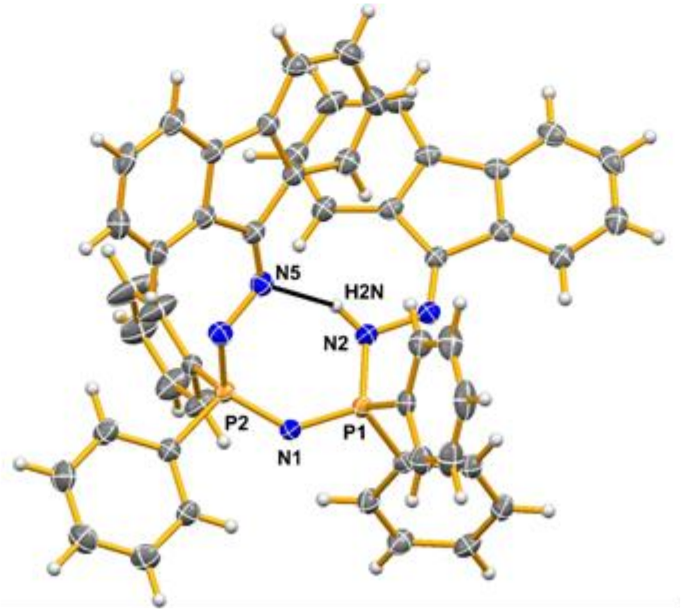

Figure *S*9: The intramolecular N-H…N hydrogen bond formed by compound **1b**. Thermal ellipsoids have been drawn with 50% probability. Only selected atoms have been labelled.

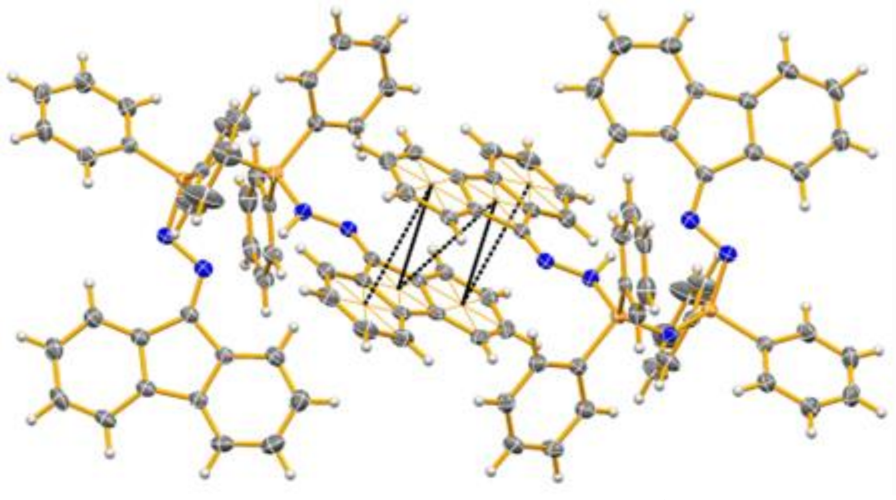

Figure *S*10: Intramolecular stacking contacts less than 3.8 Å (dashed lines) in compound **1b**. Thermal ellipsoids have been drawn with 50% probability. Atoms have not been labelled.

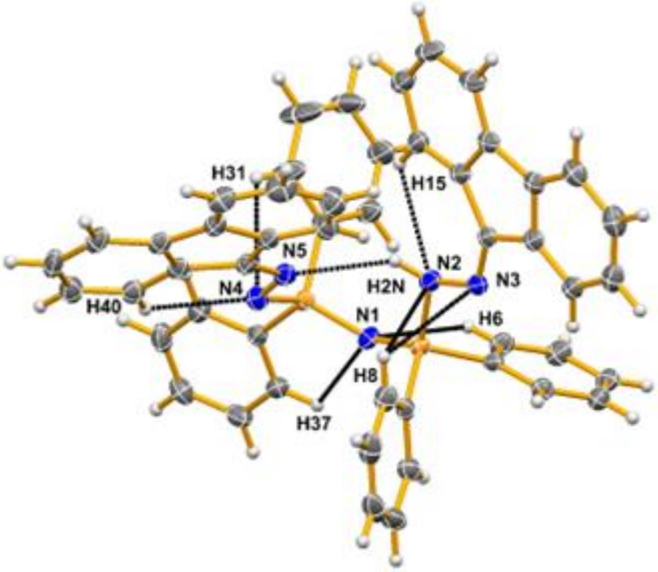

Figure *S*11: Intramolecular contacts accepted by nitrogen (dotted lines) in Compound **1b**. Contacts shown are to the limit of the sum of the van der Waals radii and H…H contacts have been omitted. Thermal ellipsoids have been drawn at the 50% probability level. Only the atoms involved in the interactions have been labelled.

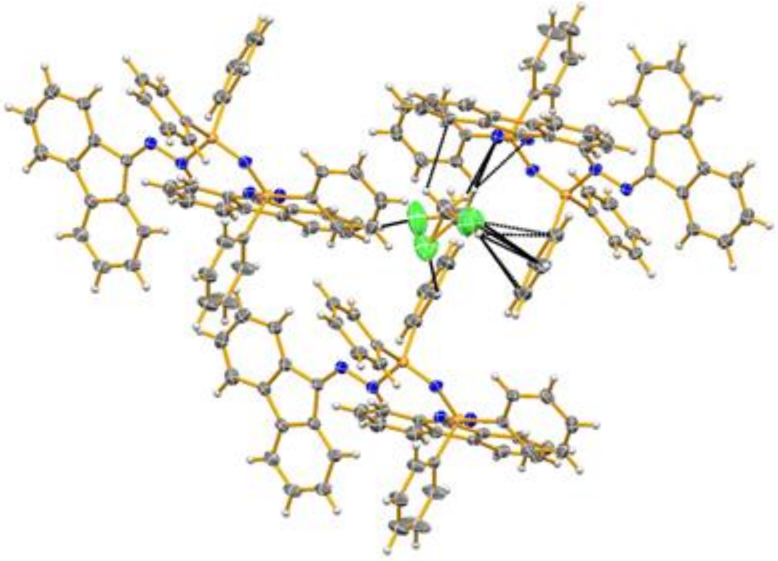

Figure *S*12: Intermolecular contacts (dotted lines) in Compound **1b** drawn from the perspective of one central disordered solvent molecule. Contacts shown are to the limit of the sum of the van der Waals radii. Thermal ellipsoids have been drawn at the 50% probability level. Atoms have not been labelled.

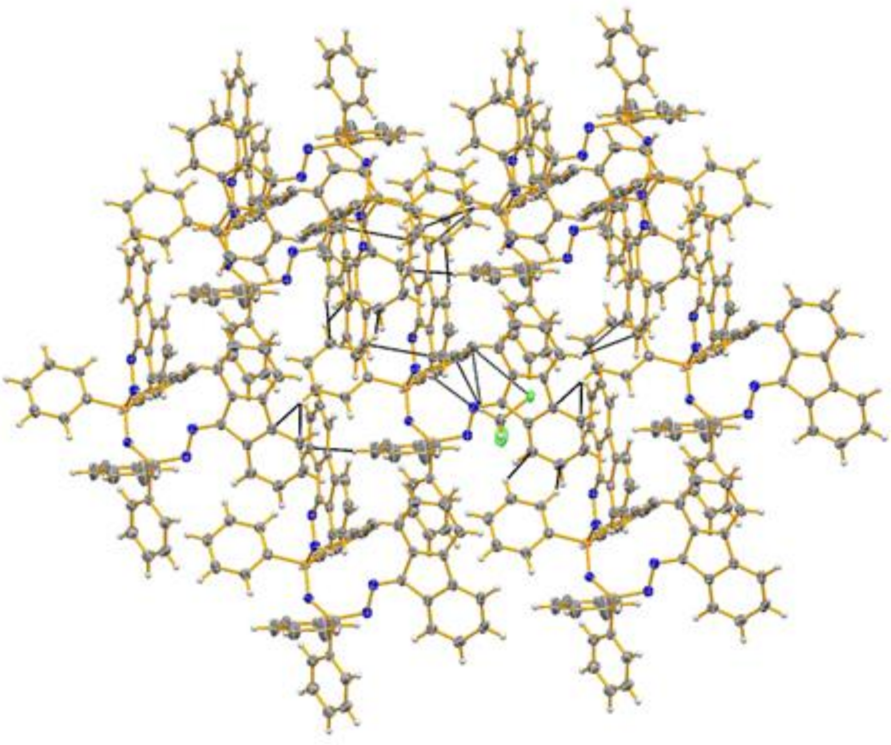

Figure *S*13: Intermolecular contacts (dotted lines) in Compound **1b** drawn from the perspective of one central molecule. Contacts shown are to the limit of the sum of the van der Waals radii. Thermal ellipsoids have been drawn at the 50% probability level. Atoms have not been labelled.

Compound 2a

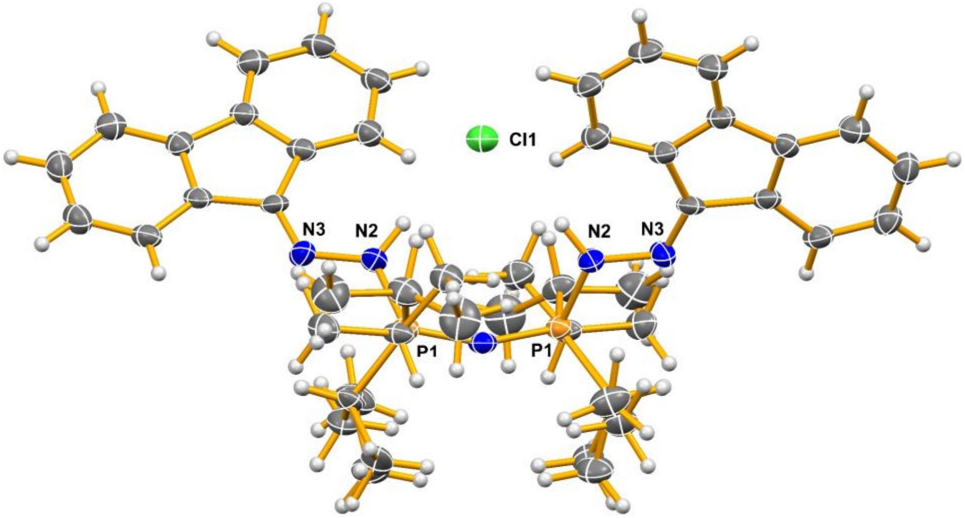

***Figure S14**: Structure of Compound **2a** with only the non-carbon atoms labelled. Disorder of the iso-propyl groups has not been removed. Thermal ellipsoids have been drawn at the 50% probability level. Hydrogen atoms are included but have not been labelled.*

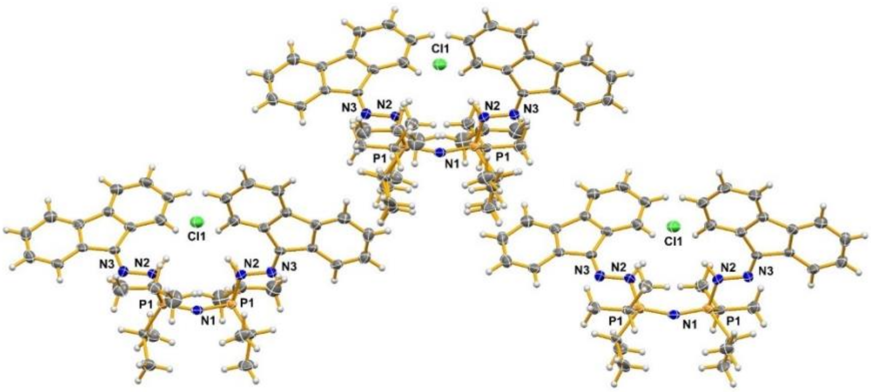

Figure S15: Composite diagram showing the disorder in Compound **2a** with only the non-carbon atoms labelled. On the top is the disordered structure while below Part A is shown on the left and Part B is on the right. Thermal ellipsoids have been drawn at the 50% probability level. Hydrogen atoms are included but have not been labelled.

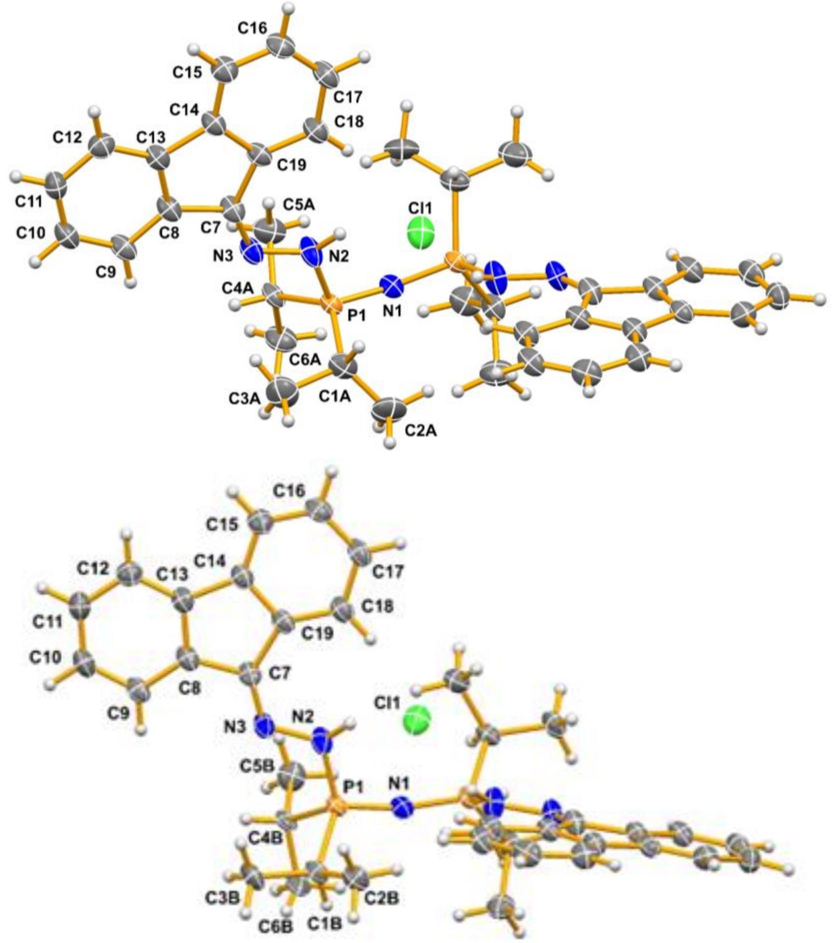

Figure S16: Structure of Compound **2a** with only the unique atoms of the asymmetric unit labelled. Part A of the disordered structure is on the top and Part B is on the bottom.

Thermal ellipsoids have been drawn at the 50% probability level. Hydrogen atoms are included but have not been labelled.

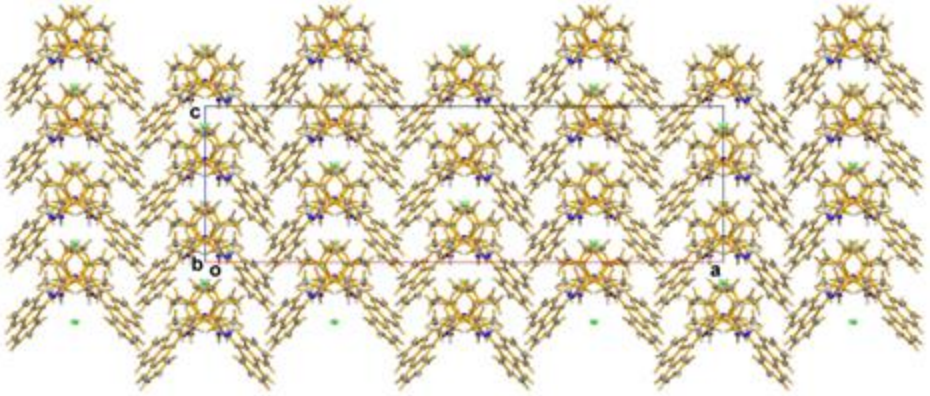

Figure S17: Packing diagram of Compound **2a** viewed down the *B*-axis. There are no stacking contacts in the structure below the 4 Å limit.

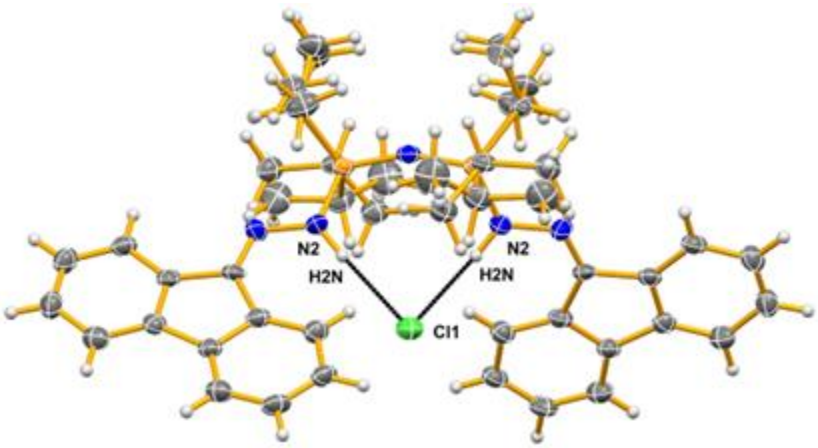

Figure S18: The N-H…Cl hydrogen bonds formed by compound **2a**. Thermal ellipsoids have been drawn with 50% probability. Only the atoms involved in the hydrogen bond have been labelled.

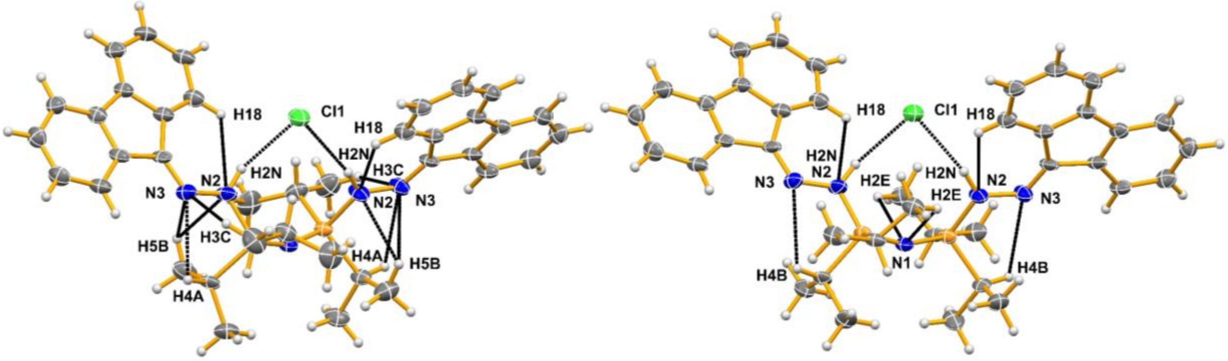

Figure S19: Intramolecular contacts accepted by nitrogen (dotted lines) in Compound **2a**. Contacts shown are to the limit of the sum of the van der Waals radii and the N-H…Cl hydrogen bonds have also been included. The interactions in Part A (left) differ from those in Part B (right). Thermal ellipsoids have been drawn at the 50% probability level. Only the atoms involved in the interactions have been labelled.

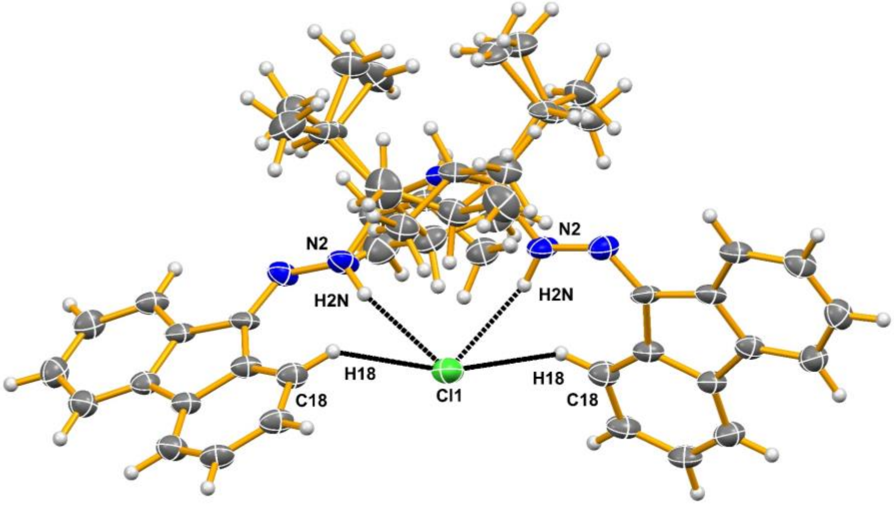

Figure S20: Intermolecular contacts (dotted lines) in Compound **2a** drawn from the perspective of one central anion. Contacts shown are to the limit of the sum of the van der Waals radii. Thermal ellipsoids have been drawn at the 50% probability level. Only selected atoms have been labelled.

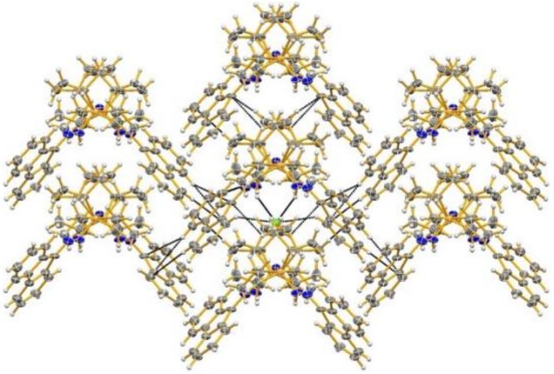

Figure S21: Intermolecular C-H contacts (dotted lines) in Compound **2a** drawn from the perspective of one central cation. The N-H…Cl hydrogen bonds have also been included. Contacts shown are to the limit of the sum of the van der Waals radii and H…H contacts have been omitted. Thermal ellipsoids have been drawn at the 50% probability level. Atoms have not been labelled.

Compound 2b

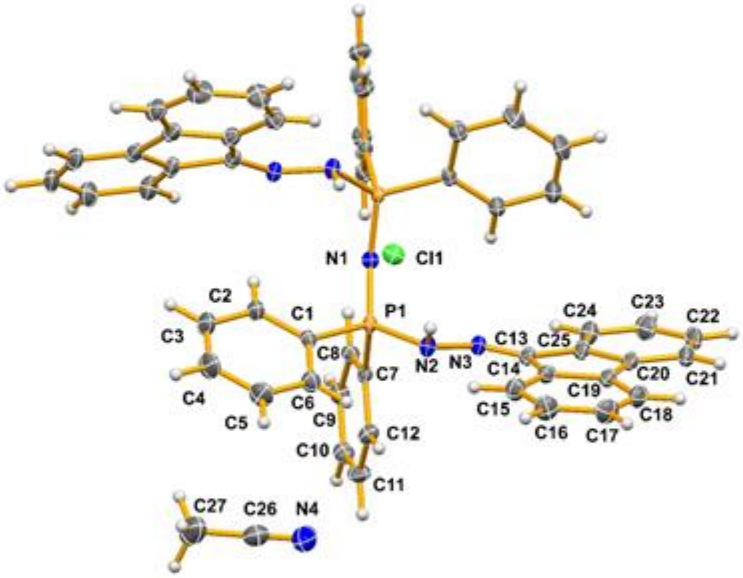

Figure S22: Structure of Compound **2b** with the unique atoms of the independent unit labelled. Thermal ellipsoids have been drawn at the 50% probability level. Hydrogen atoms are included but have not been labelled.

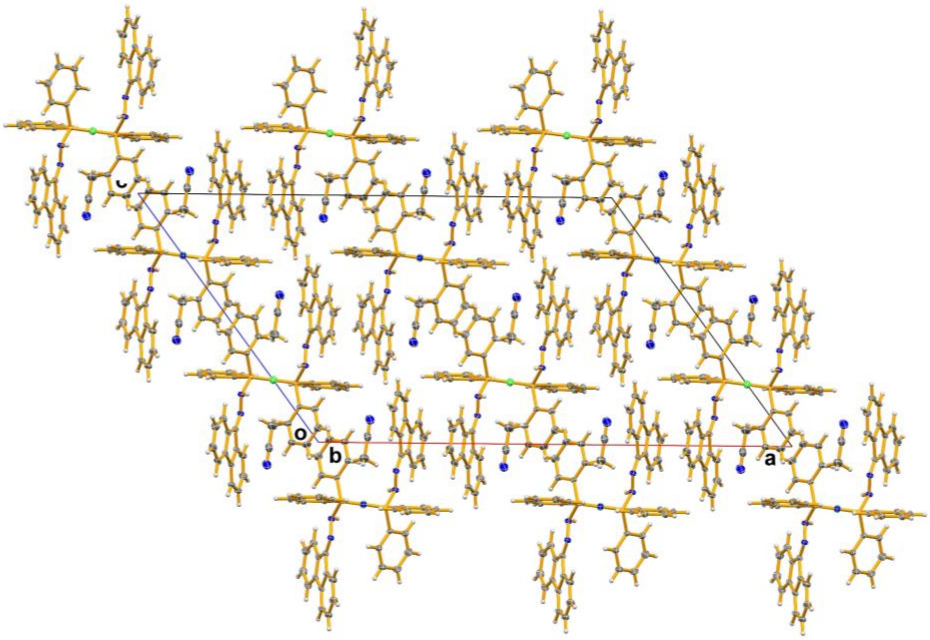

Figure S23: Packing diagram of Compound **2b** viewed down the *B*-axis.

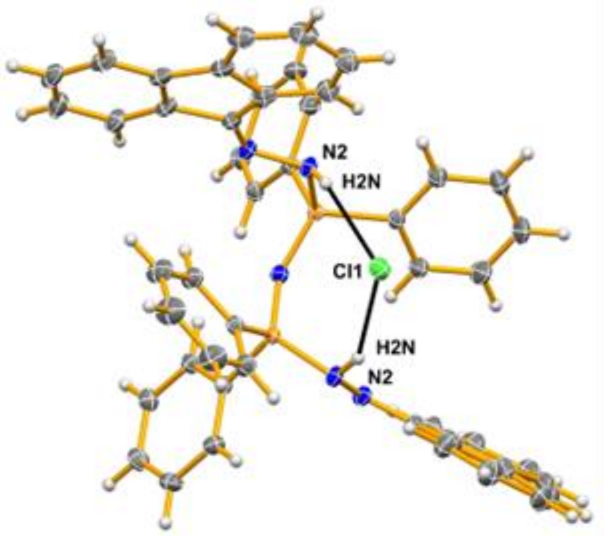

Figure S24: The intermolecular N-H…Cl hydrogen bond formed by compound **2b**. Thermal ellipsoids have been drawn with 50% probability. Only the atoms involved in the hydrogen bond have been labelled.

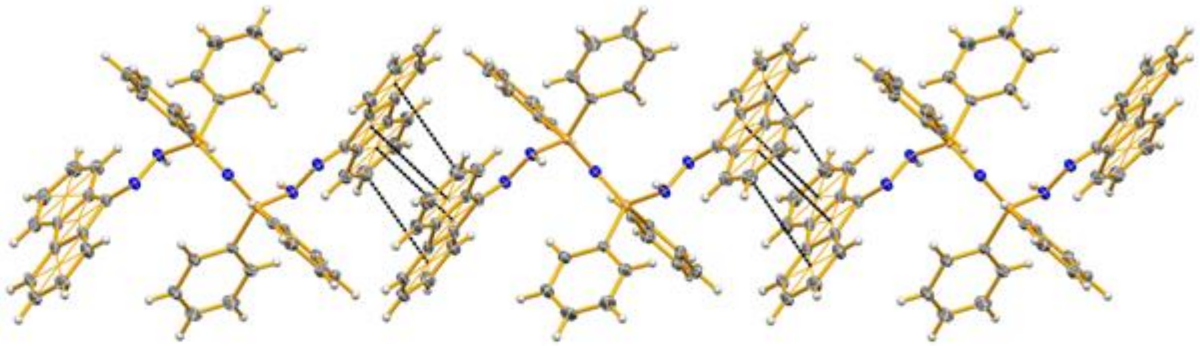

Figure S25: Intramolecular stacking contacts less than 3.8 Å (dashed lines) in compound **2b**. Thermal ellipsoids have been drawn with 50% probability. Atoms have not been labelled.

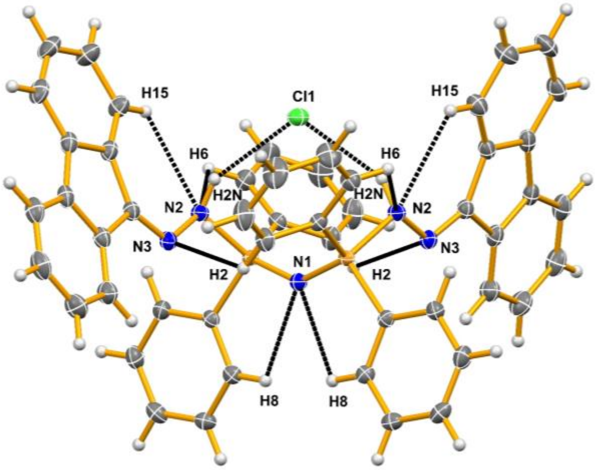

Figure S26: Intramolecular contacts accepted by nitrogen (dotted lines) in Compound **2a**. Contacts shown are to the limit of the sum of the van der Waals radii and the N-H…Cl hydrogen bonds have also been included. Thermal ellipsoids have been drawn at the 50% probability level. Only the atoms involved in the interactions have been labelled.

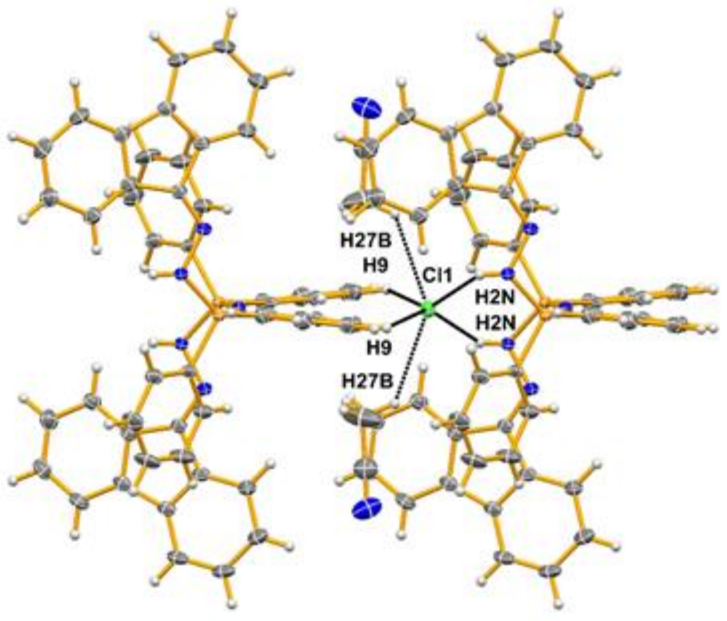

Figure S27: An overall view of the intermolecular interactions (dashed lines – less than the sum of the van der Waals radii) drawn from the perspective of one central anion in the structure of compound **2b**. Thermal ellipsoids have been drawn with 50% probability. Only selected atoms have been labelled.

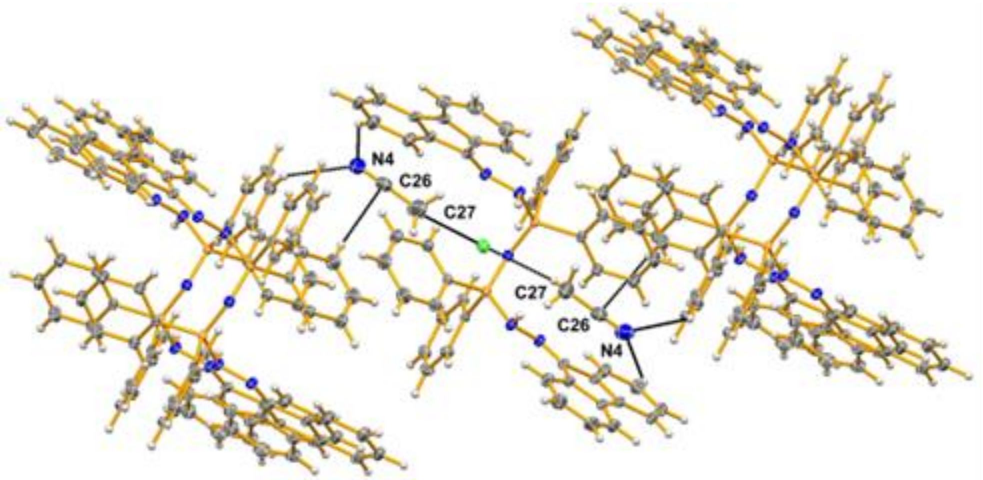

Figure S28: An overall view of the intermolecular interactions (dashed lines – less than the sum of the van der Waals radii) drawn from the perspective of two acetonitrile solvent molecules in the structure of compound **2b**. Thermal ellipsoids have been drawn with 50% probability. Only selected atoms have been labelled.

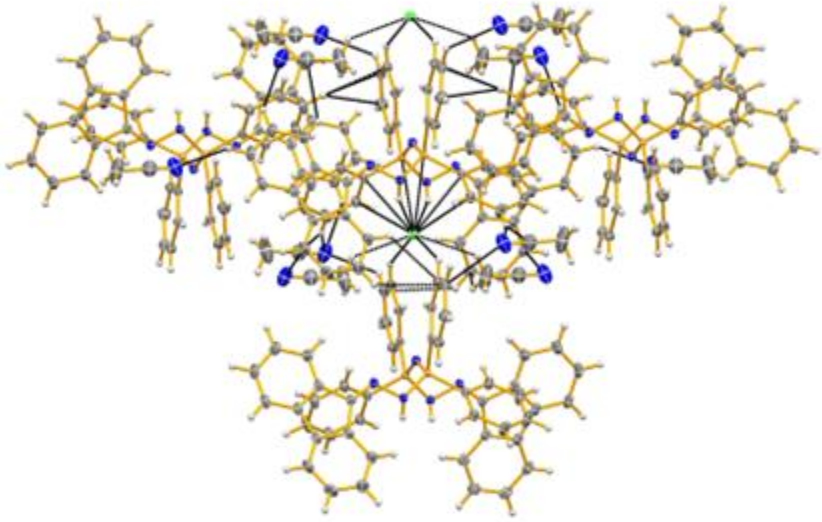

Figure S29: Intermolecular C-H contacts (dotted lines) in Compound **2b** drawn from the perspective of two central cations. The N-H…Cl hydrogen bonds have also been included. Contacts shown are to the limit of the sum of the van der Waals radii and H…H contacts have been omitted. Thermal ellipsoids have been drawn at the 50% probability level. Atoms have not been labelled.

Compound 3

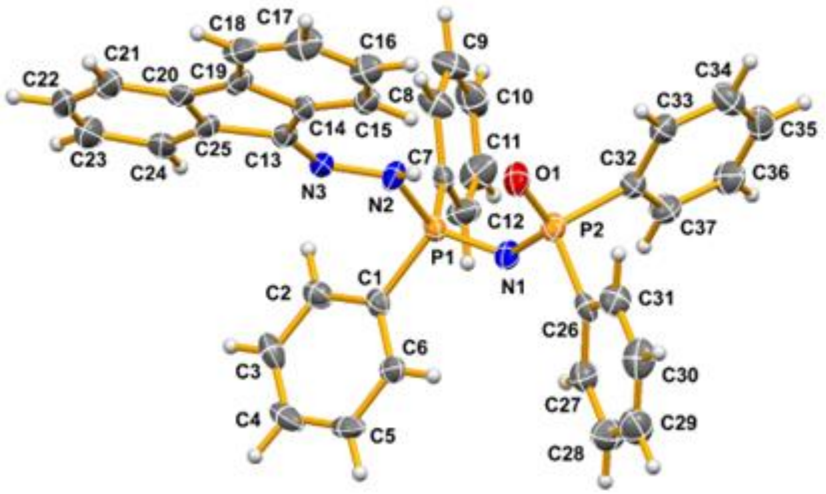

Figure S30: Structure of Compound **3** with full labelling. Thermal ellipsoids have been drawn at the 50% probability level. Hydrogen atoms are included but have not been labelled.

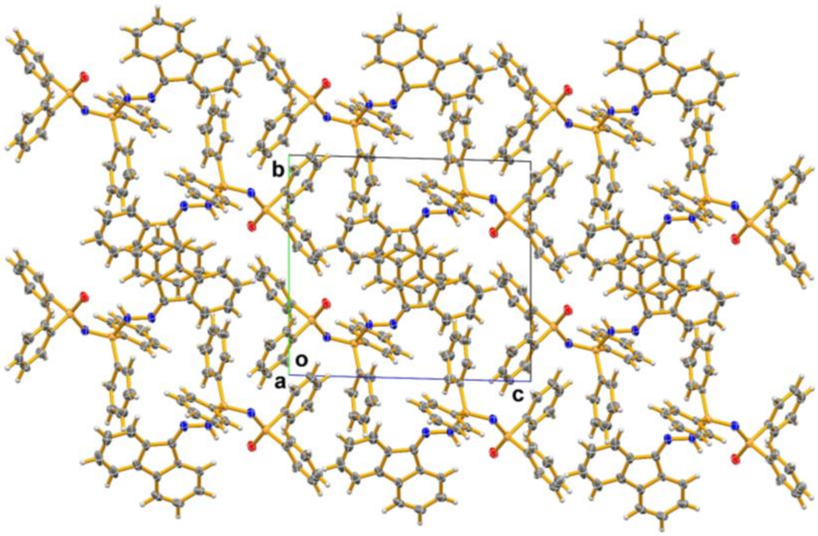

Figure S31: Packing diagram of Compound **3** viewed down the *A*-axis.

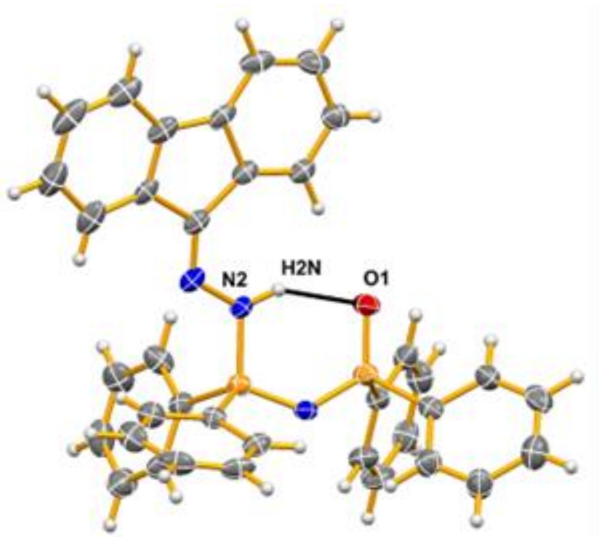

Figure S32: The intramolecular N-H…O hydrogen bond formed by compound **3**. Thermal ellipsoids have been drawn with 50% probability. Only the atoms involved in the hydrogen bond have been labelled.

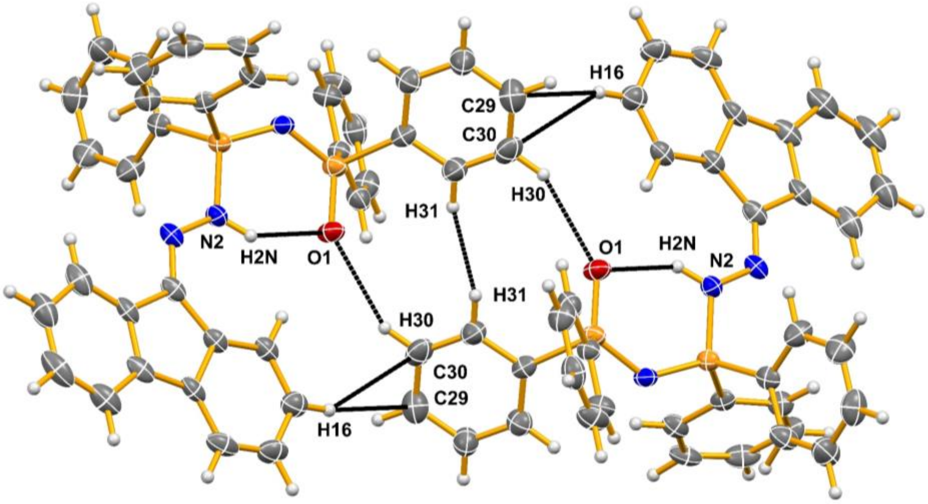

Figure S33: An overall view of the ordered network of hydrogen bonds (dashed lines – less than the sum of the van der Waals radii + 0.2 Å) joining two molecules in the structure of compound **3**. Thermal ellipsoids have been drawn with 50% probability. Only selected atoms have been labelled.

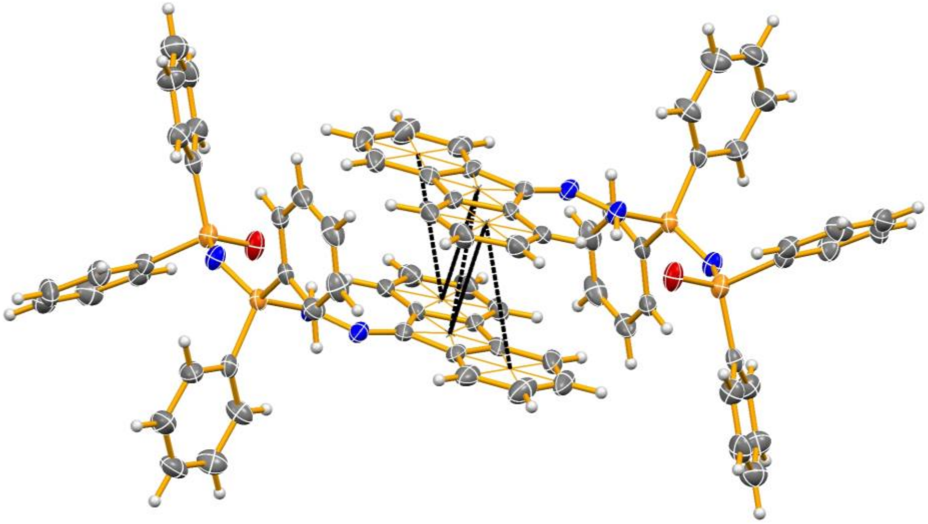

Figure S34: Intramolecular stacking contacts less than 3.8 Å (dashed lines) in compound **3**. Only the interaction in molecule 1 is below the limit chosen; the equivalent interaction in molecule 2 is slightly longer but is still shown. Thermal ellipsoids have been drawn with 50% probability.

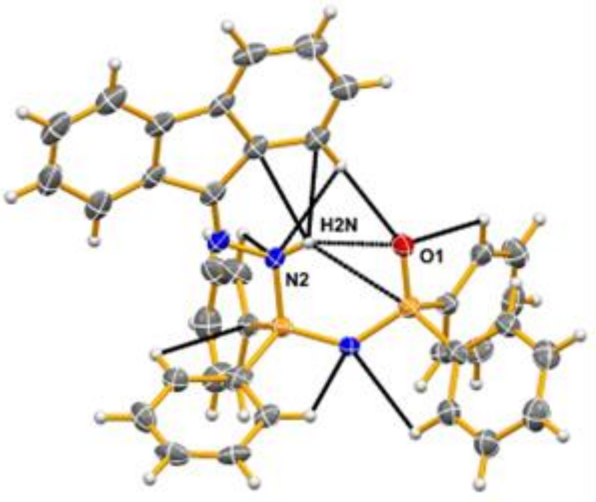

Figure S35: Intramolecular C-H contacts (dotted lines) in Compound **3**. Contacts shown are to the limit of the sum of the van der Waals radii and H…H contacts have been omitted. Thermal ellipsoids have been drawn at the 50% probability level. Only the atoms of the N-H…N hydrogen bond have been labelled.

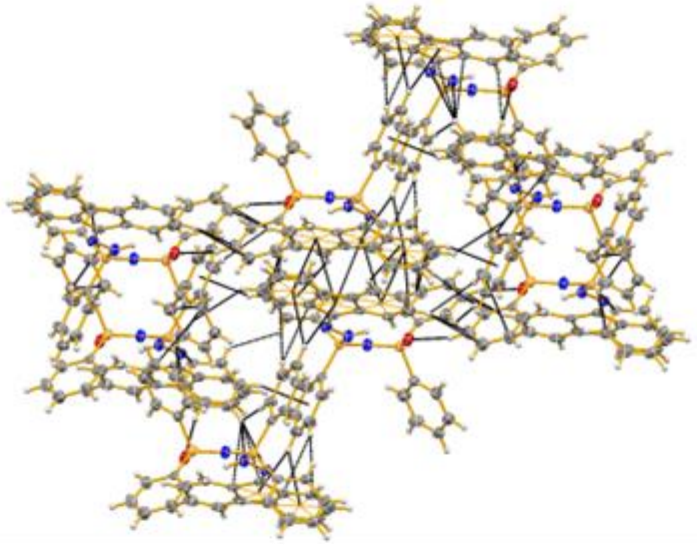

Figure S36: Intermolecular C-H contacts (dotted lines) in Compound **3** drawn from the perspective of two central (stacking also shown) molecules. Contacts shown are to the limit of the sum of the van der Waals radii + 0.2 Å and H…H contacts have been omitted. Thermal ellipsoids have been drawn at the 50% probability level. Atoms have not been labelled.

Compound 4

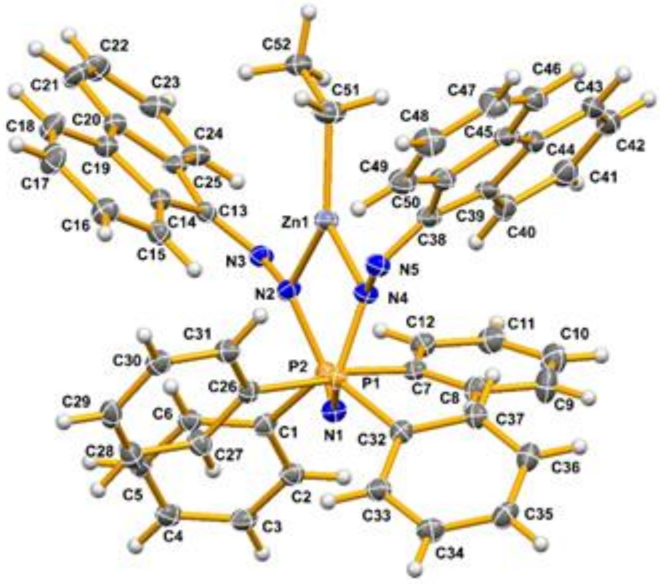

Figure S37: Structure of Compound **4** with full heavy atom labelling. Thermal ellipsoids have been drawn at the 50% probability level. Hydrogen atoms are included but have not been labelled.

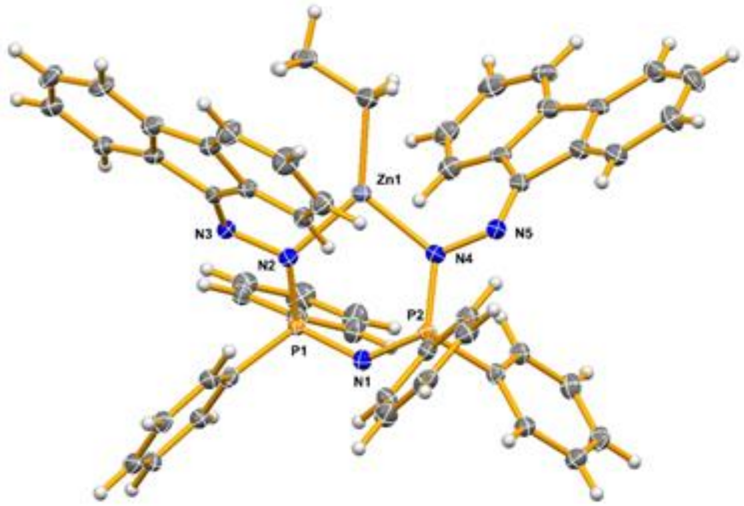

Figure S38: A second view of Compound **4**, with only select atoms labelled, drawn to more clearly show the central core. Thermal ellipsoids have been drawn at the 50% probability level. Hydrogen atoms are included but have not been labelled.

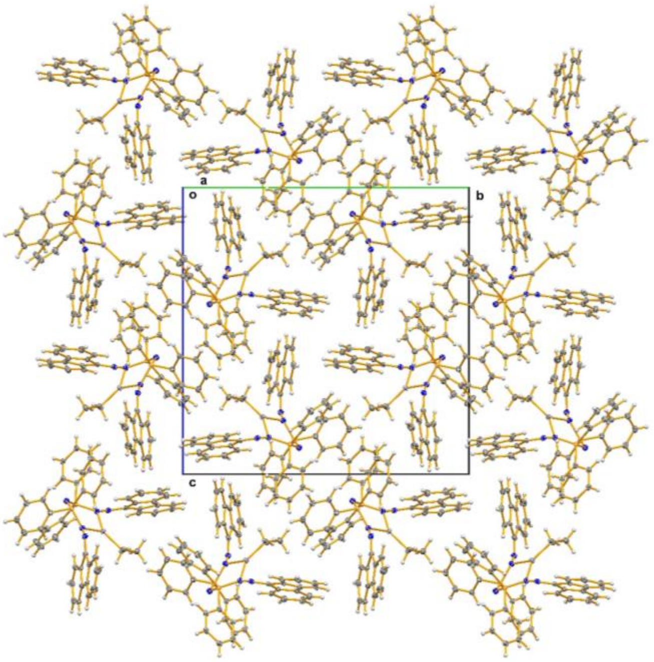

Figure S39: Packing diagram of Compound **4** viewed down the *A*-axis. There are no stacking contacts in the structure below the 4 Å limit.

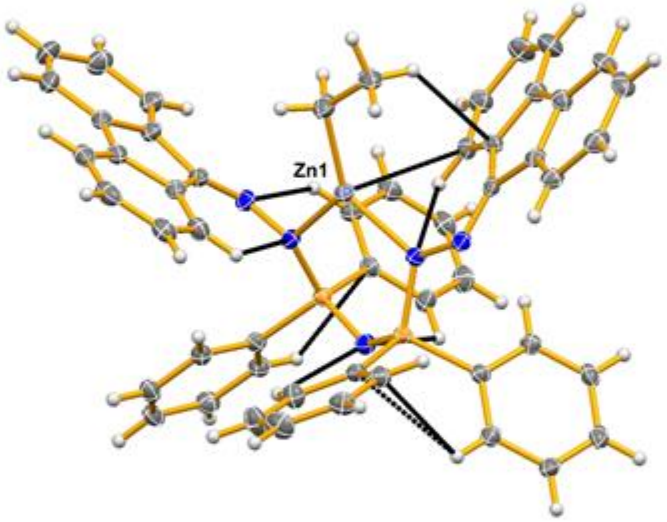

Figure S40: Intramolecular C-H contacts (dotted lines) in Compound **4**. Contacts shown are to the limit of the sum of the van der Waals radii and H…H contacts have been omitted. Thermal ellipsoids have been drawn at the 50% probability level. Only the central zinc atom has been labelled.

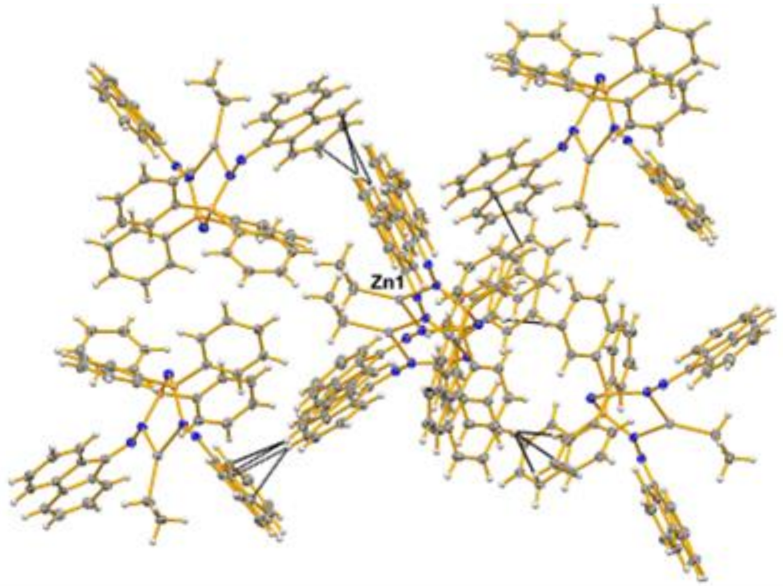

Figure S41: Intermolecular C-H contacts (dotted lines) in Compound **4** drawn from the perspective of one central molecule. Contacts shown are to the limit of the sum of the van der Waals radii and H…H contacts have been omitted. Thermal ellipsoids have been drawn at the 50% probability level. Only the central zinc atom has been labelled.

Compound 5

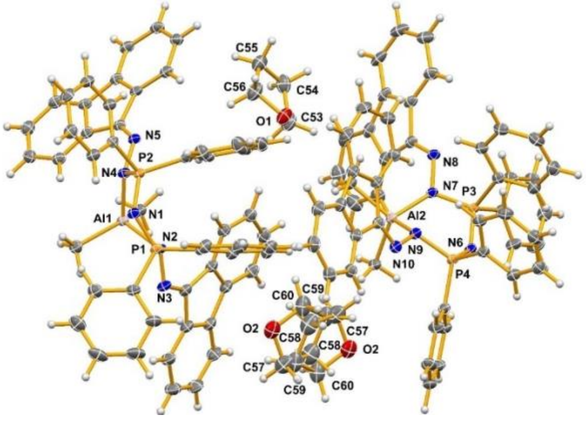

Figure S42: Structure of Compound **5**, including the two molecules and the tetrahydrofuran solvent of the independent unit. Only selected atoms in the main molecules have been labelled. Thermal ellipsoids have been drawn at the 50% probability level. Hydrogen atoms are included but have not been labelled.

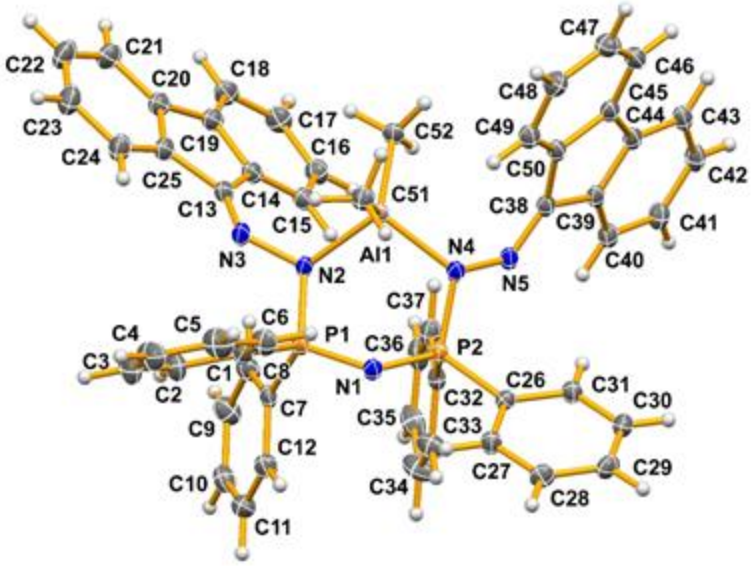

Figure S43: View of molecule 1 in Compound **5**, with full labelling. The THF solvent has been removed for clarity. Thermal ellipsoids have been drawn at the 50% probability level. Hydrogen atoms are included but have not been labelled.

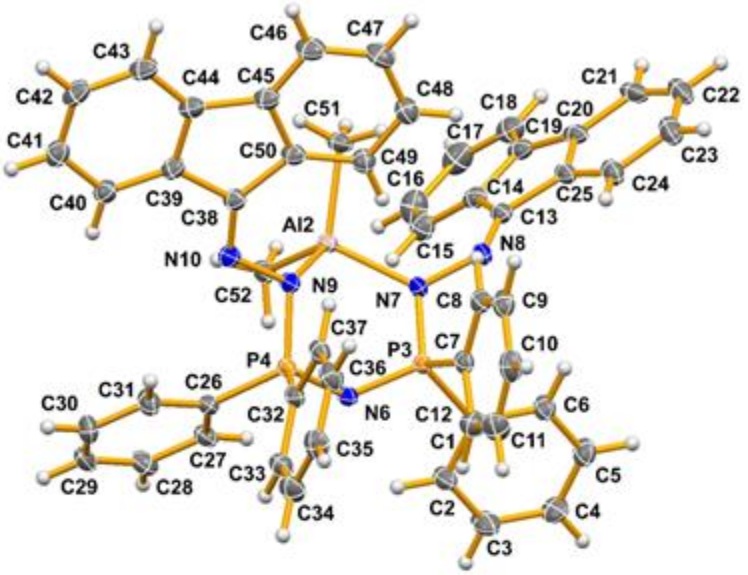

Figure S44: View of molecule 2 in Compound **5**, with full labelling. The THF solvent has been removed for clarity. Thermal ellipsoids have been drawn at the 50% probability level. Hydrogen atoms are included but have not been labelled.

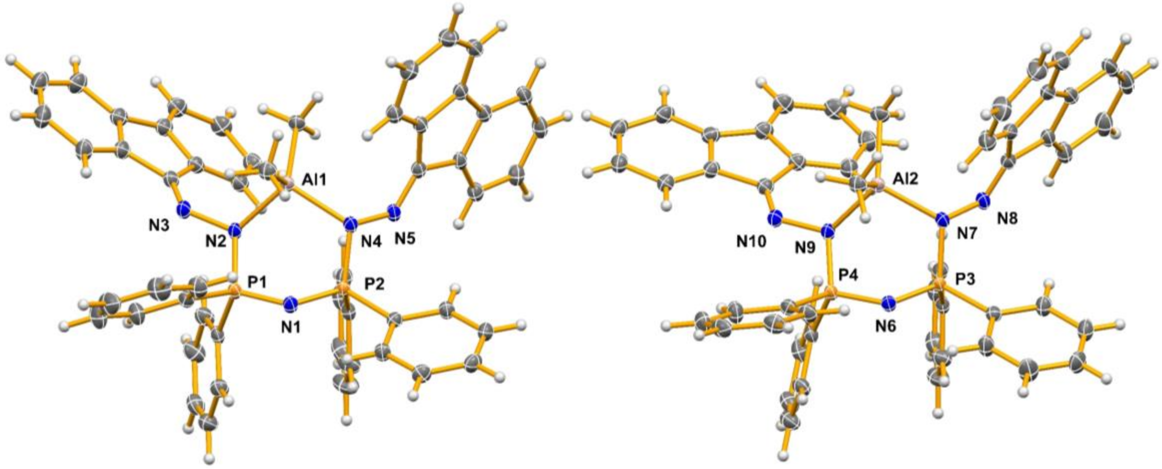

Figure S45: Composite diagram showing the two molecules in Compound **5** with selected atoms labelled. The THF solvent molecules have been removed for clarity. Molecule 1 is on the left and on the right is a view of molecule 2 after being inverted. The two molecules are shown in similar orientations so that slight differences in the two can be discerned. Thermal ellipsoids have been drawn at the 50% probability level. Hydrogen atoms are included but have not been labelled.

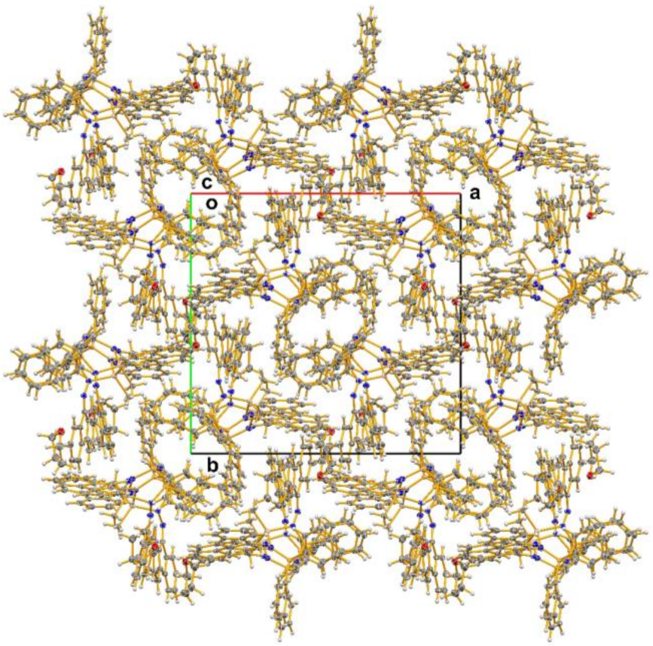

Figure S46: Packing diagram of Compound **5** viewed down the *C*-axis.

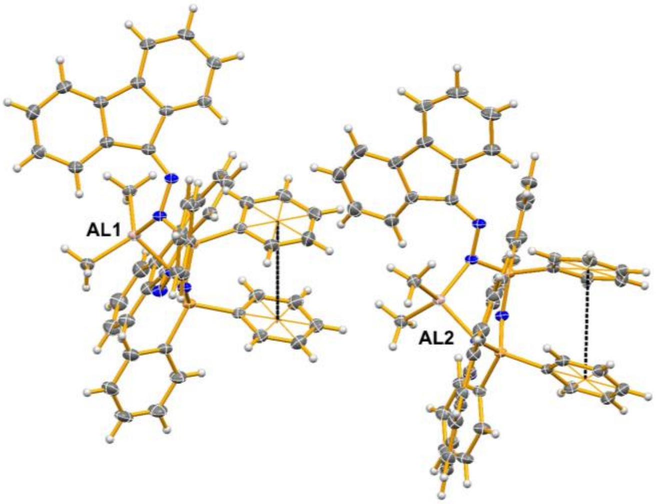

Figure S47: Intramolecular stacking contacts less than 3.8 Å (dashed lines) in compound **5**. Only the interaction in molecule 1 is below the limit chosen; the equivalent interaction in molecule 2 is slightly longer but is still shown. Thermal ellipsoids have been drawn with 50% probability.

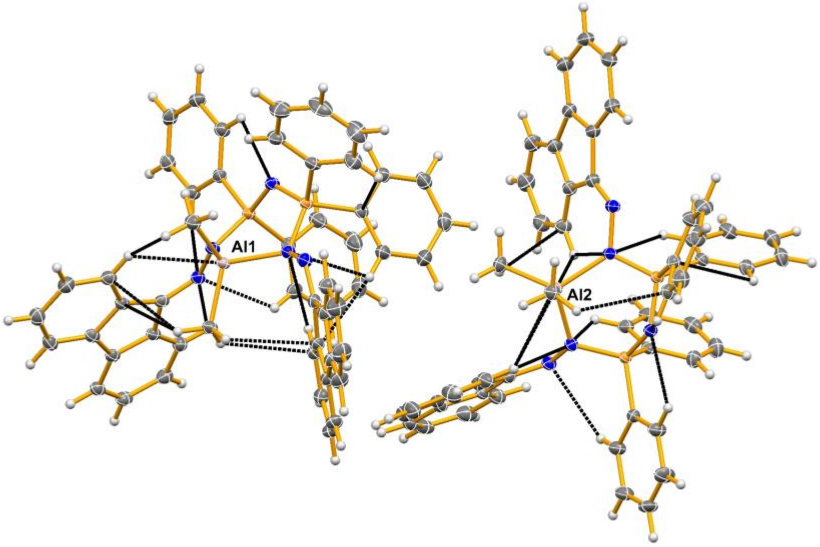

Figure S48: Intramolecular C-H contacts (dotted lines) in Compound **5**. Contacts shown are to the limit of the sum of the van der Waals radii and H…H contacts have been omitted. Thermal ellipsoids have been drawn at the 50% probability level. Only the aluminum atoms have been labelled to identify the molecules.

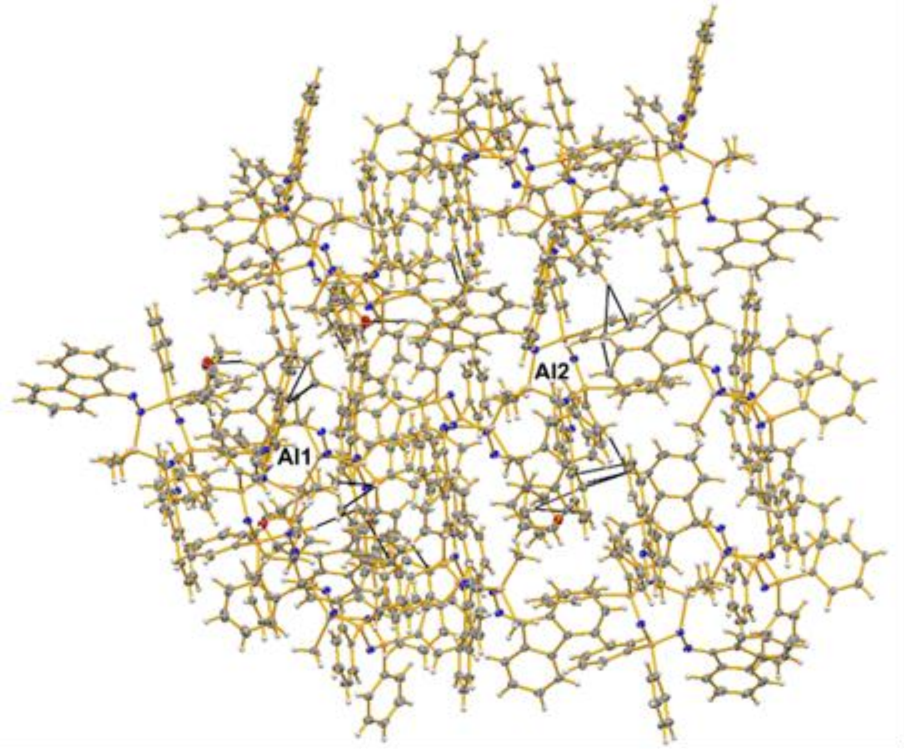

Figure S49: Intermolecular C-H contacts (dotted lines) in Compound **5** drawn from the perspective of two central molecules. Contacts shown are to the limit of the sum of the van der Waals radii and H…H contacts have been omitted. Thermal ellipsoids have been drawn at the 50% probability level. Only the central aluminum atoms have been labelled.

Compound 6

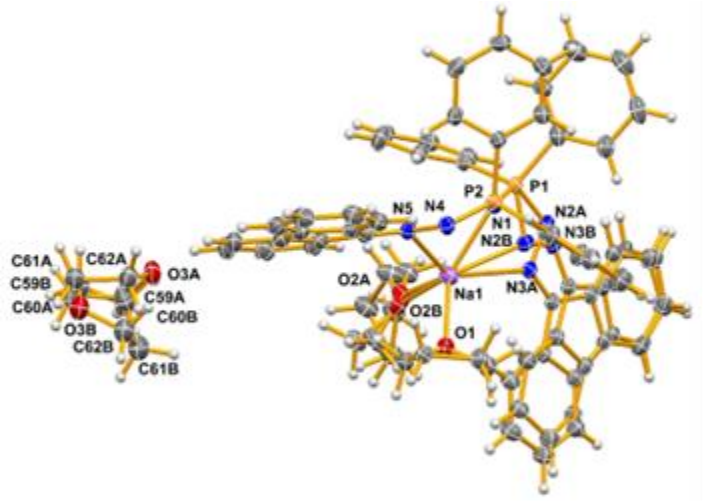

Figure S50: Structure of Compound **6**, including one molecule of disordered tetrahydrofuran solvent. Only selected atoms in the main molecule have been labelled.

Thermal ellipsoids have been drawn at the 50% probability level. Hydrogen atoms are included but have not been labelled.

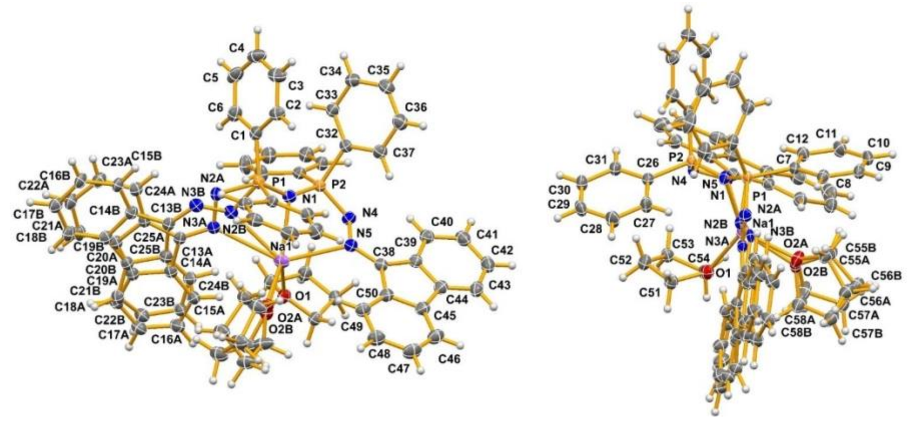

Figure S51: Composite diagram showing two views of Compound **6**, with full labelling. One molecule of disordered THF solvent has been removed for clarity. Thermal ellipsoids have been drawn at the 50% probability level. Hydrogen atoms are included but have not been labelled.

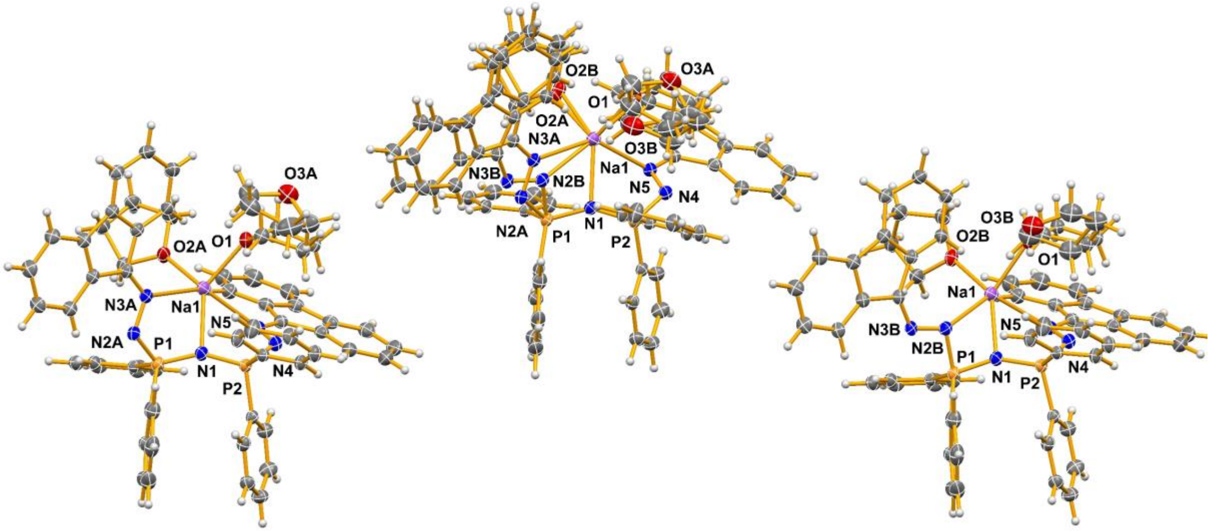

Figure S52: Composite diagram showing the two components of the disordered model used to refine Compound **6** with selected atoms labelled. The THF solvent molecule has not been removed. In the center is the disordered molecule, while on the left is the contribution of part A (major) and on the right is part B (minor). Thermal ellipsoids have been drawn at the 50% probability level. Hydrogen atoms are included but have not been labelled.

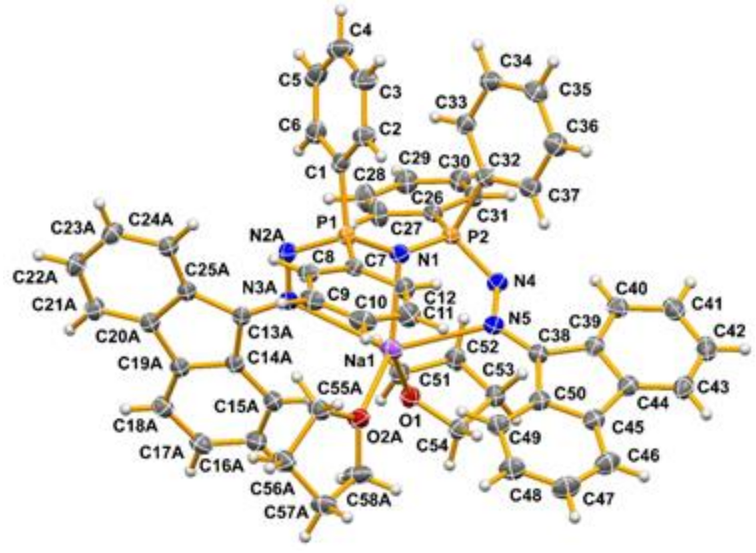

Figure S53: Fully labelled diagram of the structure of Compound **6**, with the free solvent and disorder removed for clarity. Thermal ellipsoids have been drawn at the 50% probability level. Hydrogen atoms are included but have not been labelled.

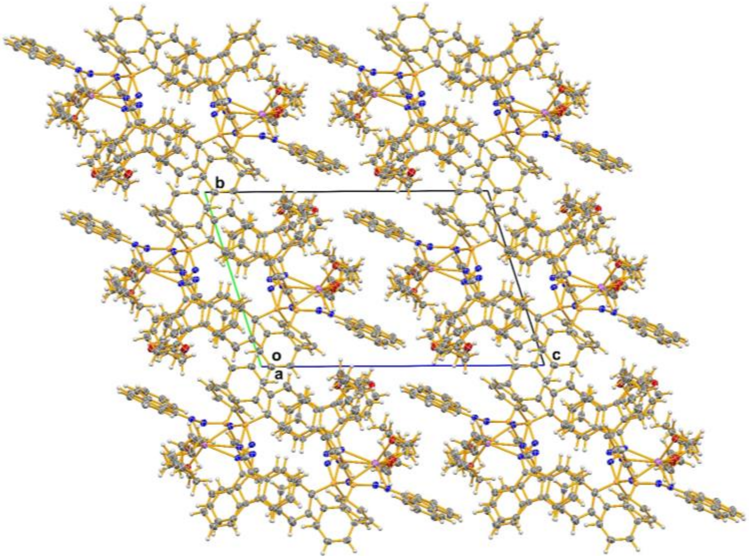

Figure S54: Packing diagram of Compound **6** viewed down the *A*-axis. There are no stacking contacts in the structure below the 4 Å limit.

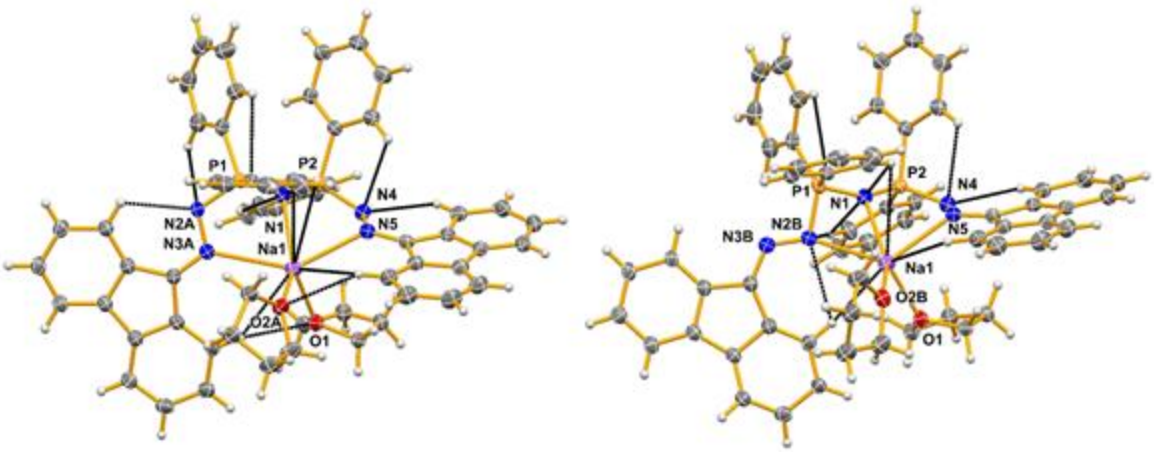

Figure S55: Composite diagram showing the intramolecular C-H contacts (dotted lines) in Compound **6**. Part A of the disordered structure is shown on the left and Part B is on the right. Contacts shown are to the limit of the sum of the van der Waals radii and H…H contacts have been omitted. Thermal ellipsoids have been drawn at the 50% probability level. Only selected atoms have been labelled.

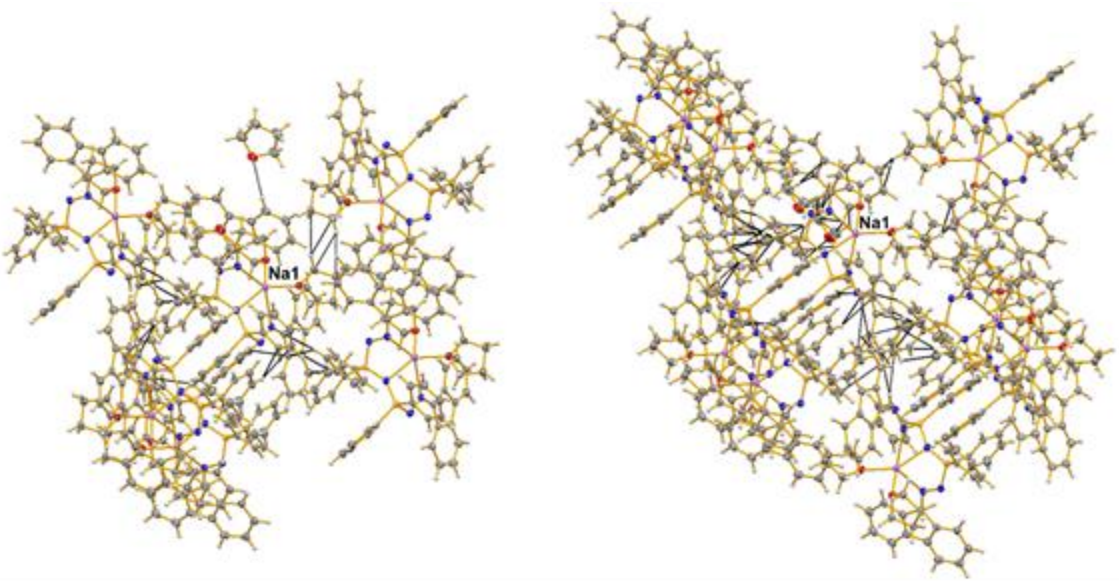

Figure S56: Composite diagram showing the intermolecular C-H contacts (dotted lines) in Compound **6** drawn from the perspective of one central cation. Part A of the disordered structure is shown on the left and Part B is on the right. Contacts shown are to the limit of the sum of the van der Waals radii and H…H contacts have been omitted. Thermal ellipsoids have been drawn at the 50% probability level. Only the central sodium atoms have been labelled.

Characterization Data of 1a

Sum Formula	Sigma	m/z	Err [ppm]	Mean Err [ppm]	rdb	N Rule	e⁻
C 38 H 46 N 5 P 2	0.06	634.3223	-0.31	-0.37	19.50	ok	even

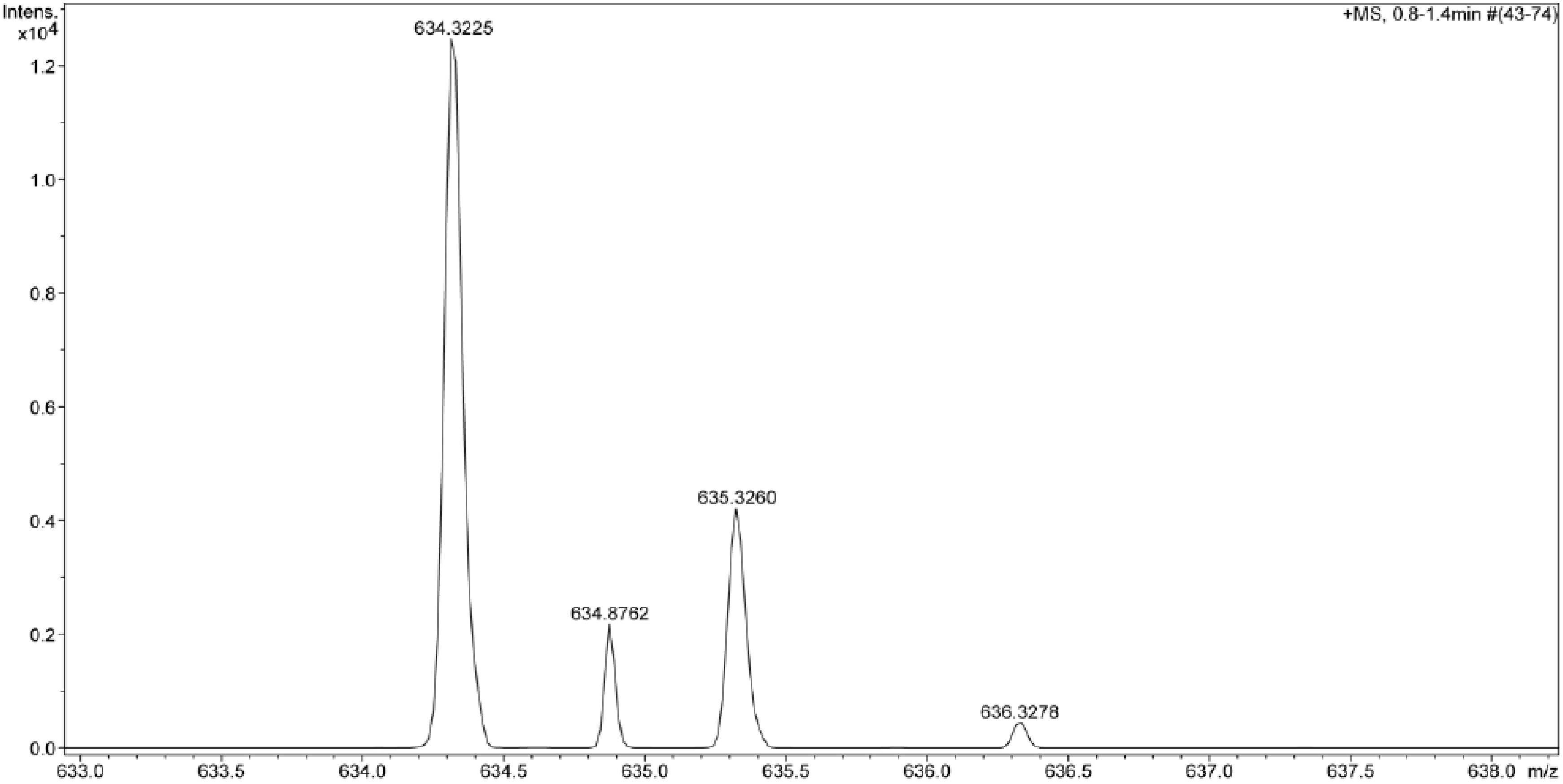

Figure S57: HRMS of **1a** (Spectrum also shows **2a** at 635.3260).

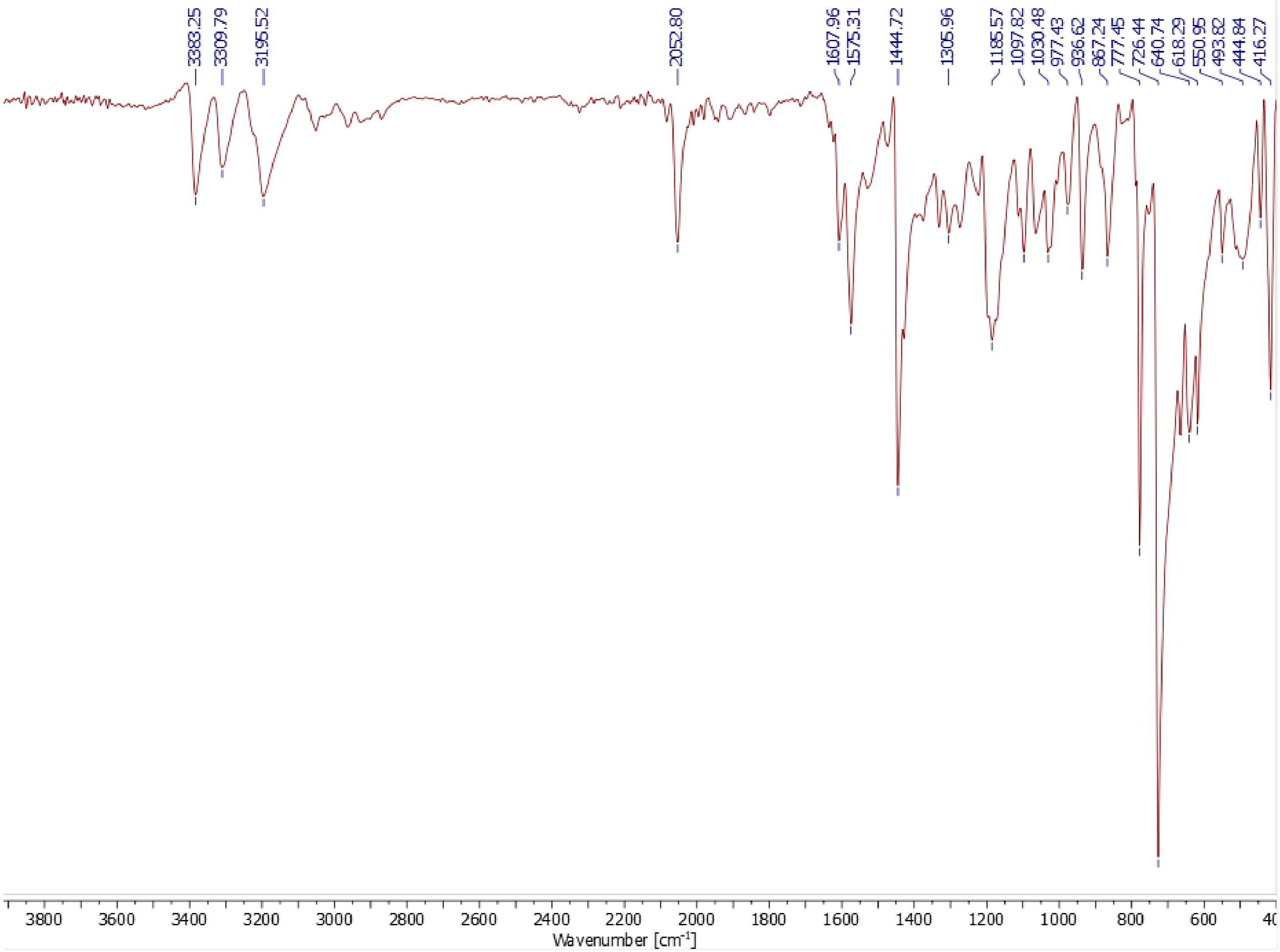

Figure S58: IR Spectrum (ATR) of **1a**.

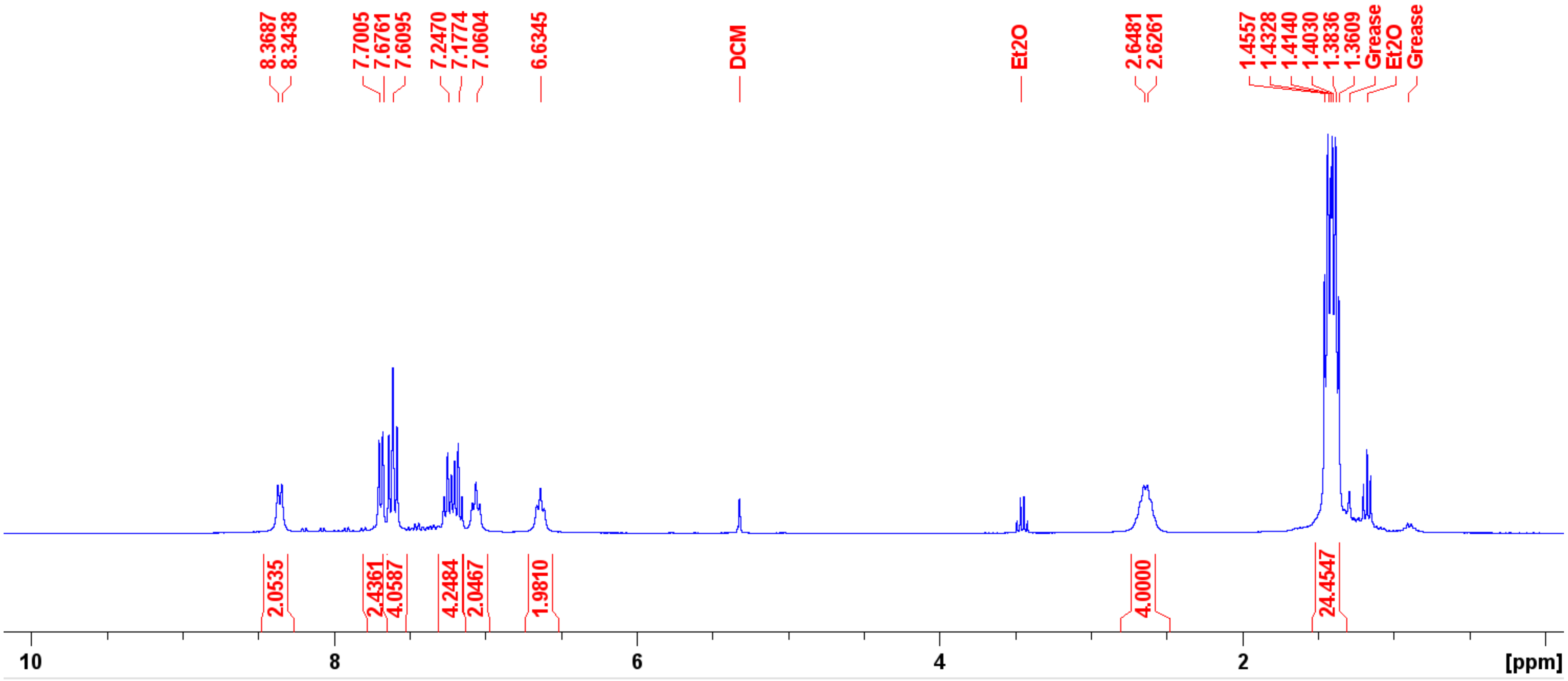

Figure S59:^{1}H NMR (300 MHz, CD_2Cl_2) spectrum of **1a**.

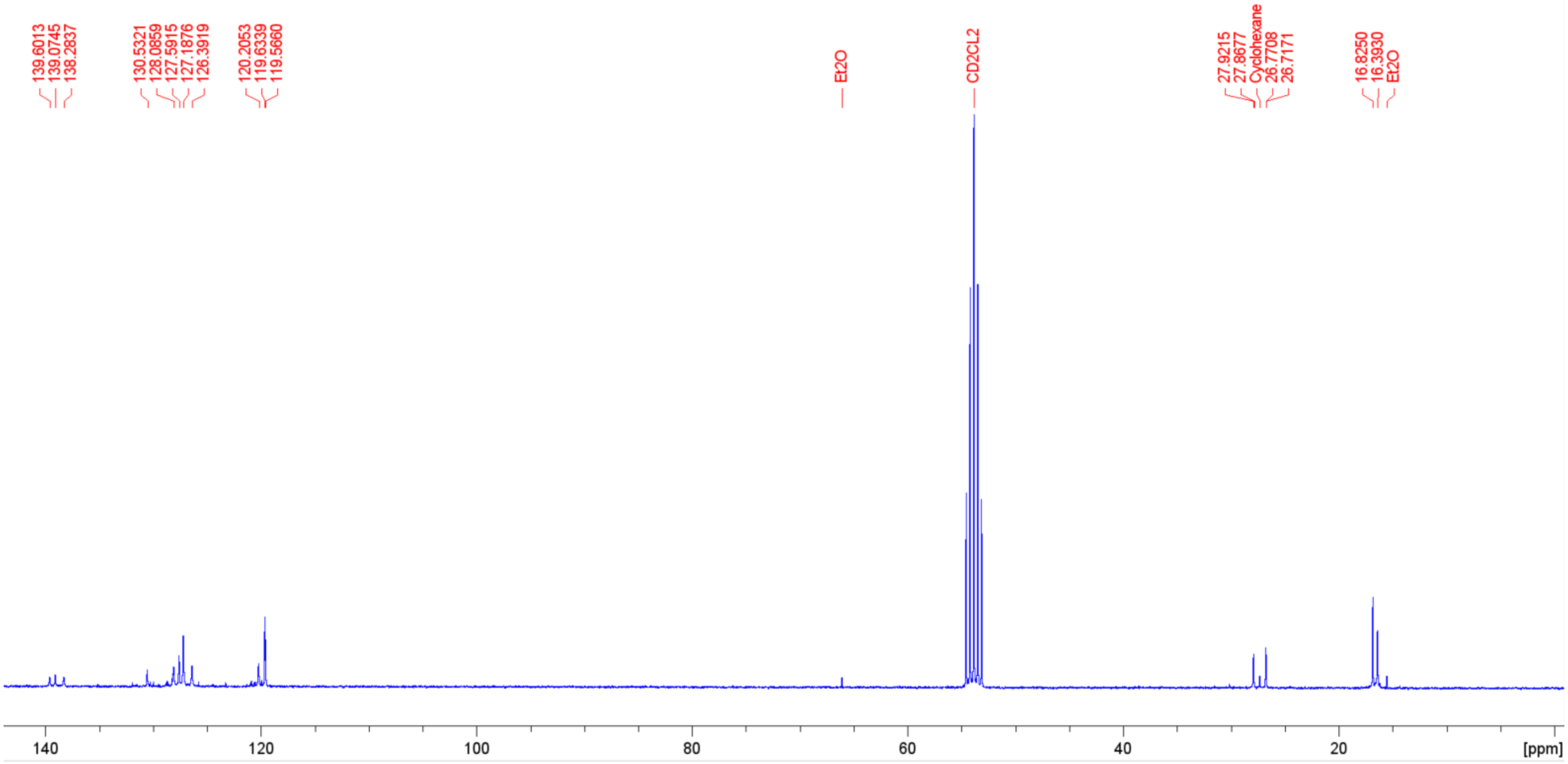

Figure S60: $^{13}C\{^{1}H\}$ NMR (75 MHz, CD_2Cl_2) spectrum of **1a**.

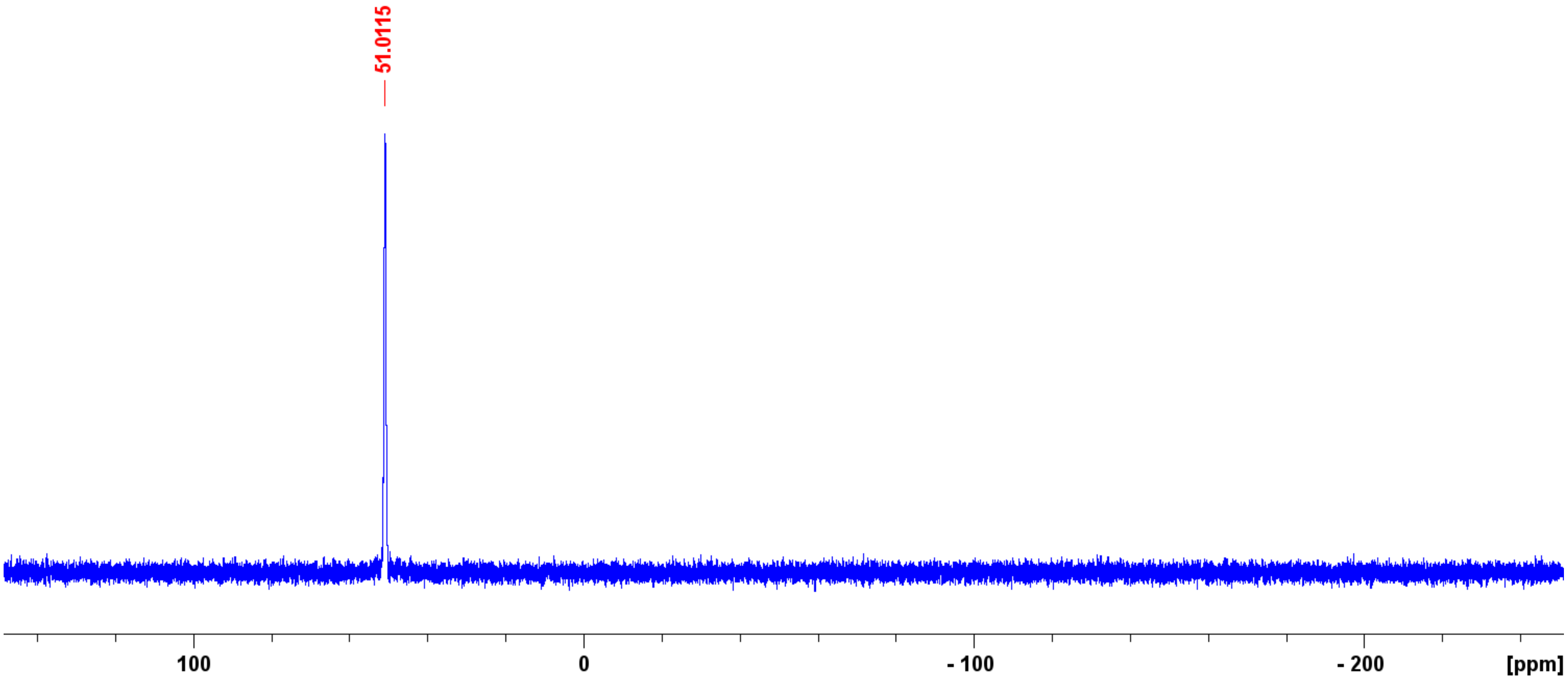

Figure S61: $^{31}P\{^1H\}$ NMR (121 MHz, CD_2Cl_2) spectrum of **1a**.

Characterization Data of 1b

Sum Formula	Sigma	m/z	Err [ppm]	Mean Err [ppm]	rdb	N Rule	e^-
C 50 H 38 N 5 P 2	0.10	770.2597	2.12	2.31	35.50	ok	even

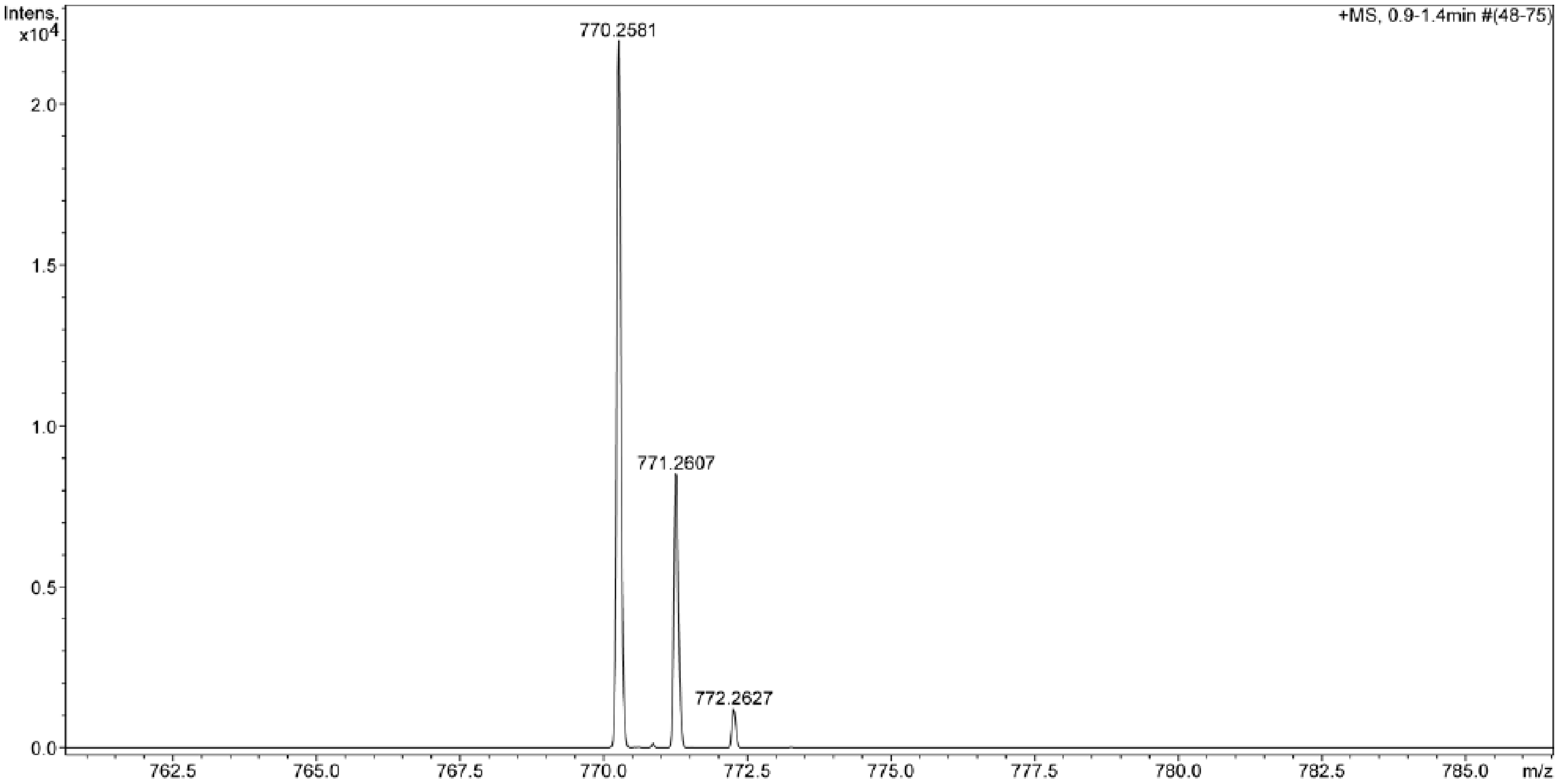

Figure S62: HRMS of **1b**.

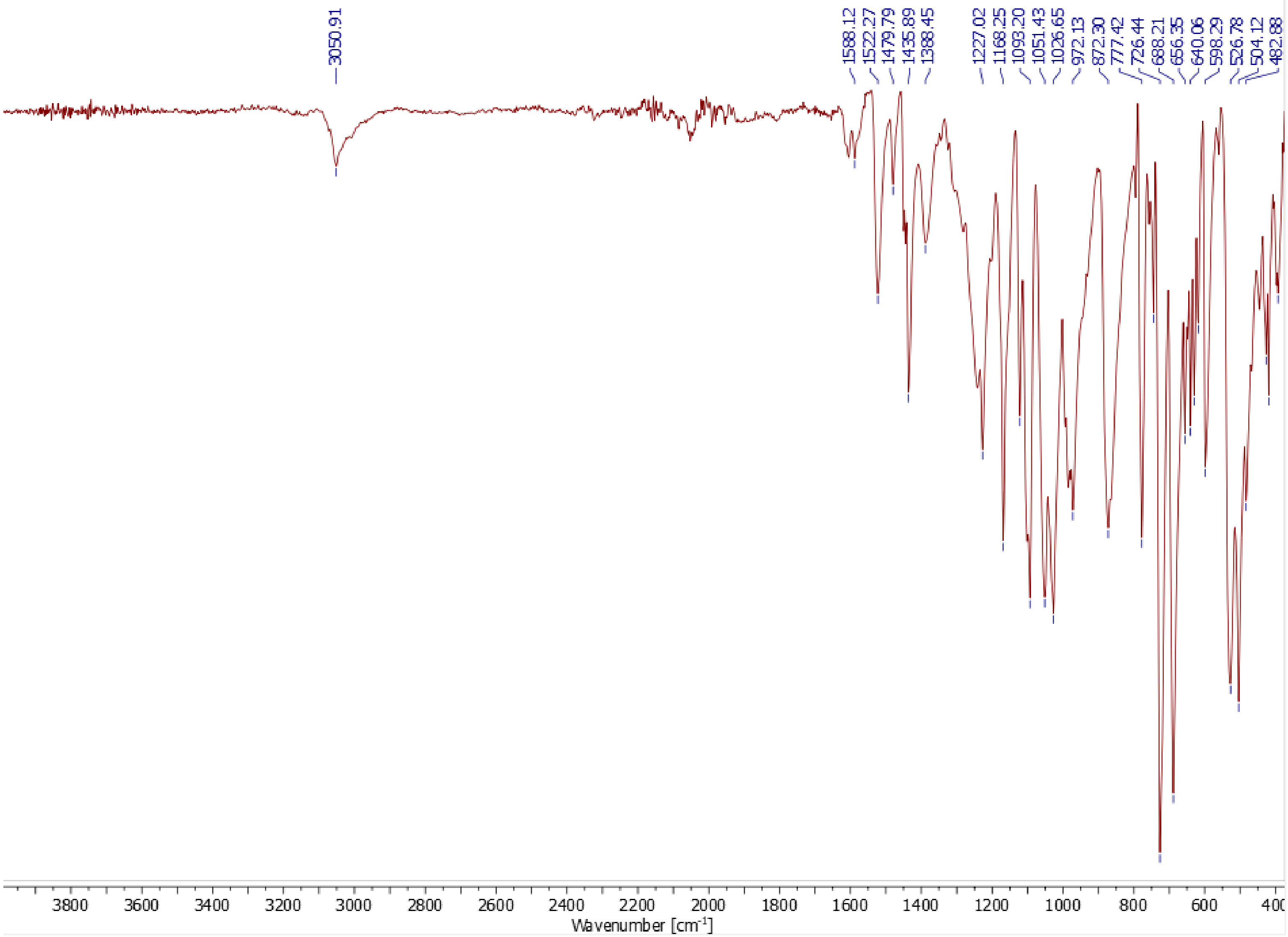

Figure S63: IR Spectrum (ATR) of **1b**.

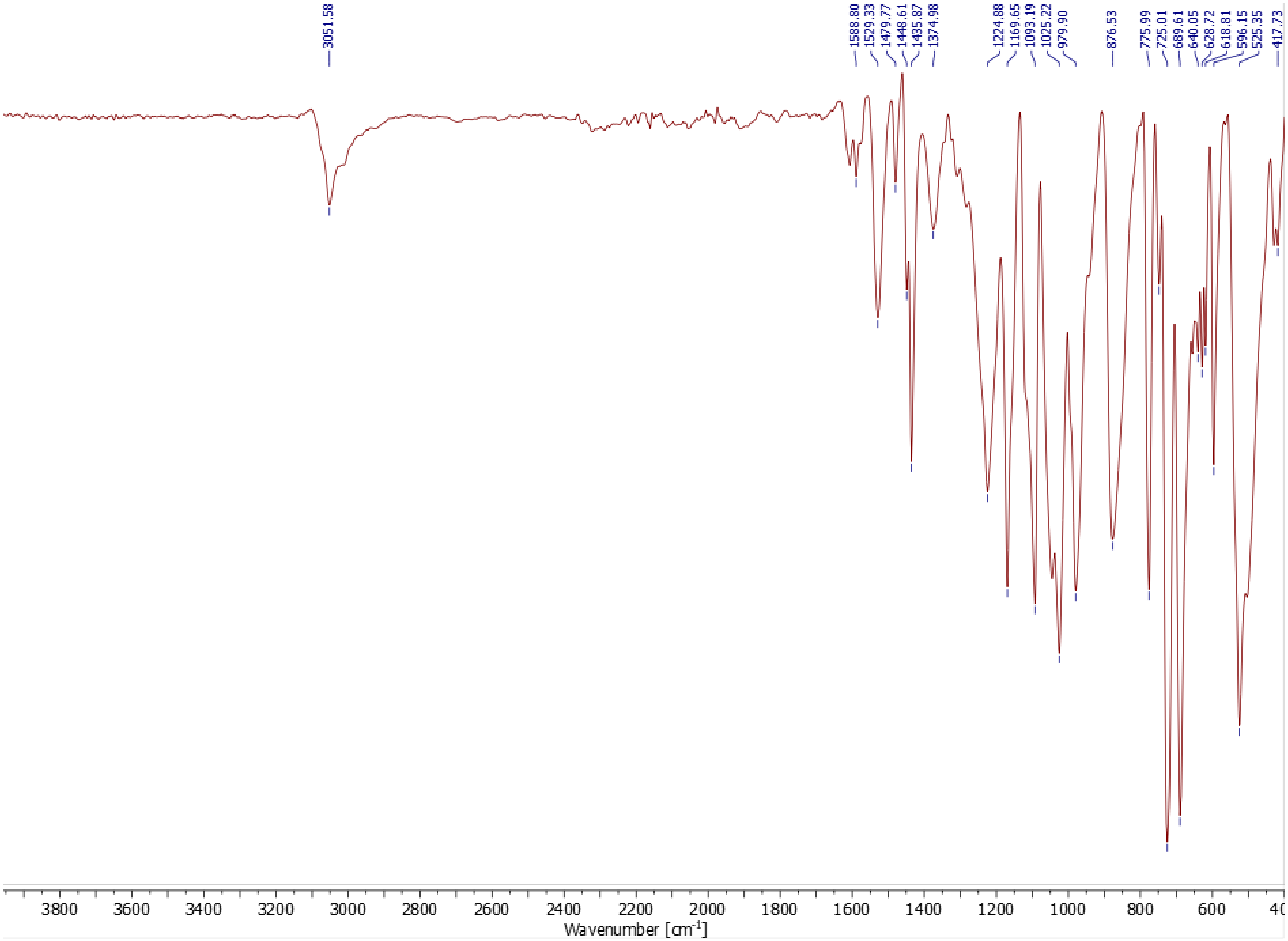

Figure S64: IR spectrum (ATR) of **1b** after heating at 180 °C for 5 h.

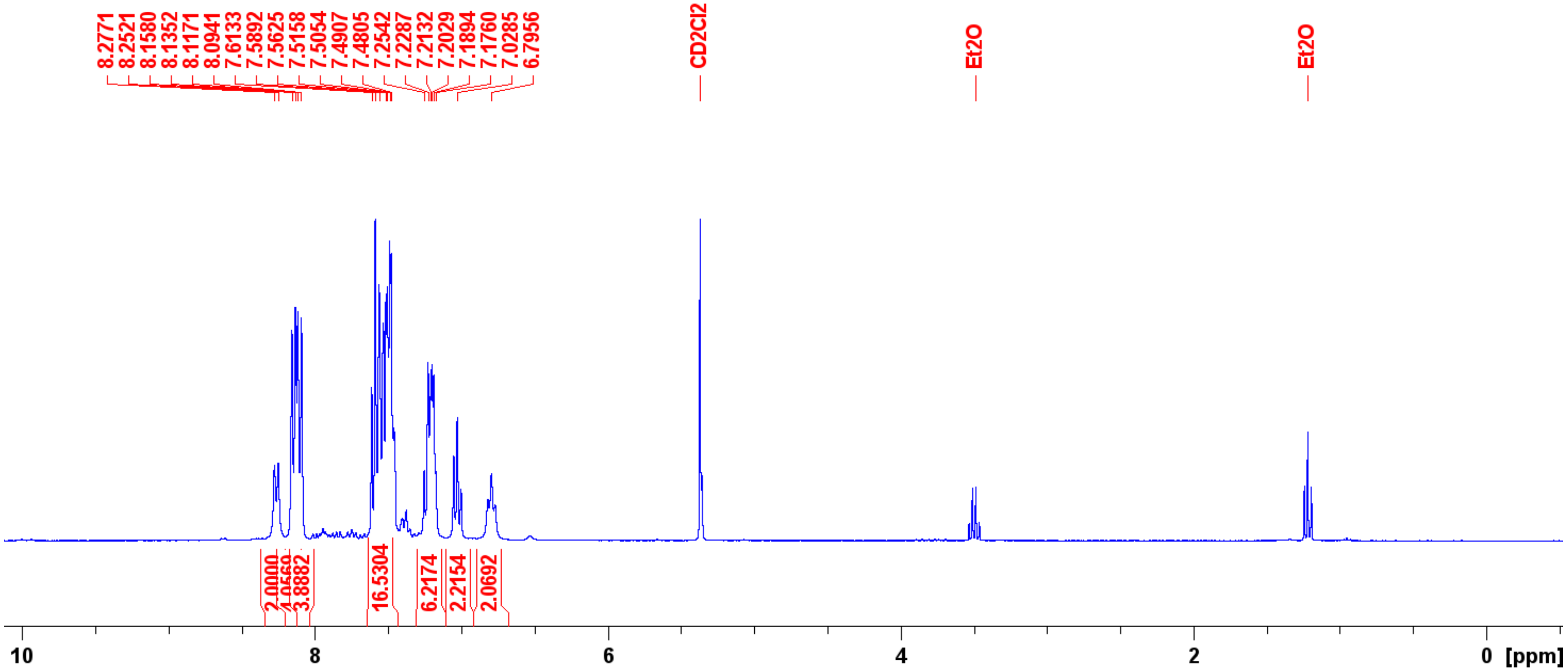

Figure S65: ^{1}H NMR (300 MHz, CD_2Cl_2) spectrum of **1b**.

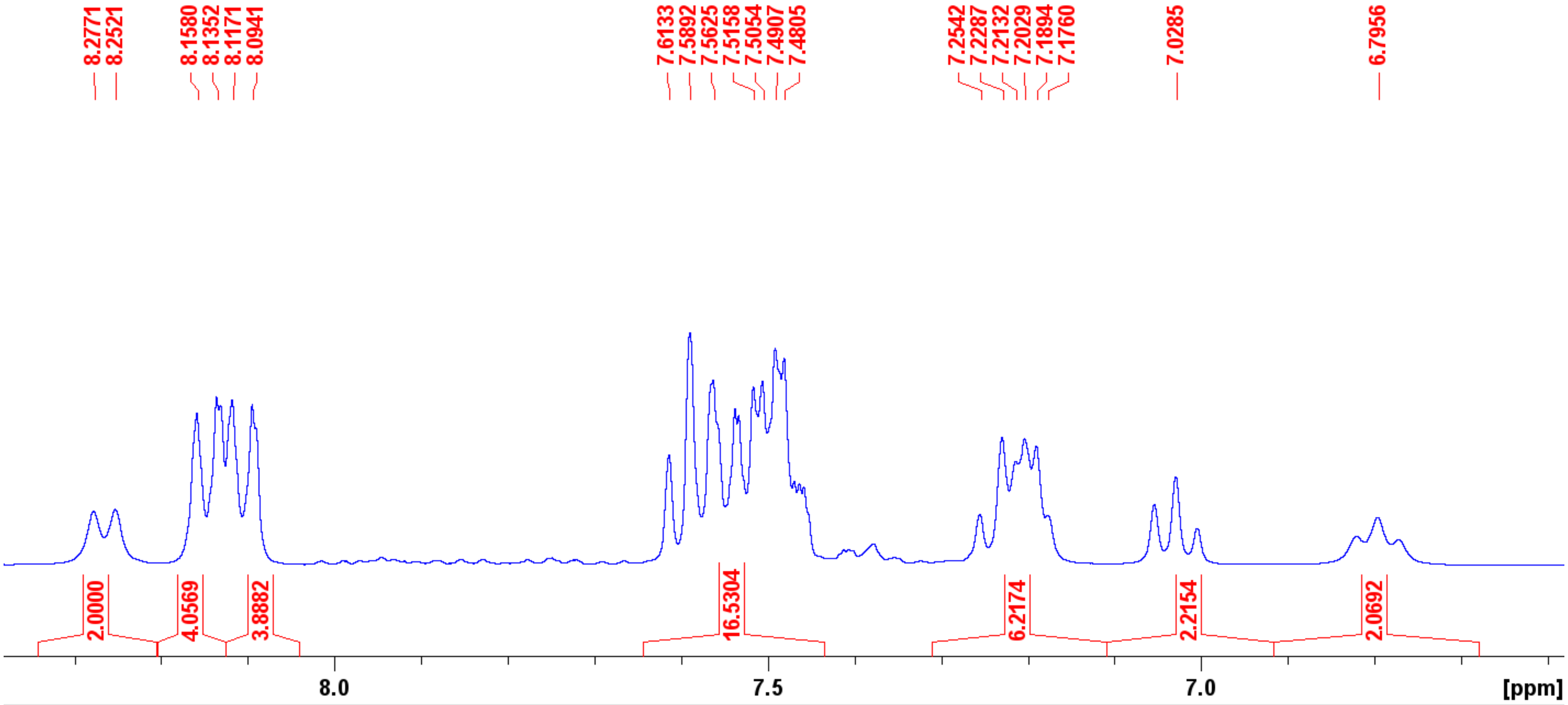

Figure S66: ^{1}H NMR (300 MHz, CD_2Cl_2) spectrum of **1b**, expansion of the aromatic region.

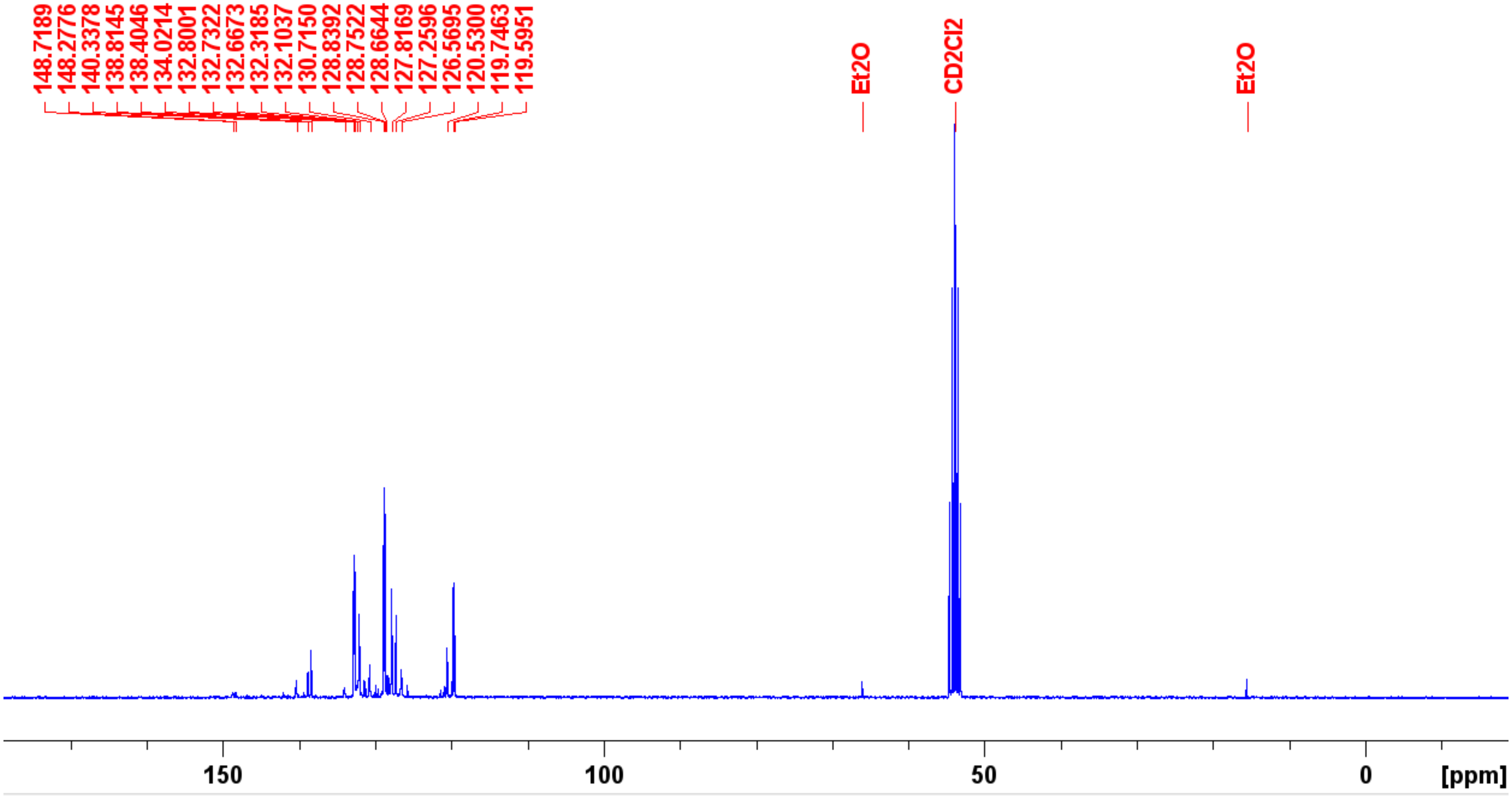

Figure S67: $^{13}C\{1H\}$ NMR (75 MHz, CD_2Cl_2) spectrum of **1b**.

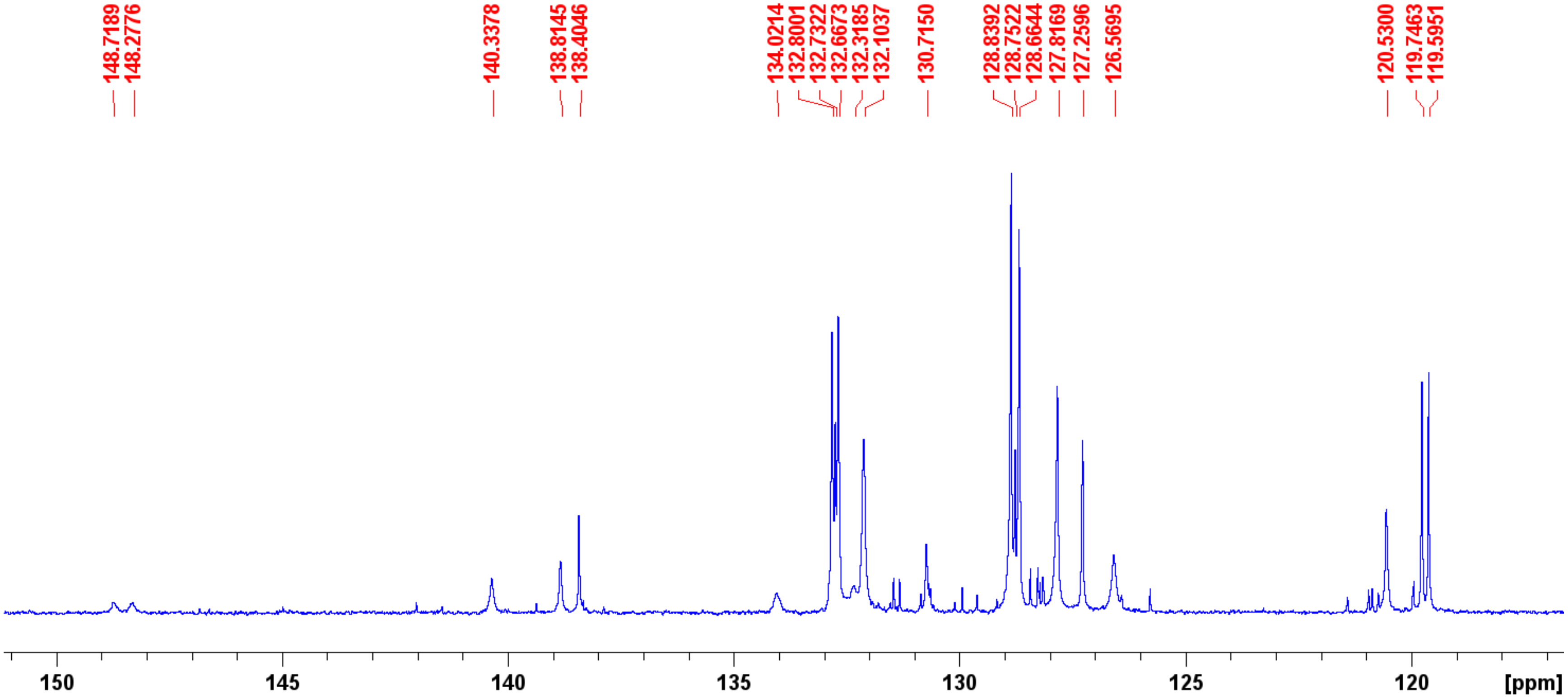

Figure S68: $^{13}C\{^1H\}$ NMR (75 MHz, CD_2Cl_2) spectrum of **1b**, expansion of the aromatic region,

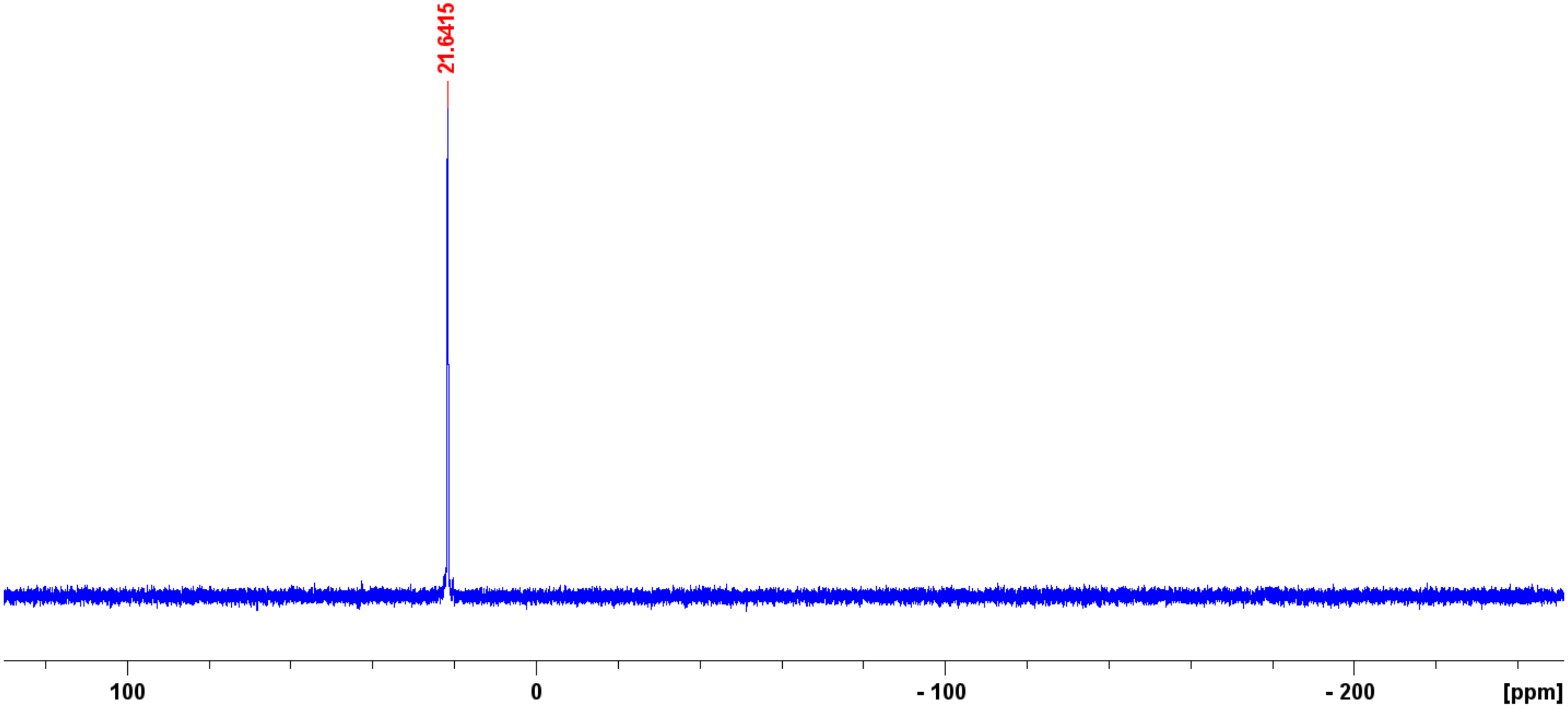

Figure S69: $^{31}P\{^1H\}$ NMR (121 MHz, CD_2Cl_2) spectrum of **1b**.

NMR Data before and after heating 1b in DMSO solution

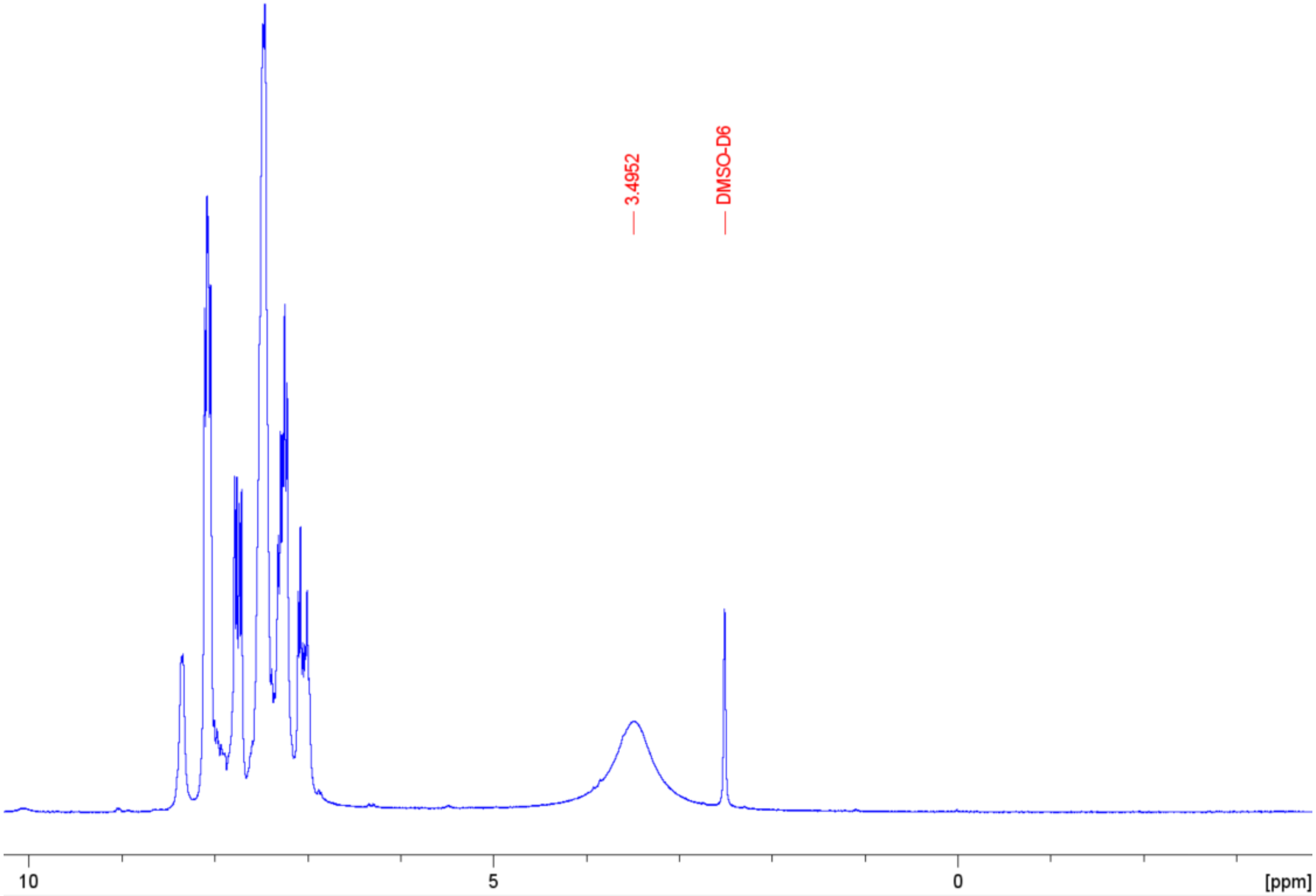

Figure S70: ^{1}H NMR (300 MHz, DMSO-D$_6$) spectrum of **1b** prior to heating.

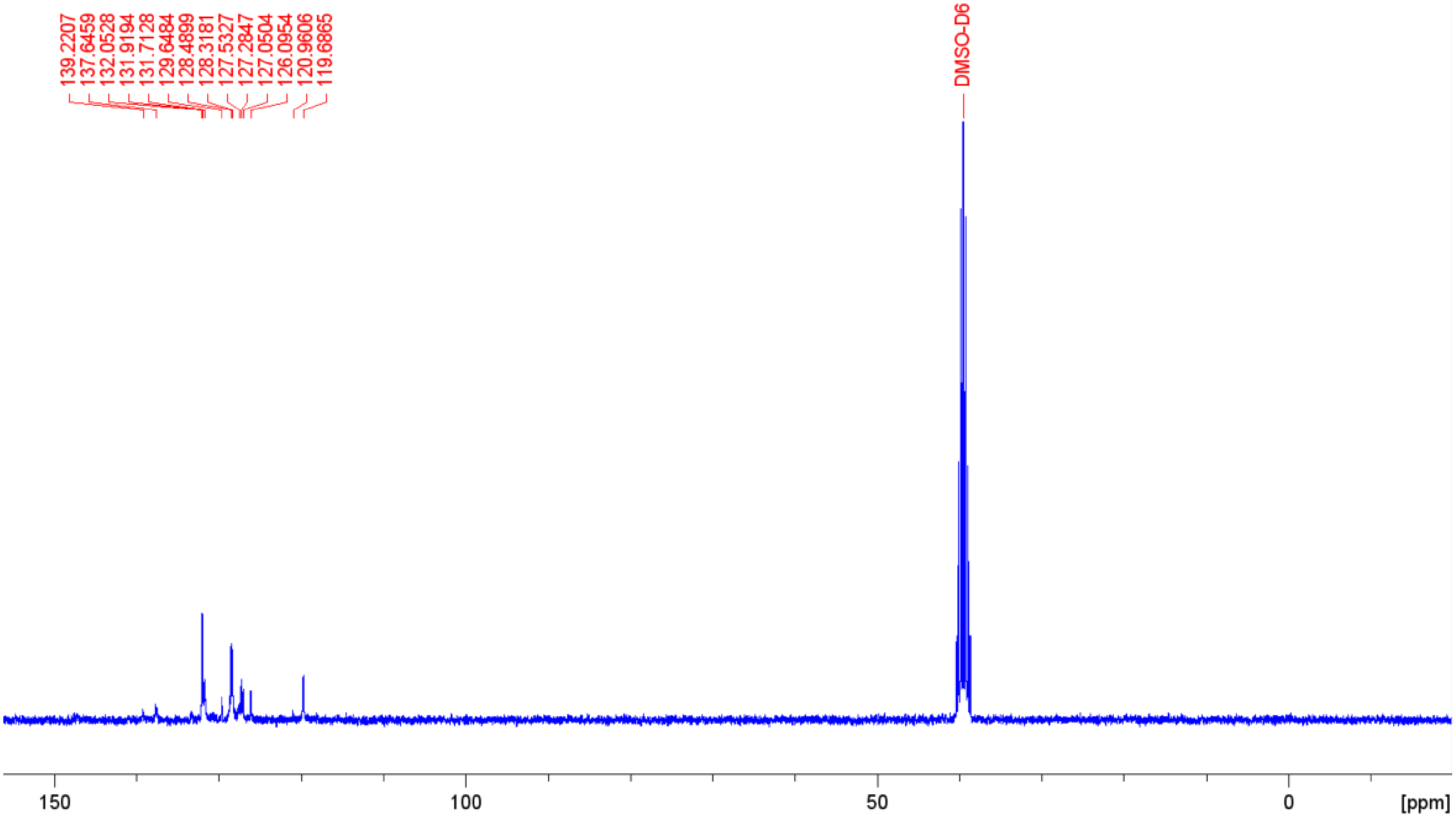

Figure S71: $^{13}C\{^1H\}$ NMR (75 MHz, DMSO-D$_6$) spectrum of **1b** prior to heating.

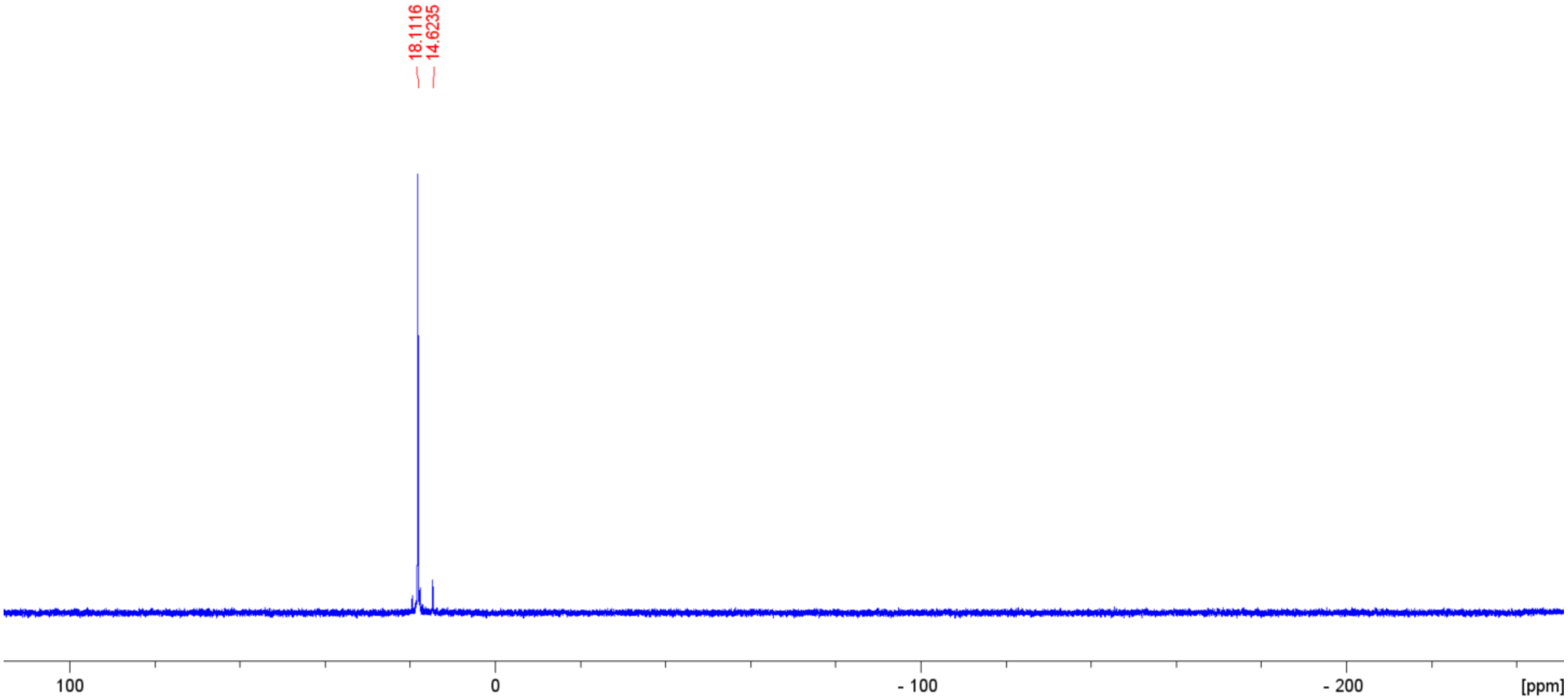

Figure S72: $^{31}P\{^{1}H\}$ NMR (121 MHz, DMSO-D_6) spectrum of **1b** prior to heating.

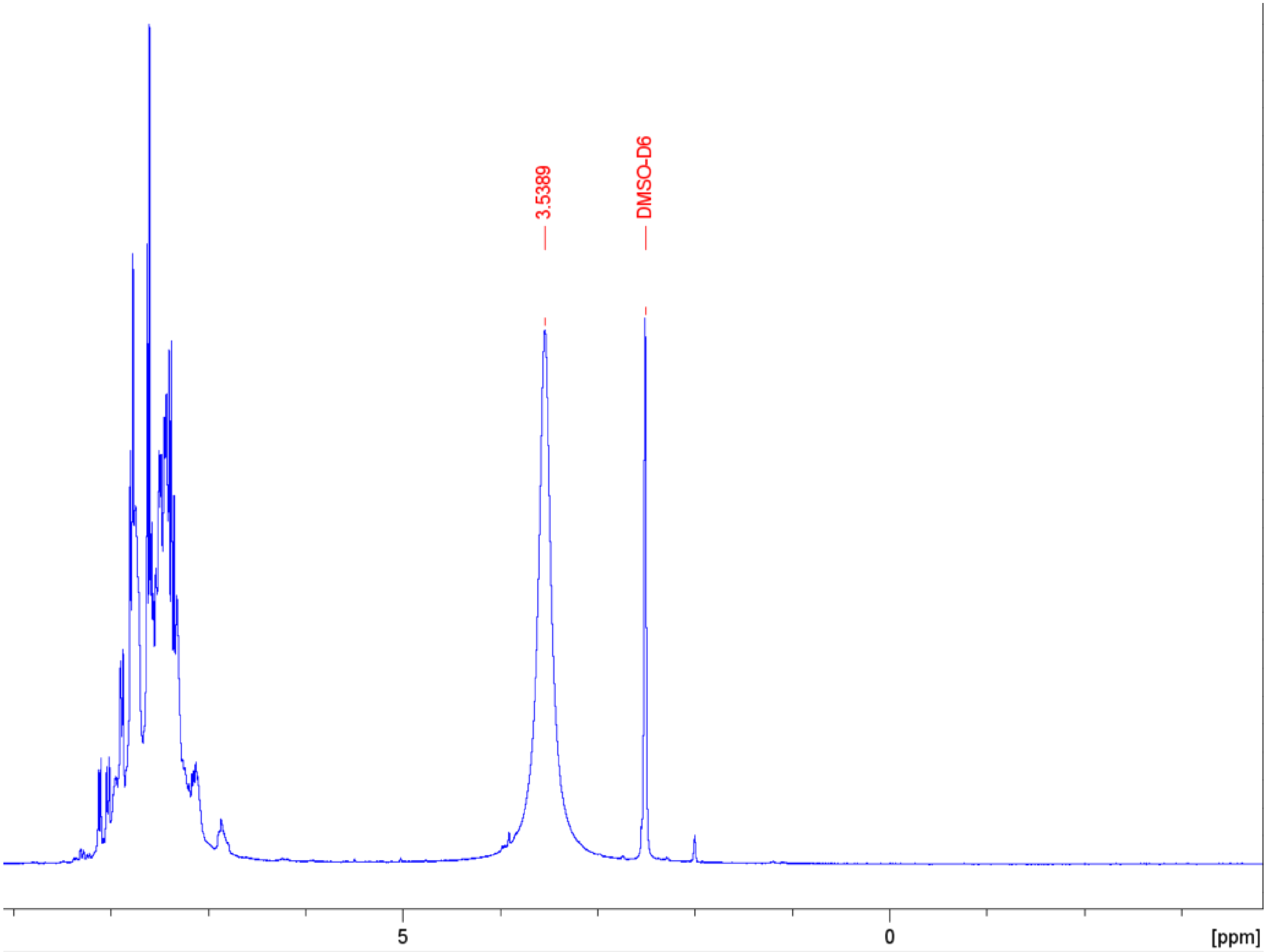

Figure S73: ^{1}H NMR (300 MHz, DMSO-D$_6$) spectrum of **1b** after heating at 180 °C for 5 h.

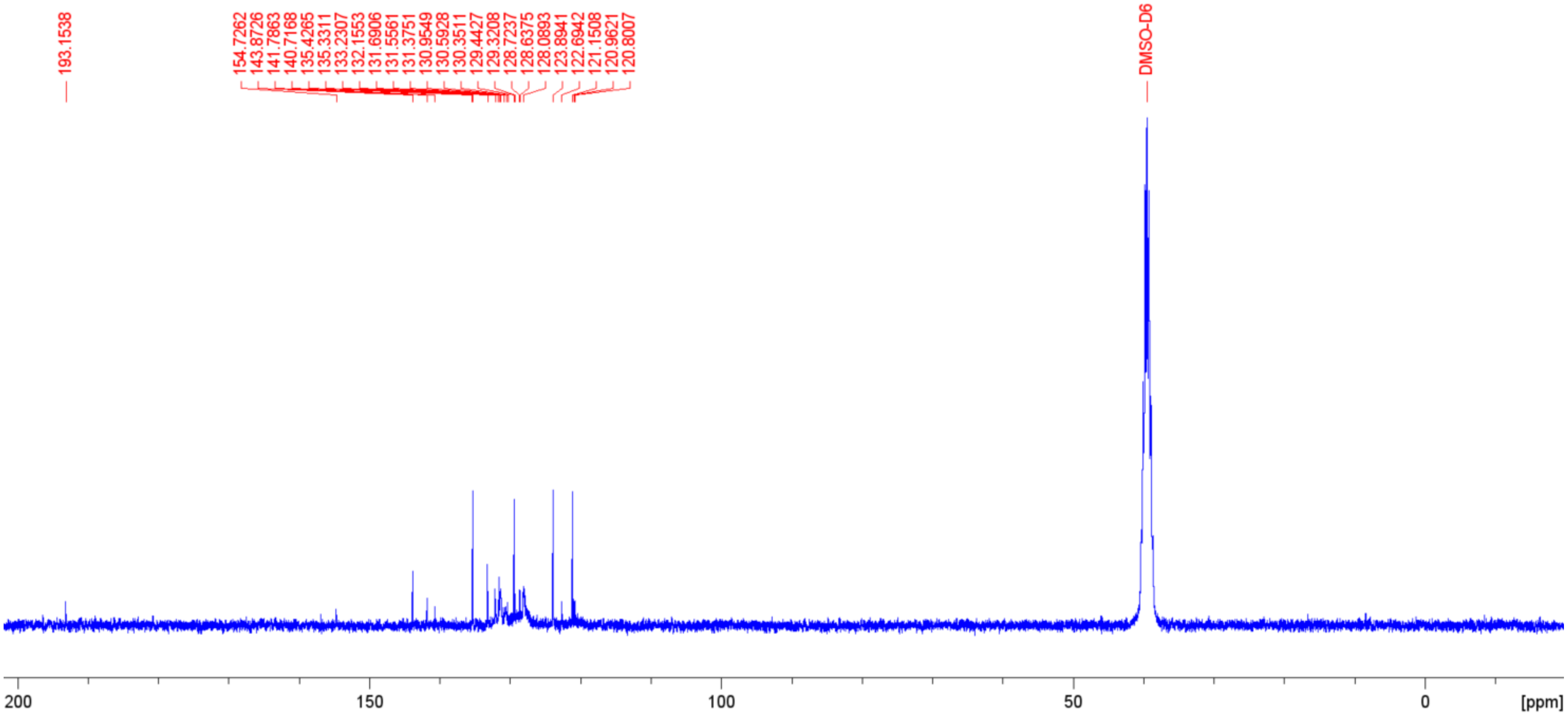

Figure S74: $^{13}C\{^{1}H\}$ NMR (75 MHz, DMSO-D_6) spectrum of **1b** after heating at 180 °C for 5 h.

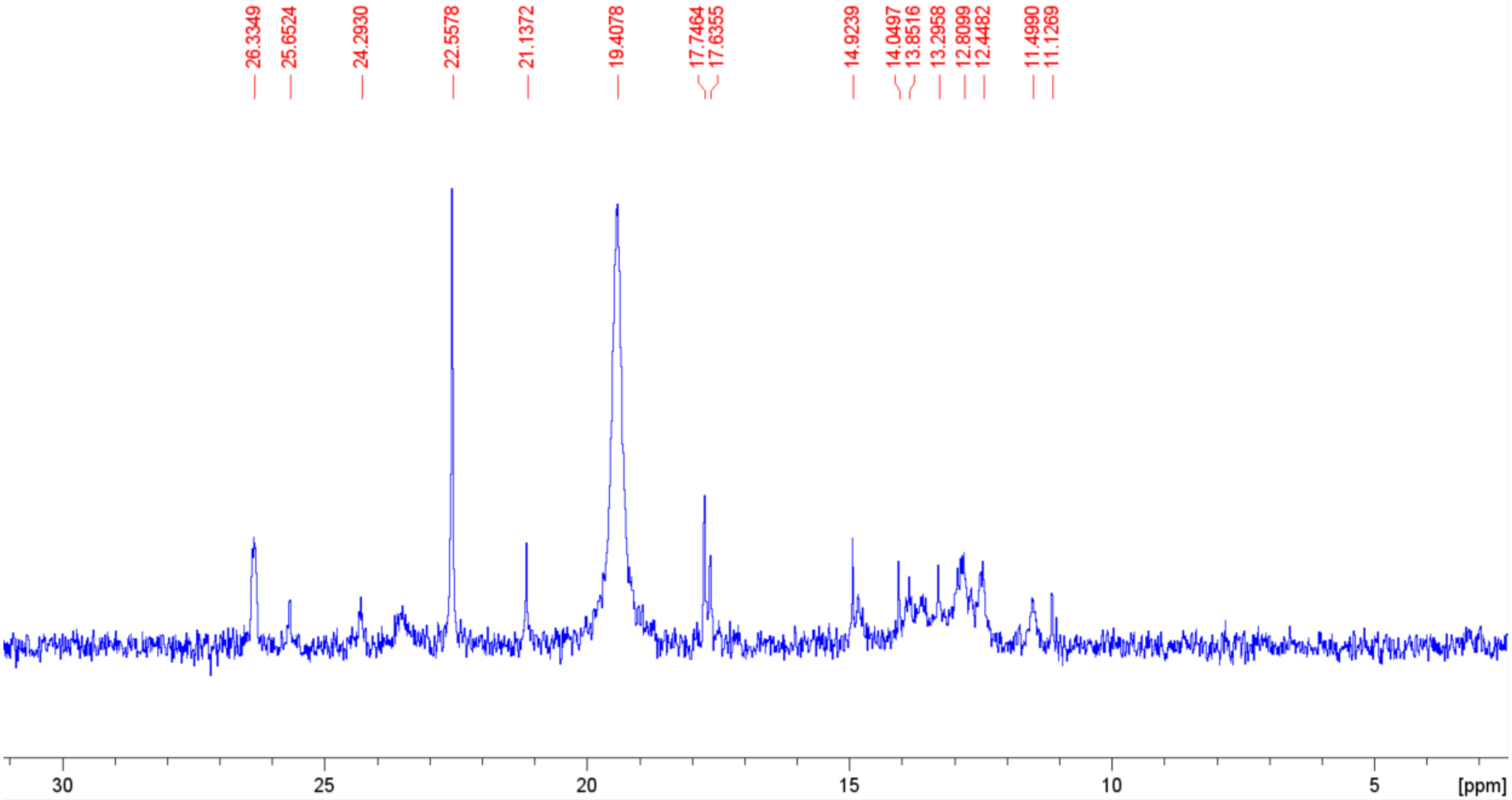

Figure S75: $^{31}P\{^1H\}$ NMR (121 MHz, DMSO-D$_6$) spectrum of **1b** after heating at 180 °C for 5 h.

Characterization Data of 2b

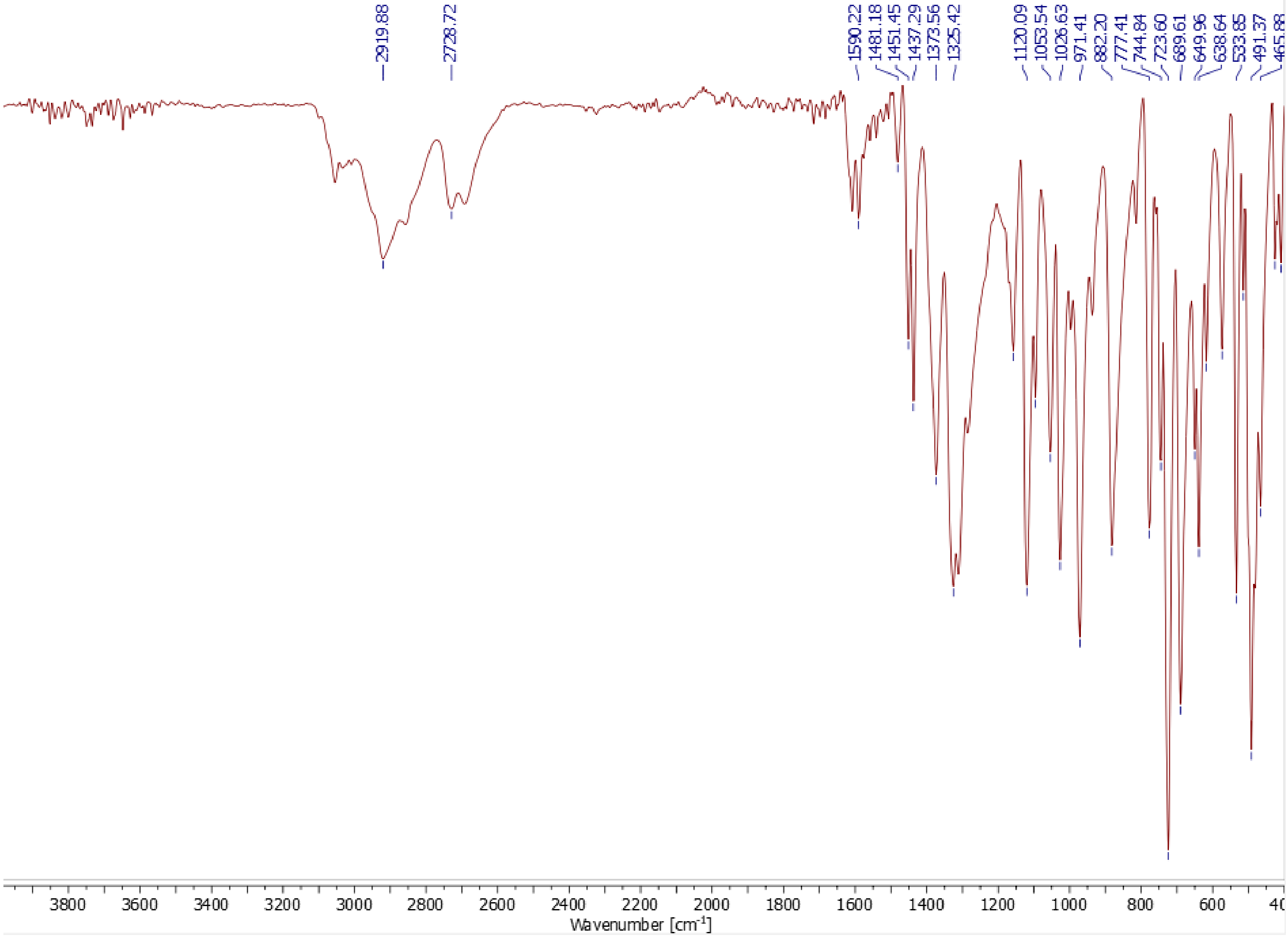

Figure S76: IR Spectrum (ATR) of **2b**.

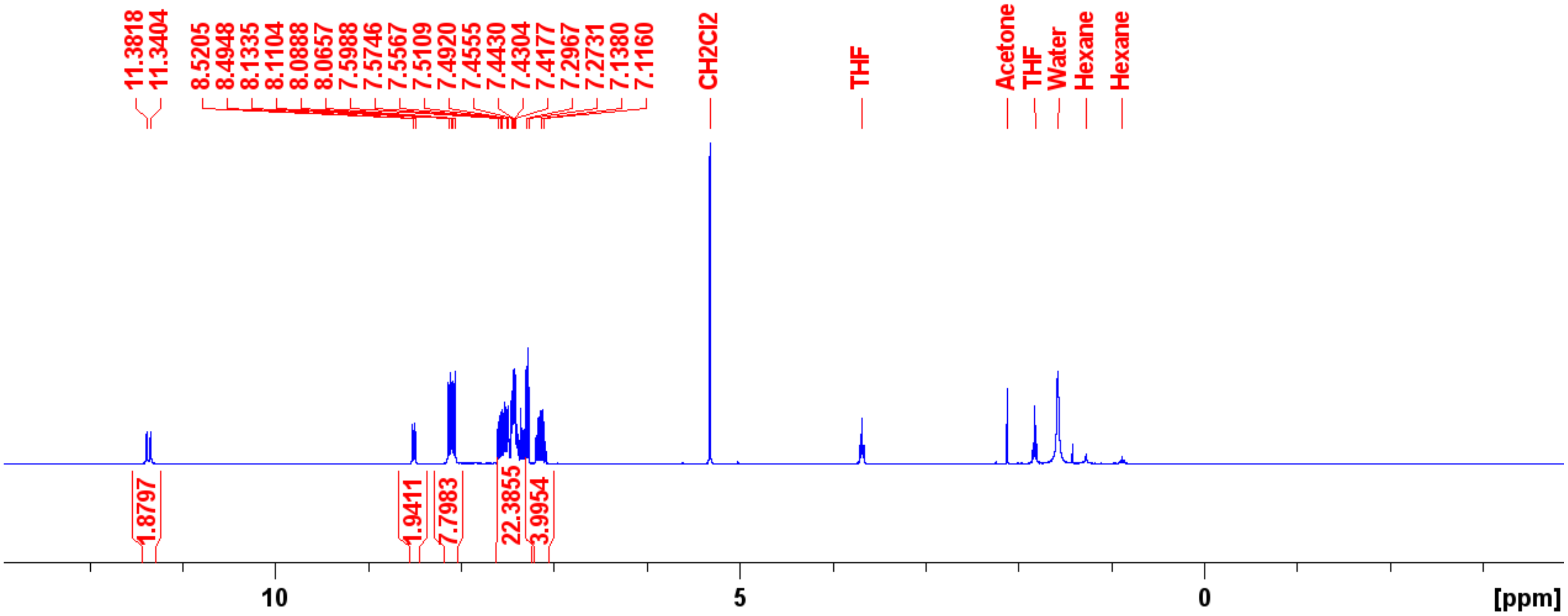

Figure S77:^{1}H NMR (300 MHz, CD_2Cl_2) spectrum of **2b**.

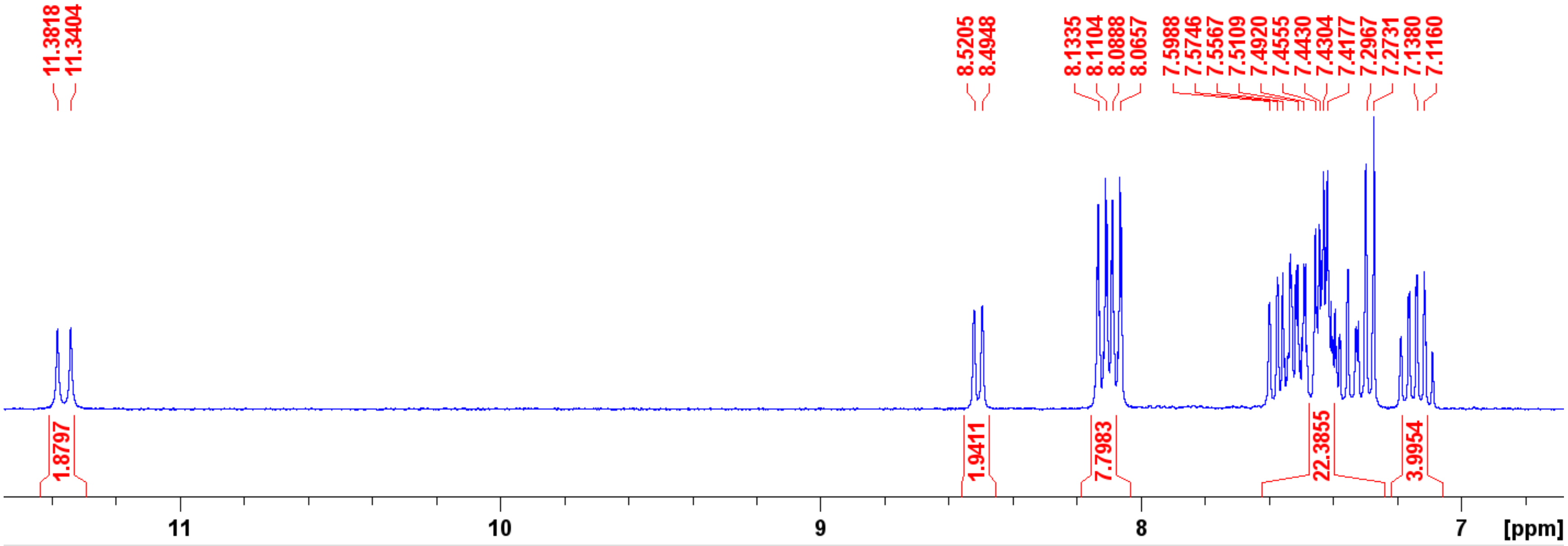

Figure S78: ^{1}H NMR (300 MHz, CD_2Cl_2) spectrum of **2b**, expansion of aromatic region.

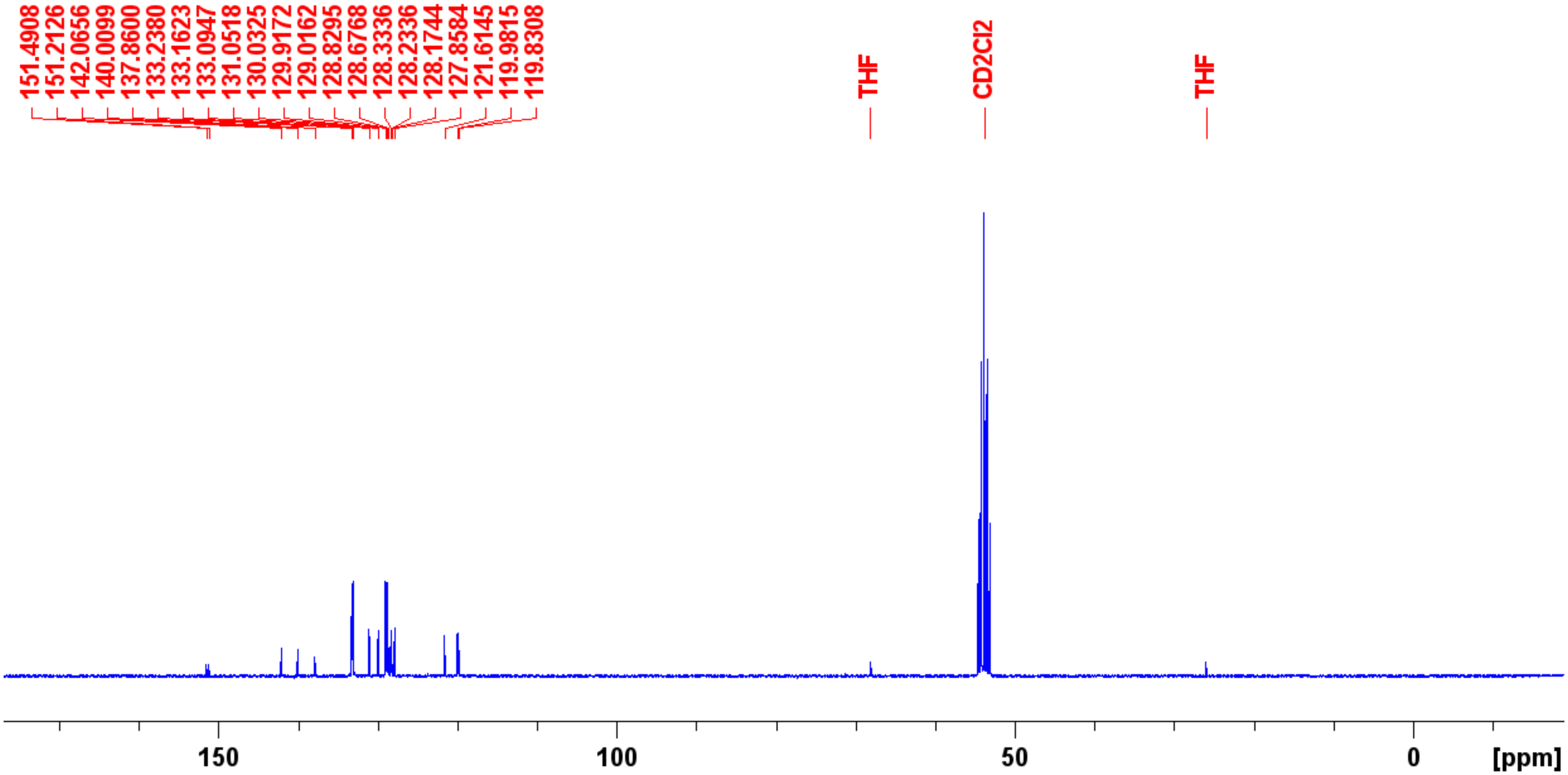

Figure S79: $^{13}C\{^{1}H\}$ NMR (75 MHz, CD_2Cl_2) spectrum of **2b**.

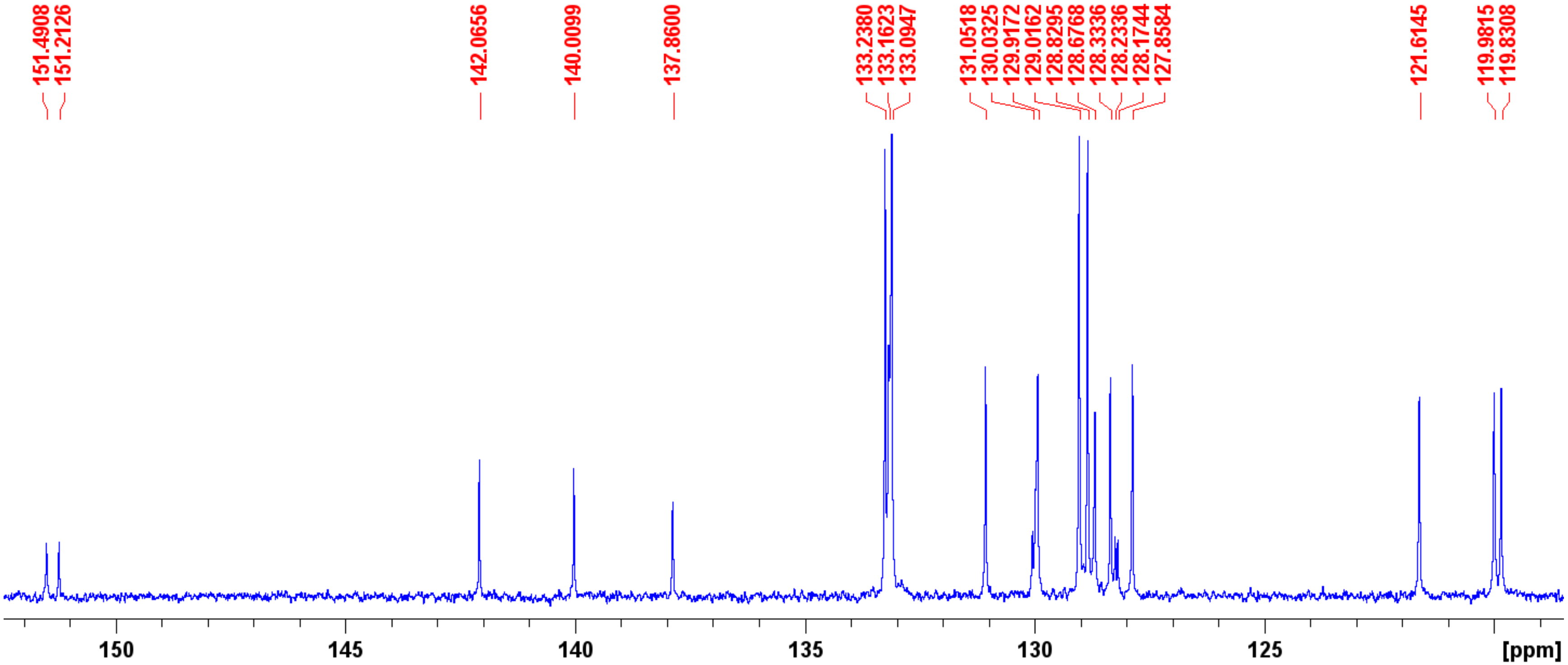

Figure S80: $^{13}C\{^1H\}$ NMR (75 MHz, CD_2Cl_2) spectrum of **2b**, expansion of aromatic region.

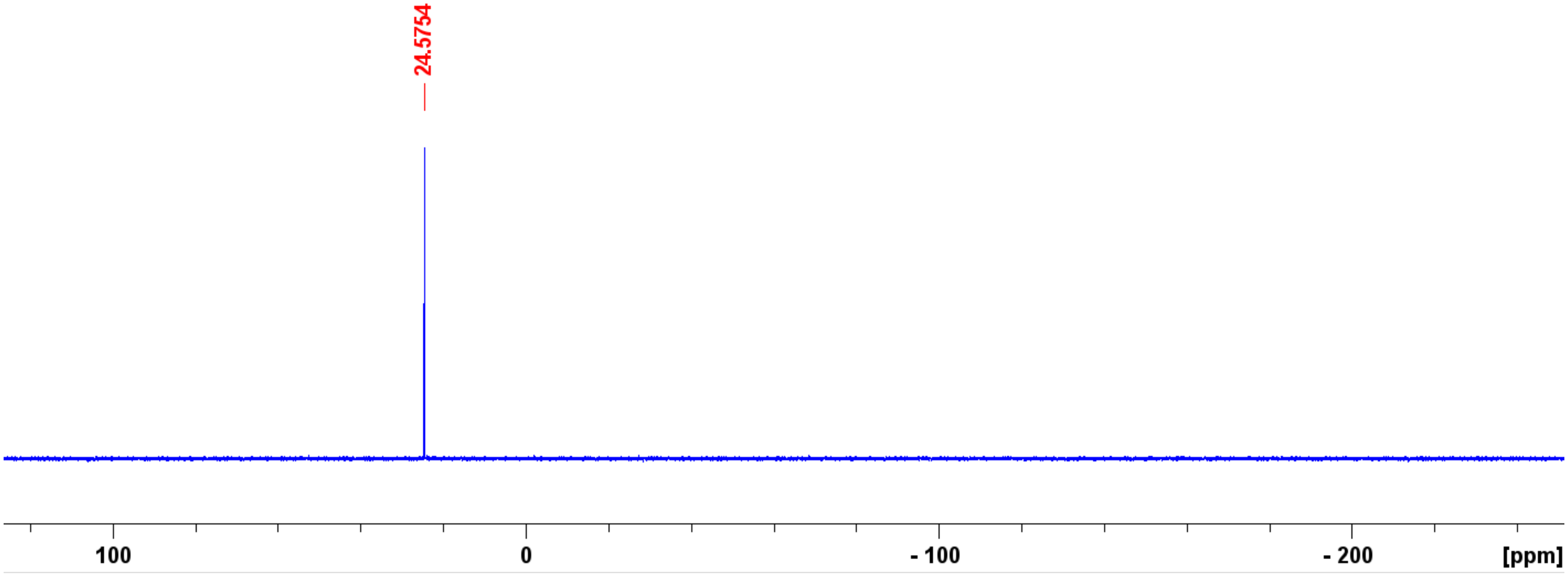

Figure S81: $^{31}P\{^1H\}$ NMR (121 MHz, CD_2Cl_2) spectrum of **2b**.

Characterization Data of 3

Sum Formula	Sigma	m/z	Err [ppm]	Mean Err [ppm]	rdb	N Rule	e⁻
C 37 H 30 N 3 O 1 P 2	0.13	594.1859	-2.28	-2.03	25.50	ok	even

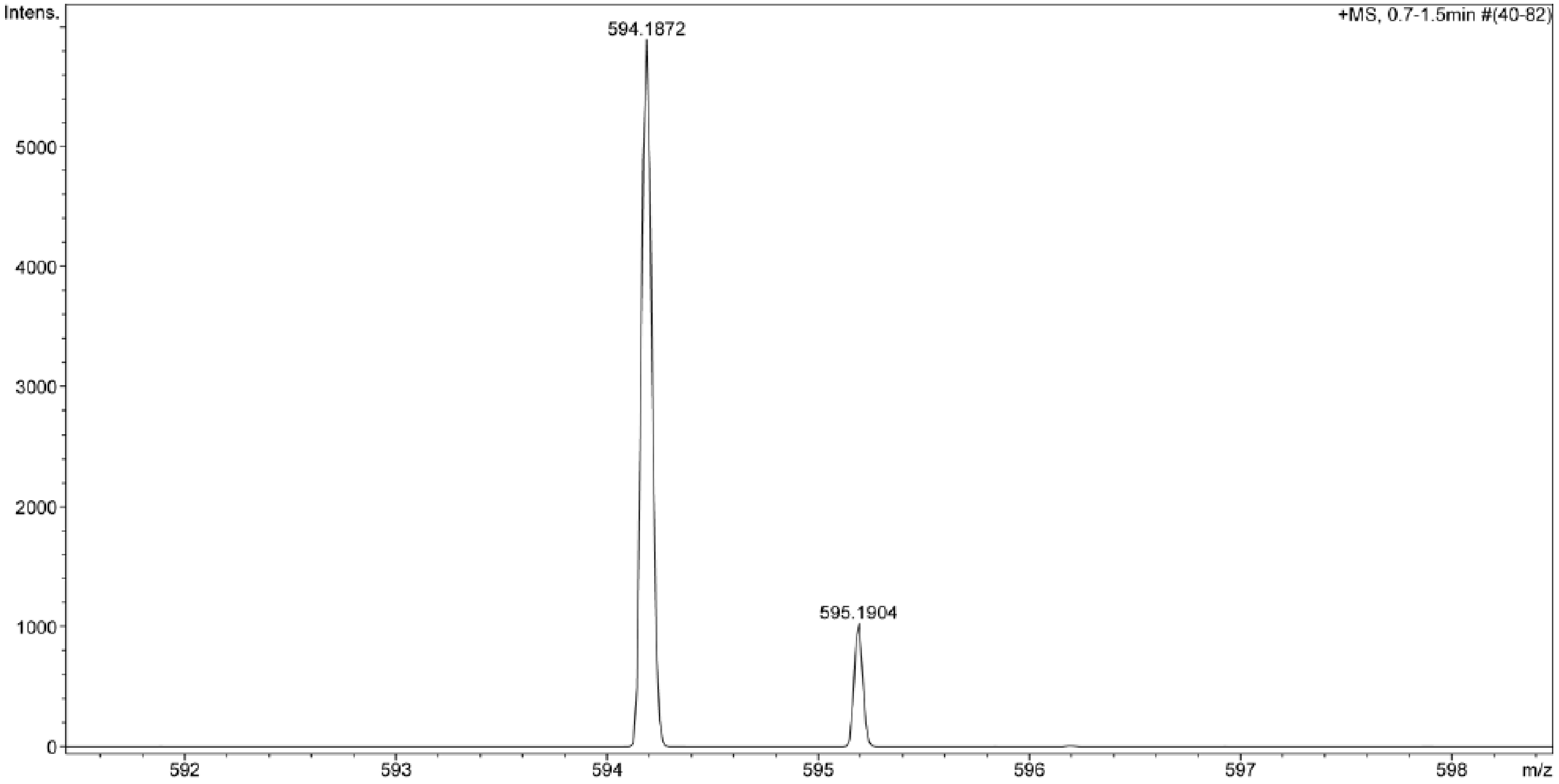

Figure S82: HRMS of **3**.

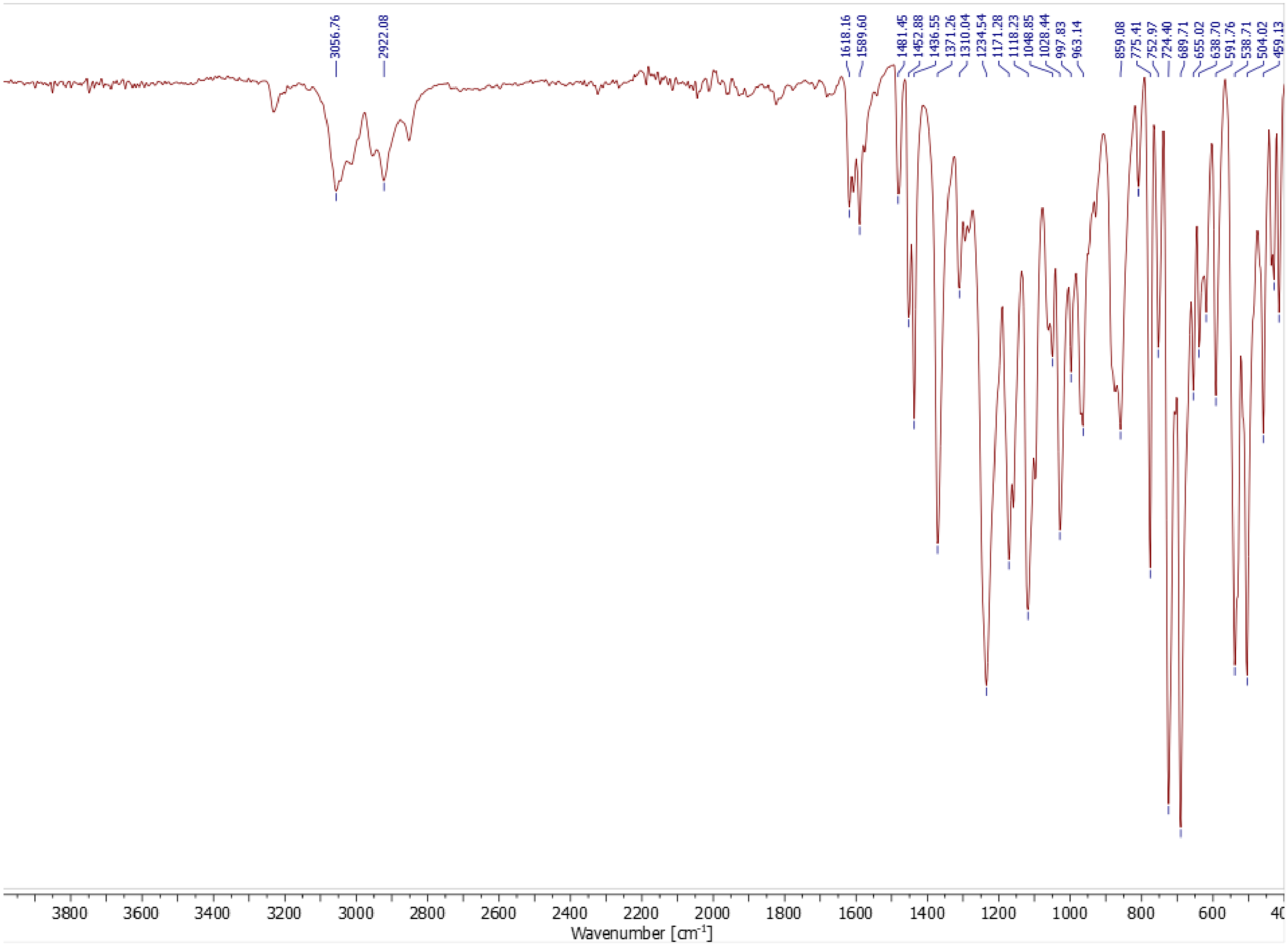

Figure S83: IR Spectrum (ATR) of **3**.

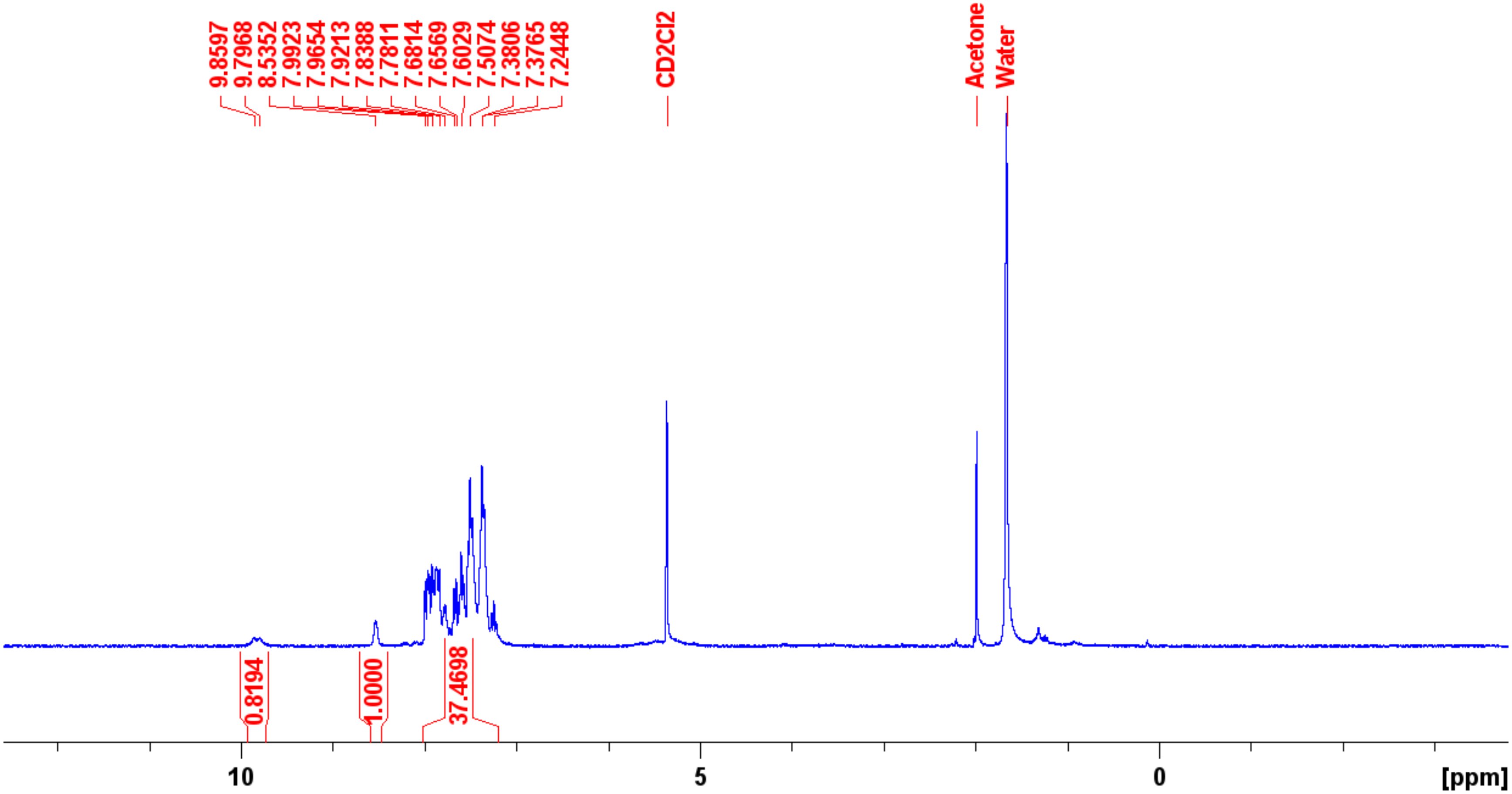

Figure S84: ^{1}H NMR (300 MHz, CD_2Cl_2) spectrum of **3**.

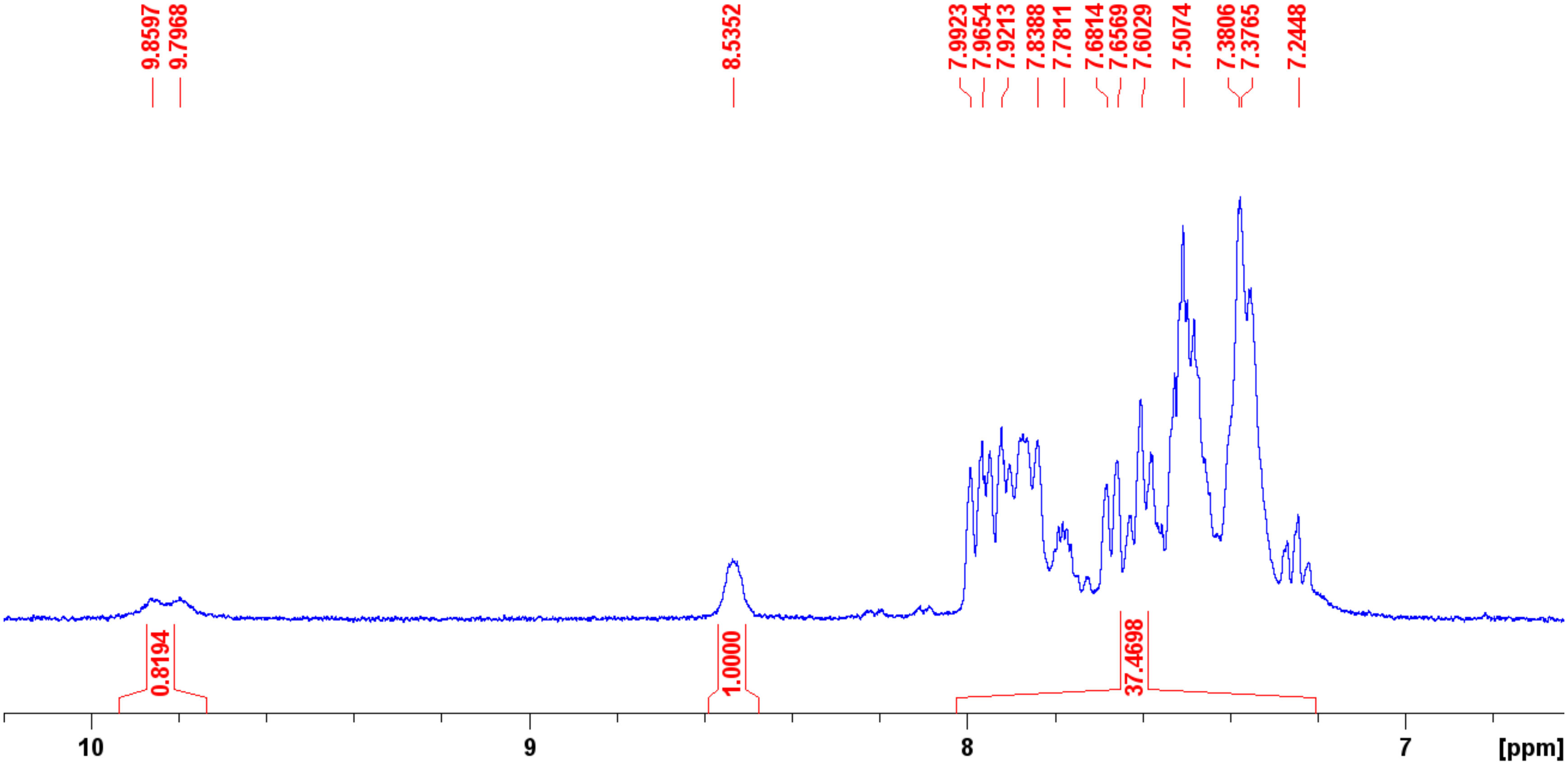

Figure S85: ^{1}H NMR (300 MHz, CD_2Cl_2) spectrum of **3**, expansion of aromatic region.

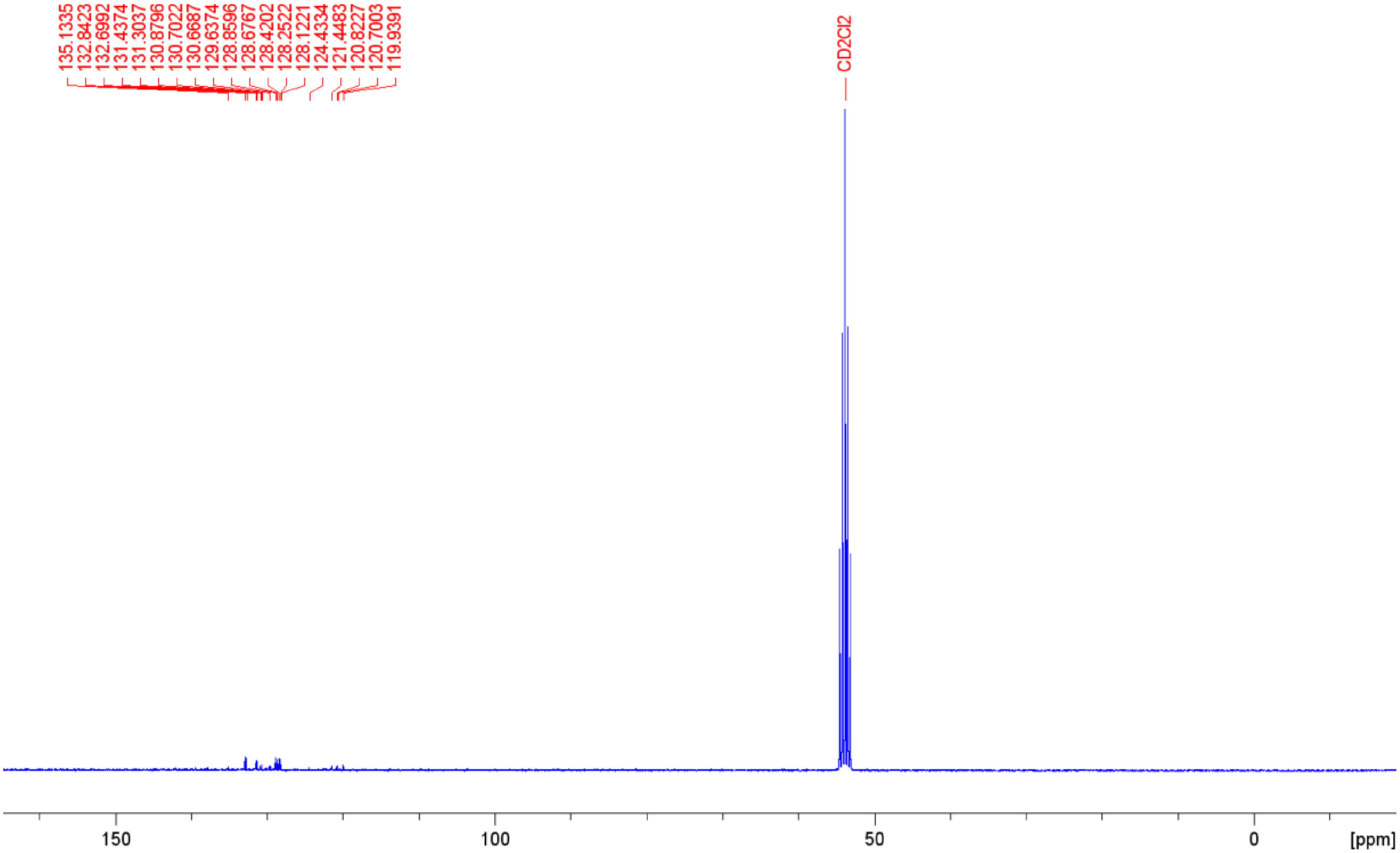

Figure S86: $^{13}C\{^1H\}$ NMR (75 MHz, CD_2Cl_2) spectrum of **3**.

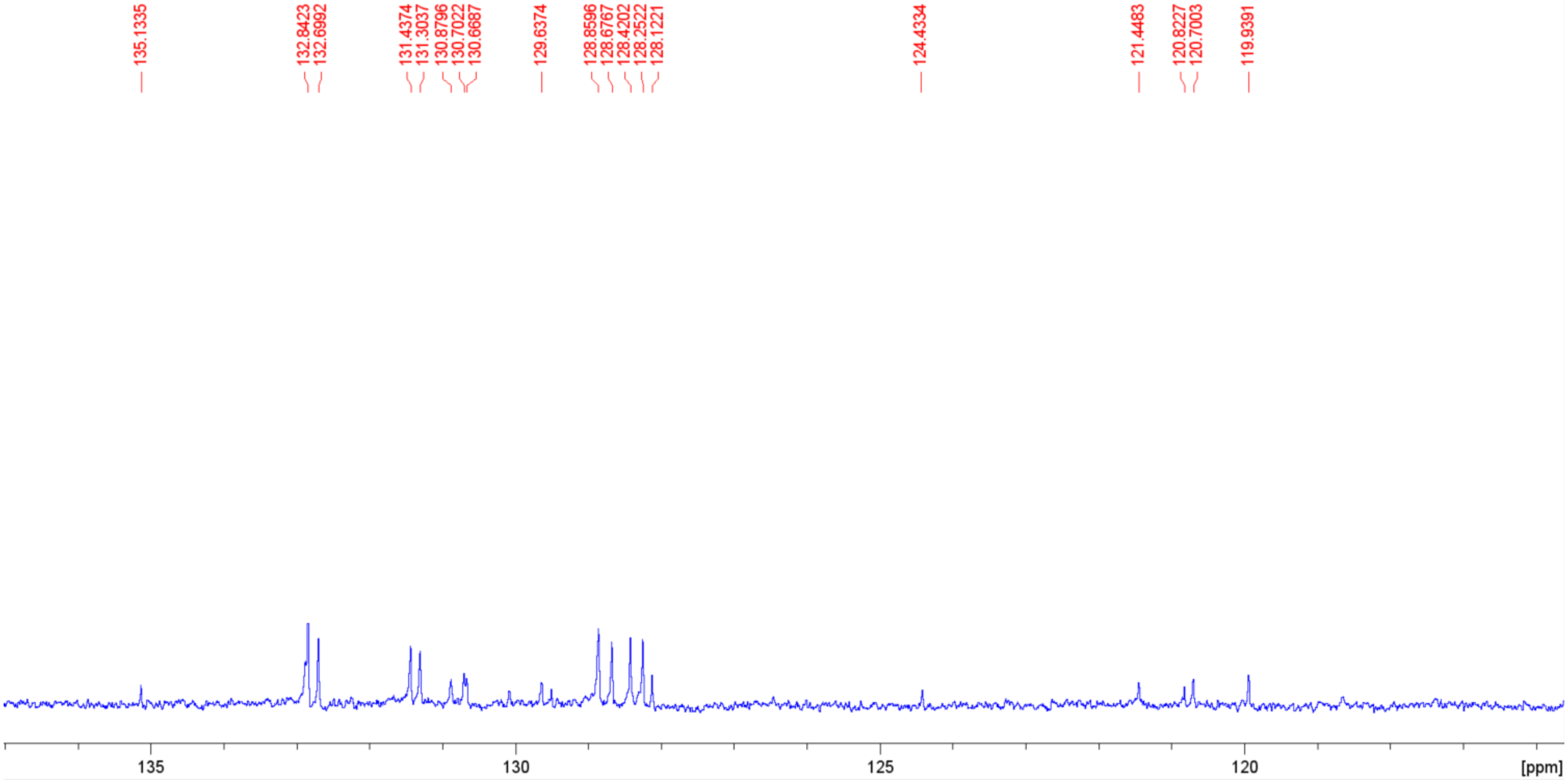

Figure S87: $^{13}C\{^{1}H\}$ NMR (75 MHz, CD_2Cl_2) spectrum of **3**, expansion of aromatic region.

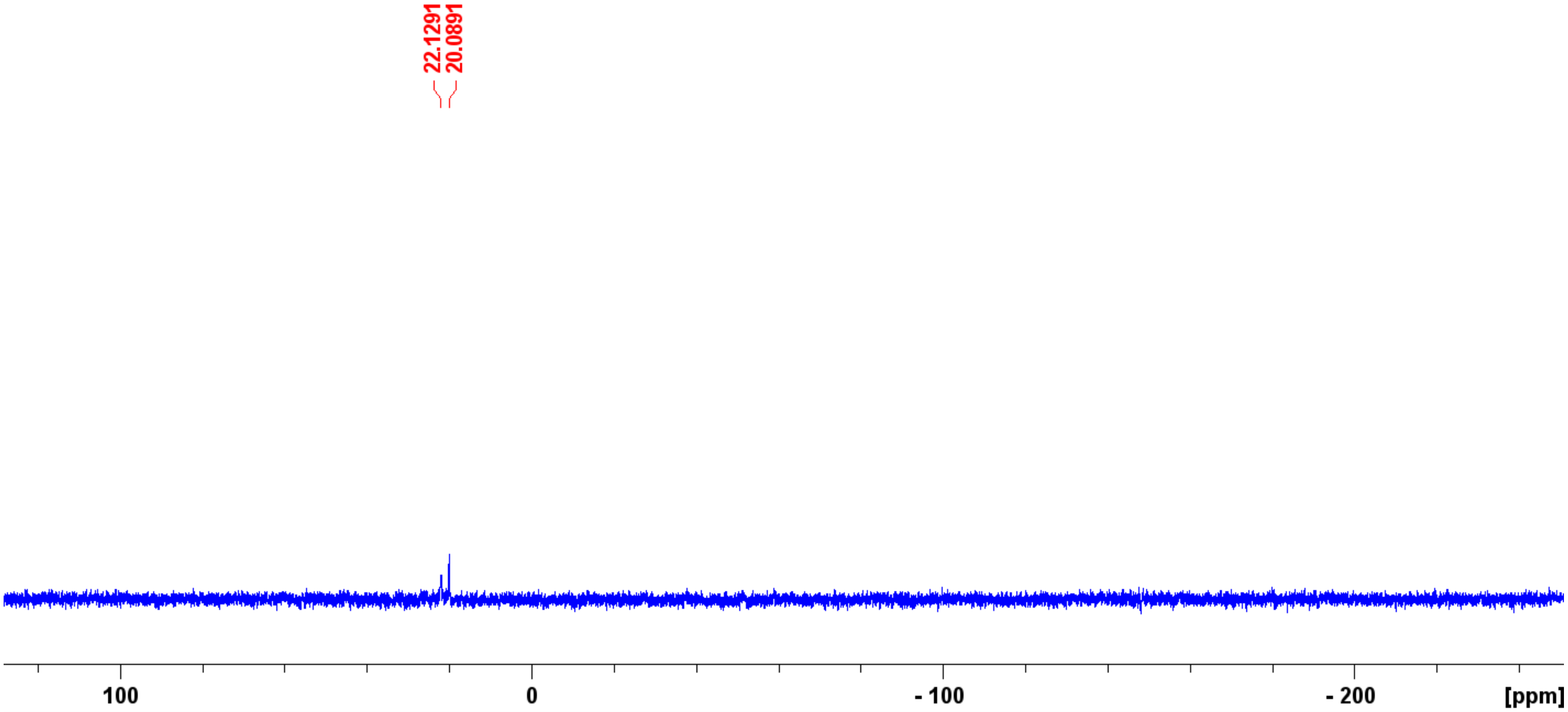

Figure S88: ${}^{31}P\{{}^{1}H\}$ NMR (121 MHz, CD_2Cl_2) spectrum of **3**.

Characterization Data of 4

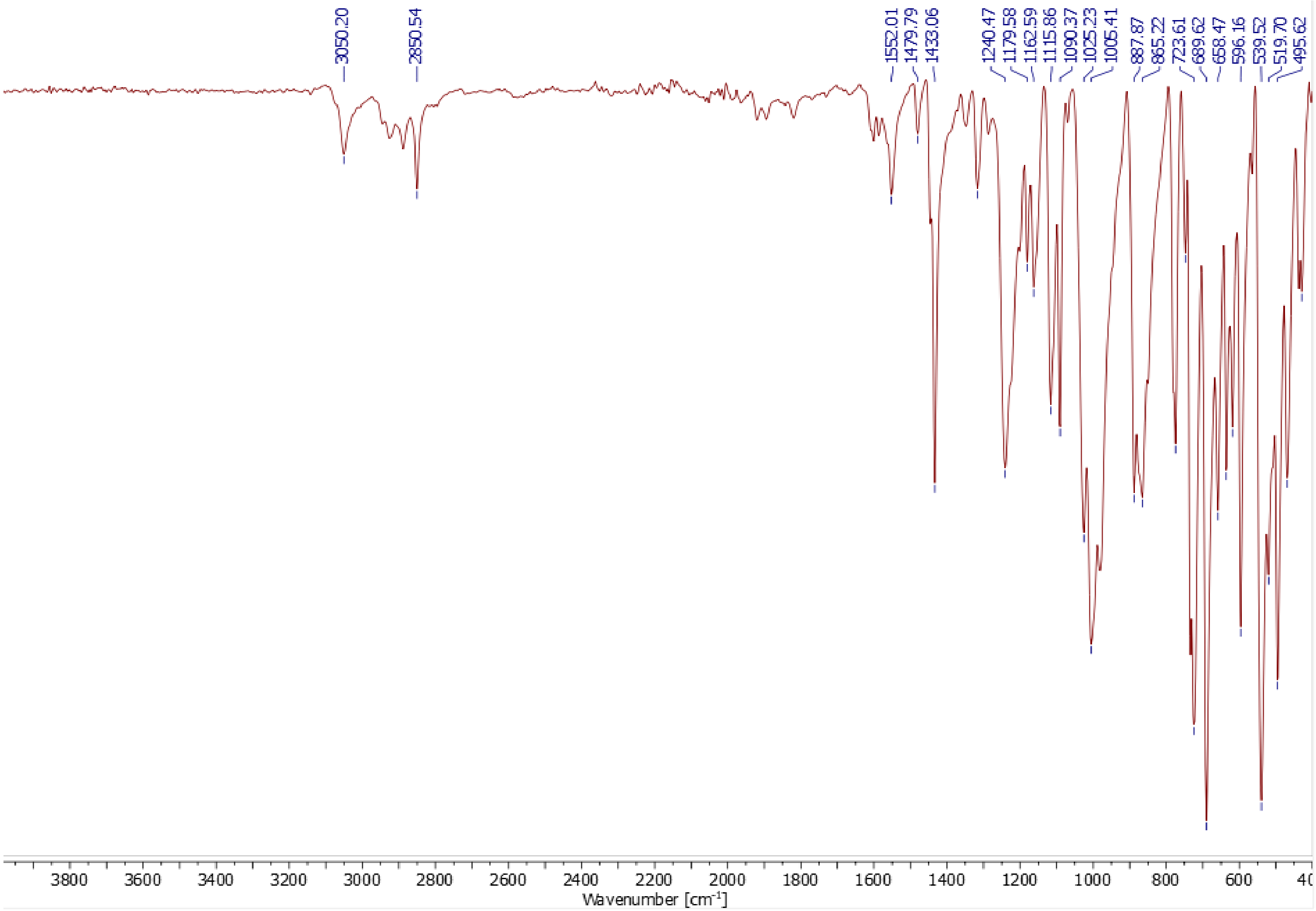

Figure S89: IR Spectrum (ATR) of **4**.

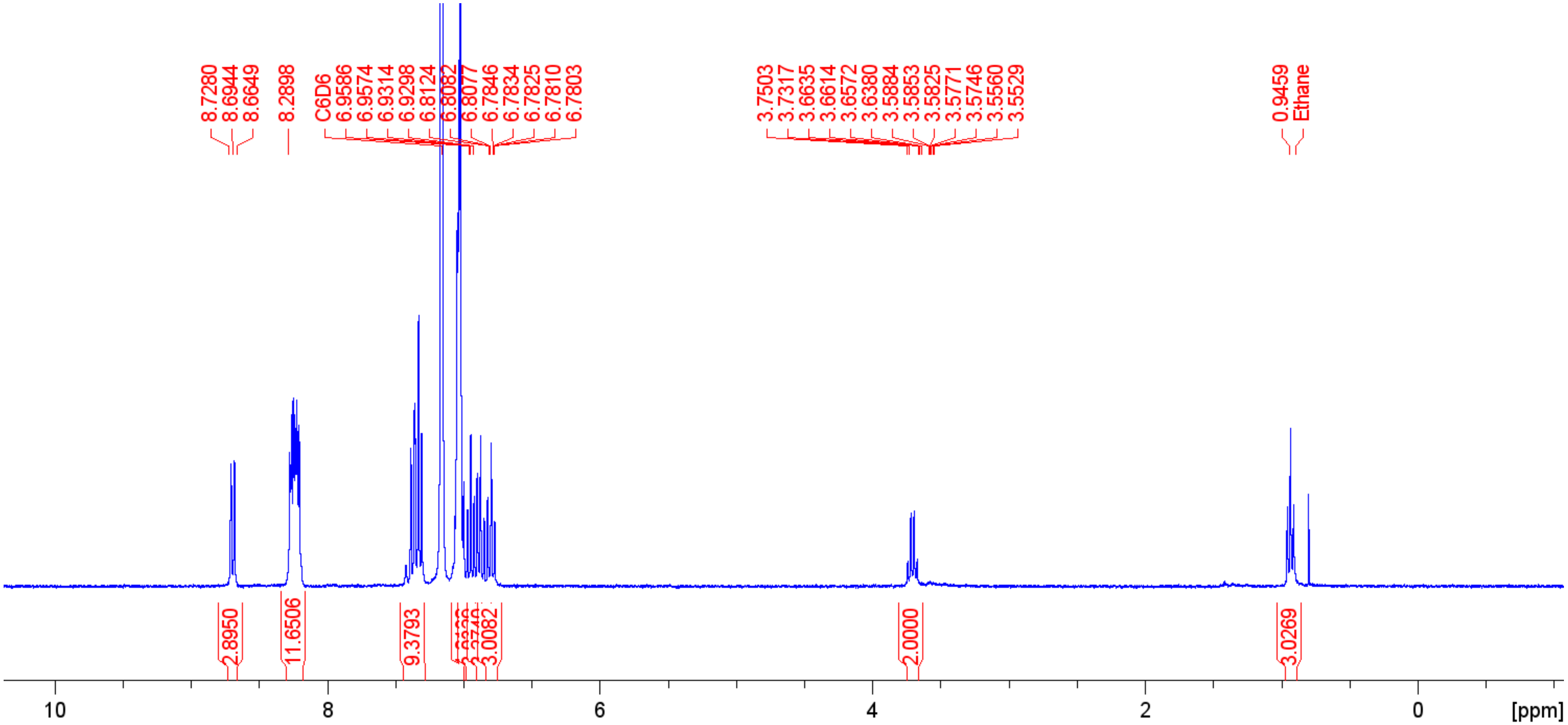

Figure S90: ^{1}H NMR (300 MHz, C_6D_6) spectrum of **4**.

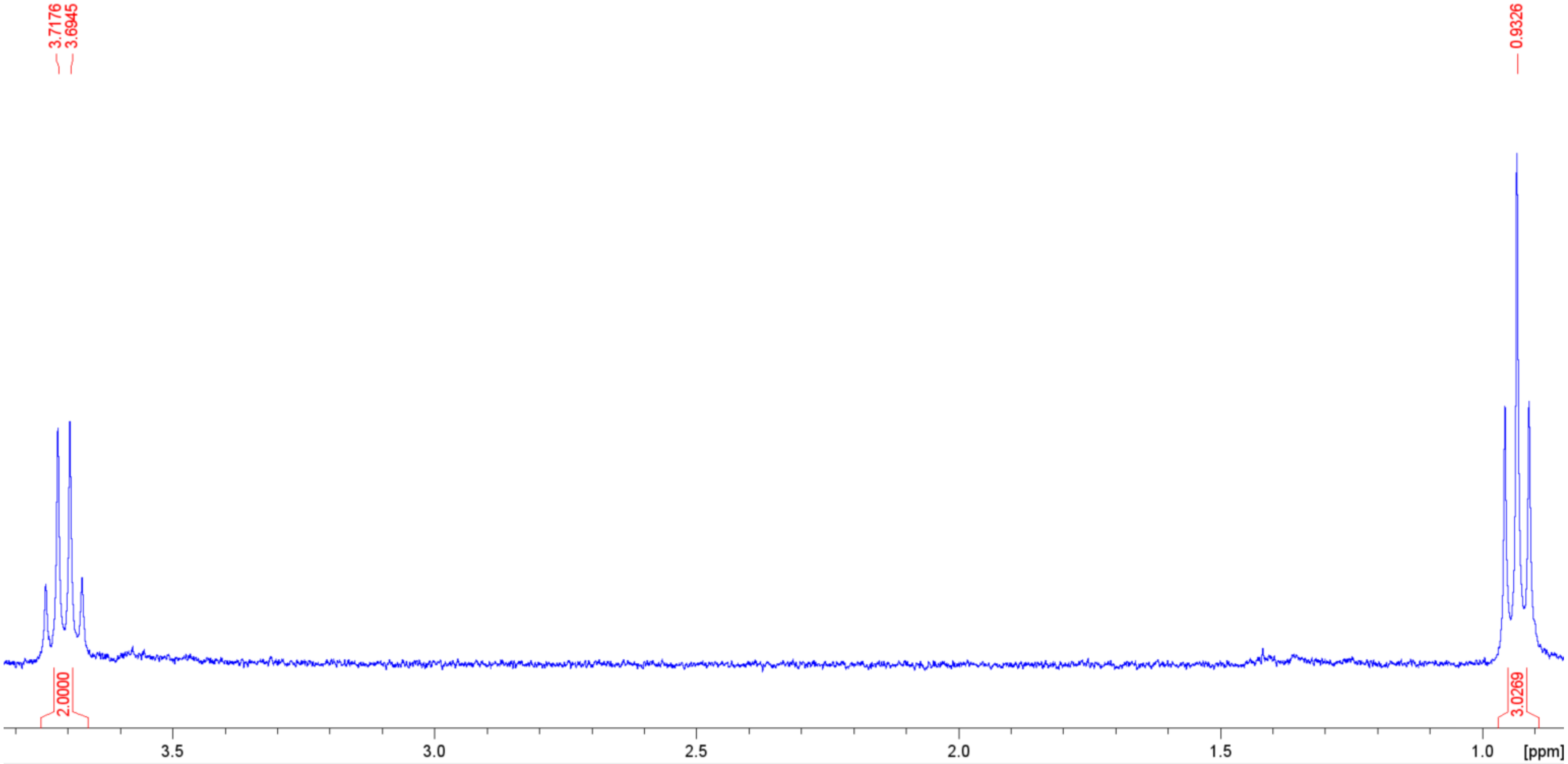

Figure S91: ^{1}H NMR (300 MHz, C_6D_6) spectrum of **4**, expansion on the metal alkyl peaks.

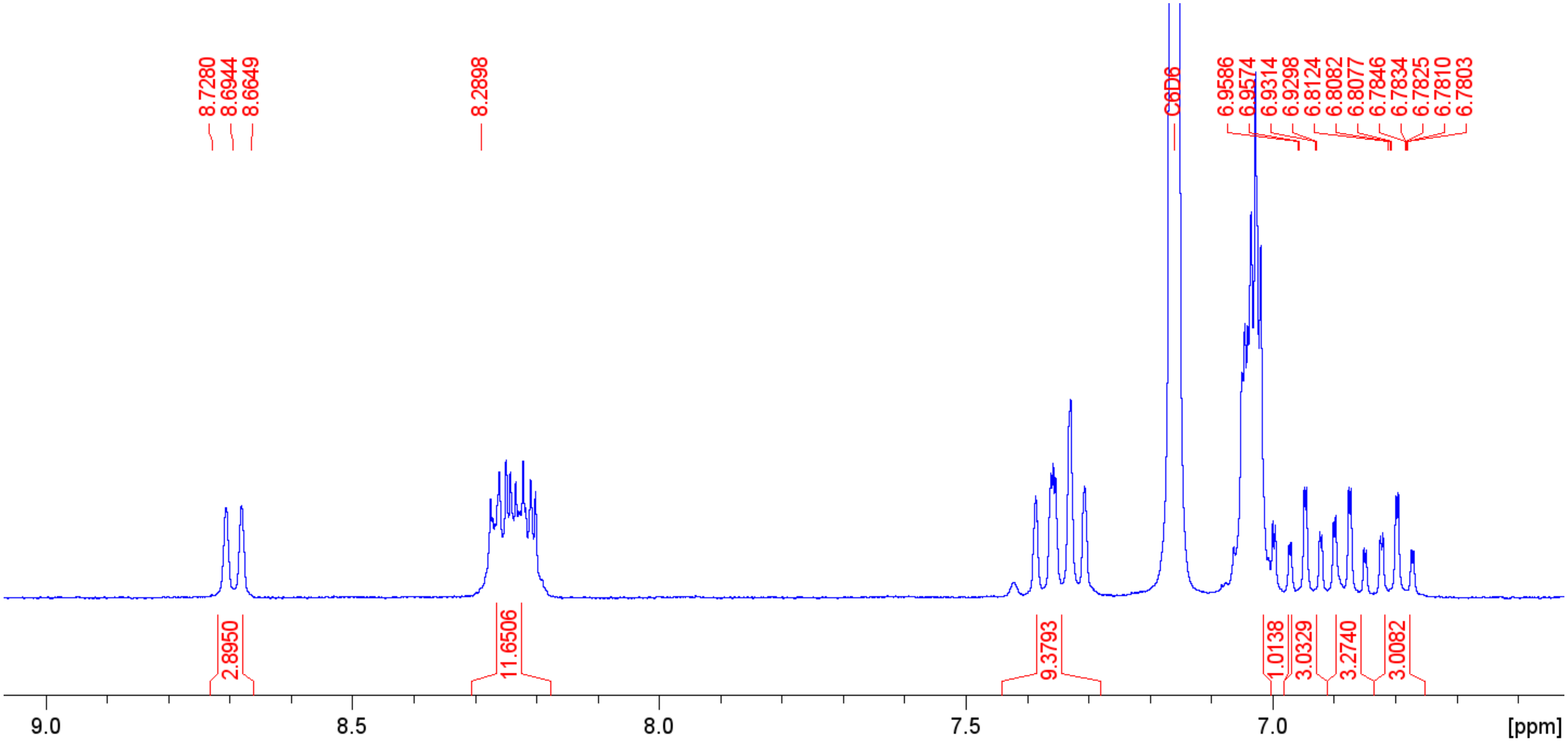

Figure S92: ^{1}H NMR (300 MHz, C_6D_6) spectrum of **4**, expansion on the aromatic region.

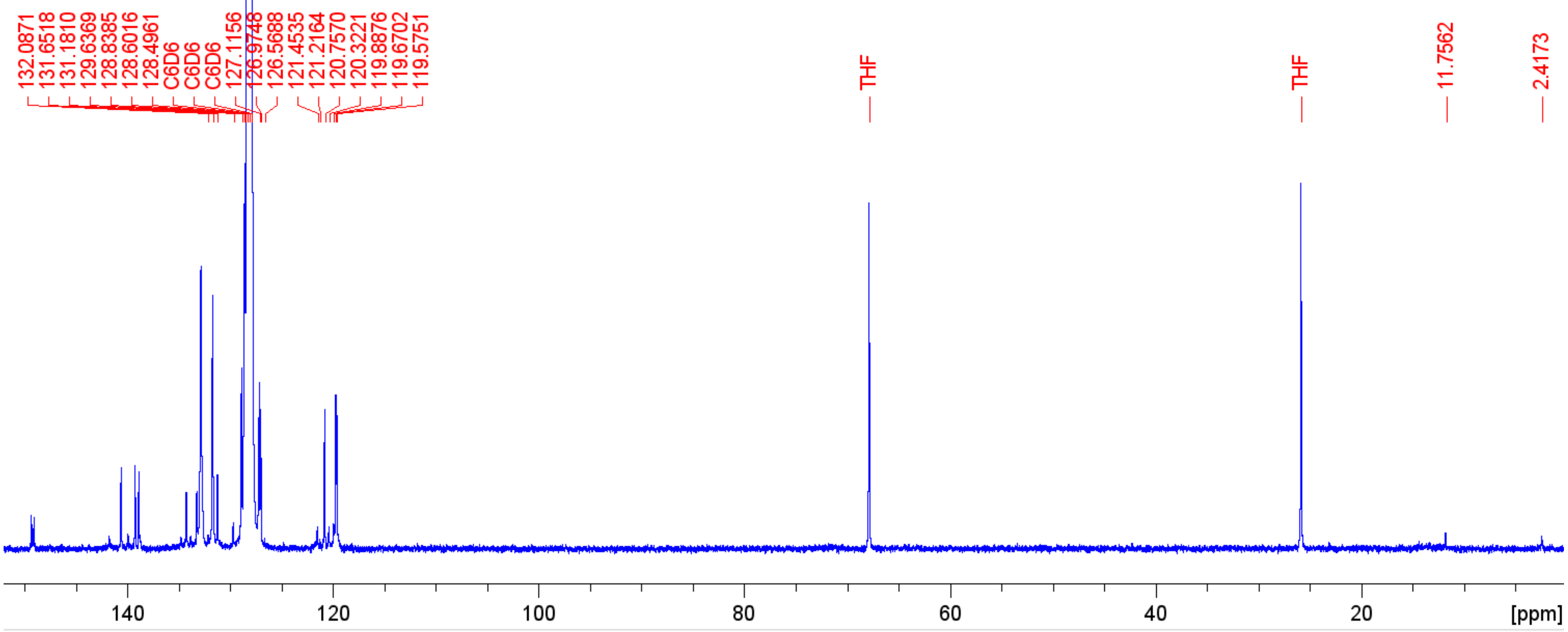

Figure S93: $^{13}C\{^1H\}$ NMR (126 MHz, C_6D_6) spectrum of **4**. Spectrum obtained with separate sample of **4** with respect to ^1H and ^{31}P spectra.

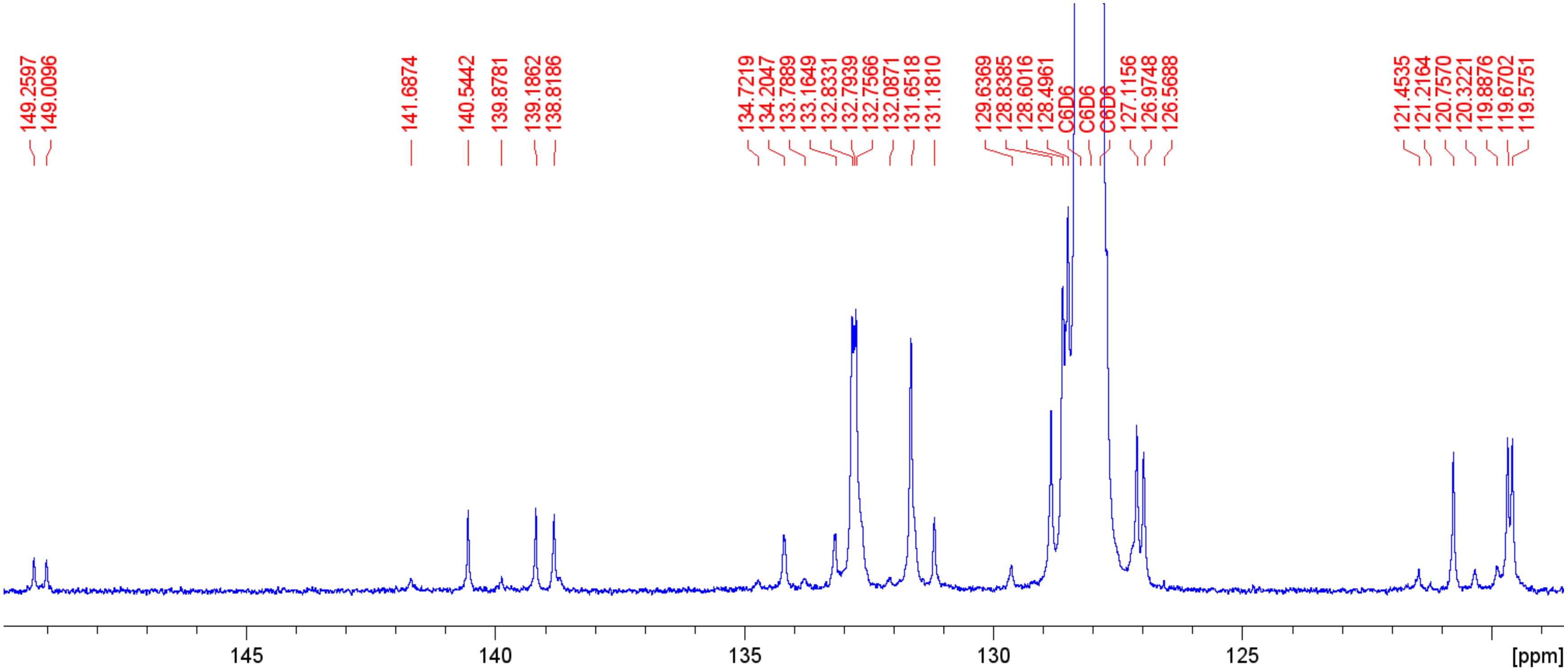

Figure S94: $^{13}C\{^1H\}$ NMR (126 MHz, C_6D_6) spectrum of **4**, expansion on the aromatic region. Spectrum obtained with separate sample of **4** with respect to ^1H and ^{31}P spectra.

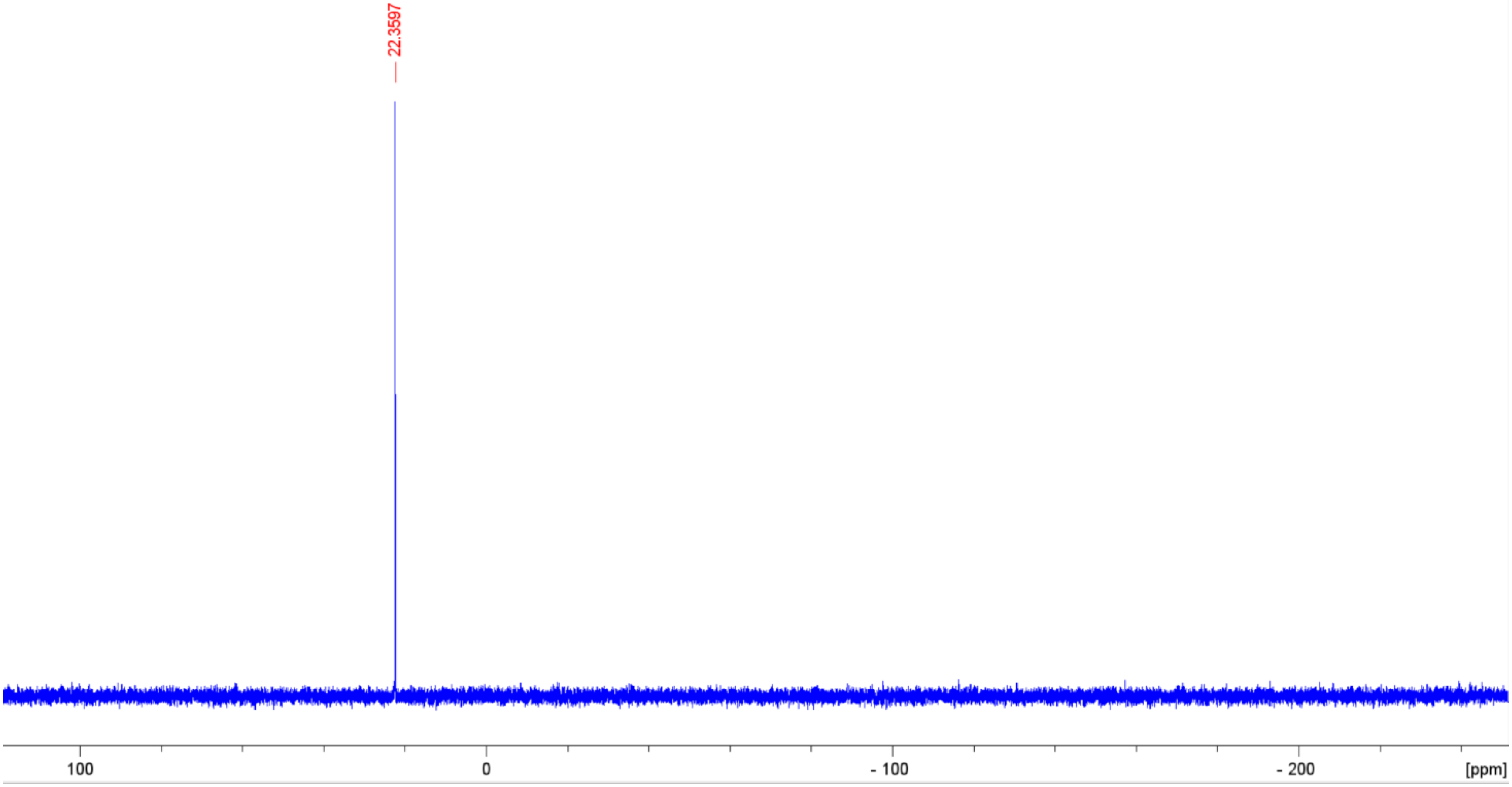

Figure S95: $^{31}P\{^{1}H\}$ NMR (121 MHz, C_6D_6) spectrum of **4.**

Characterization Data of 5

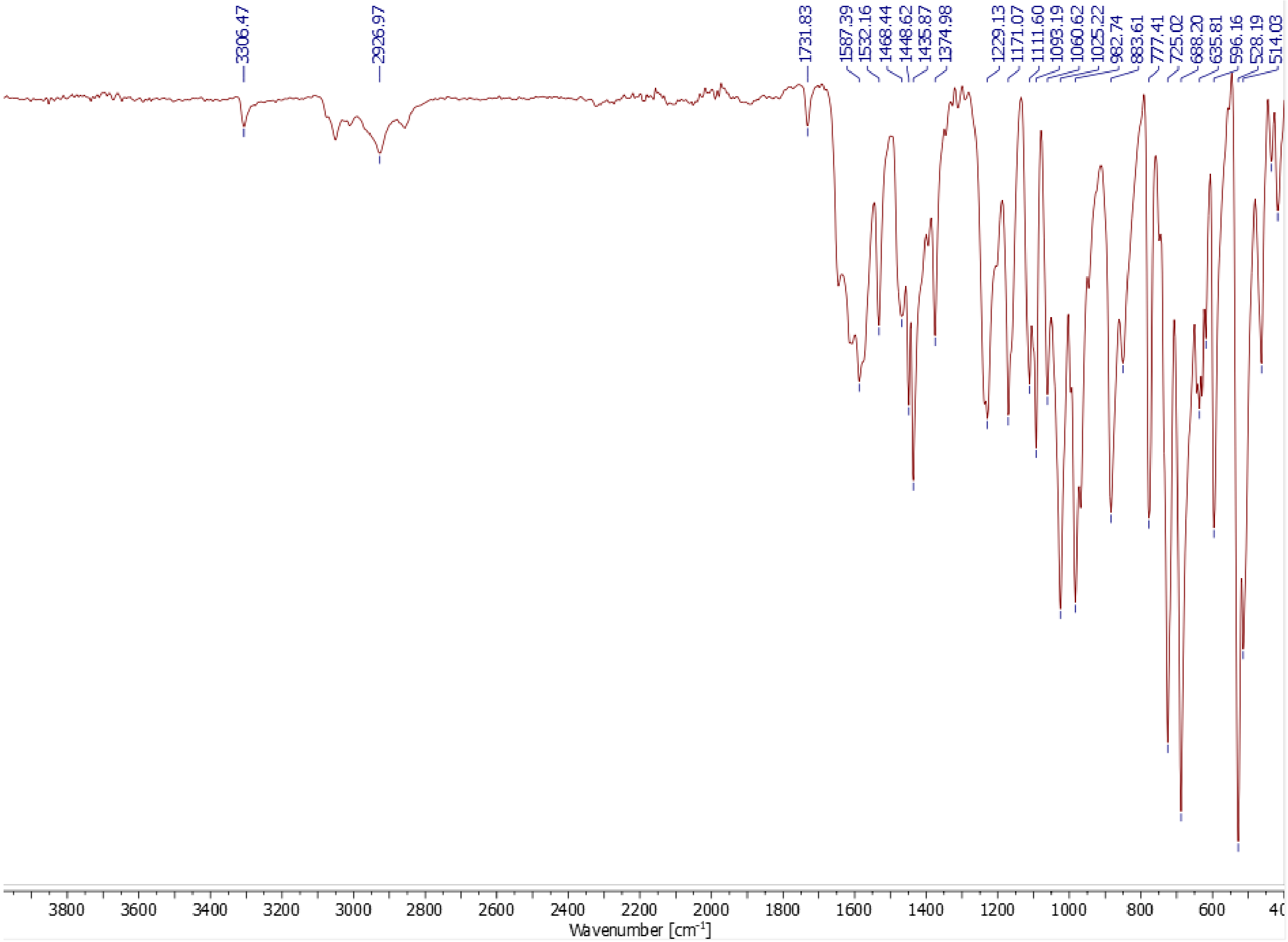

Figure S96: IR Spectrum (ATR) of **5**.

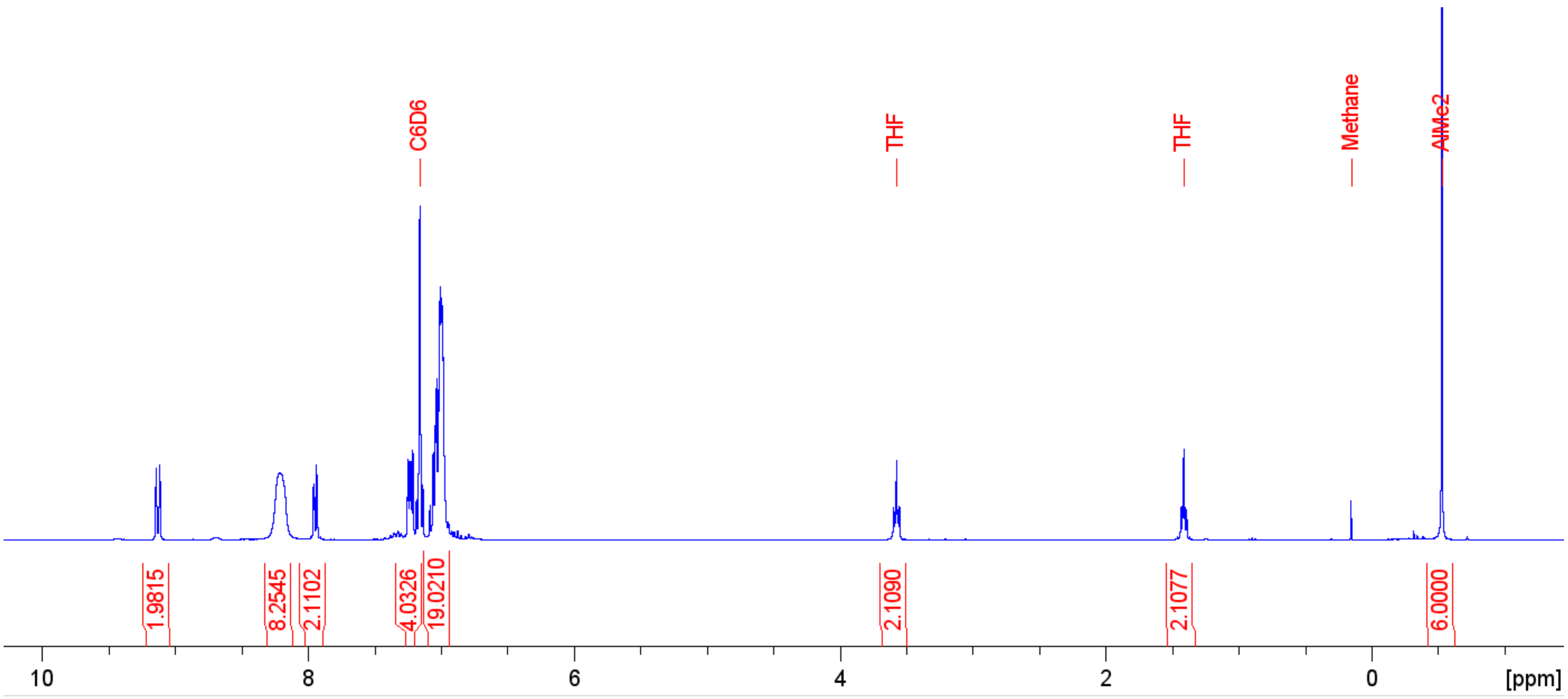

Figure S97: ^{1}H NMR (300 MHz, C_6D_6) spectrum of **5**.

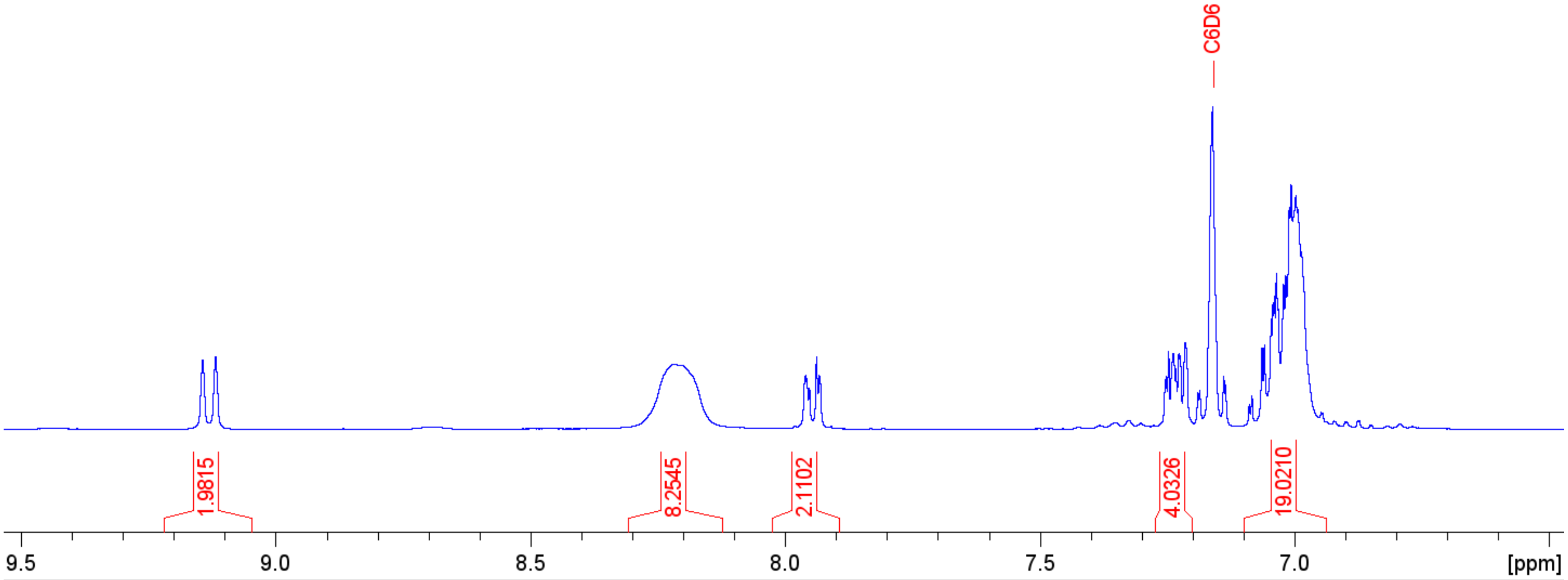

Figure S98: ^{1}H NMR (300 MHz, C_6D_6) spectrum of **5**, expansion on the aromatic region.

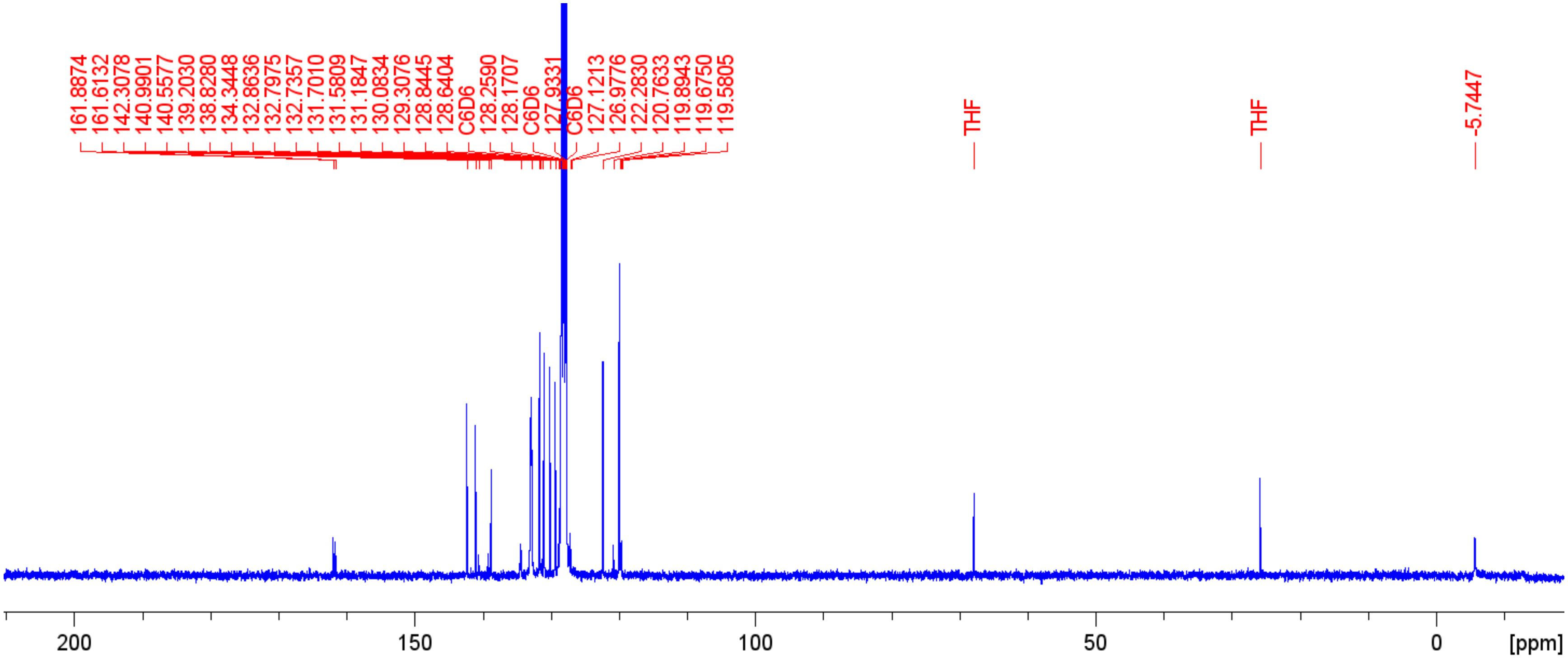

Figure S99: $^{13}C\{^{1}H\}$ NMR (75 MHz, C_6D_6) spectrum of **5**.

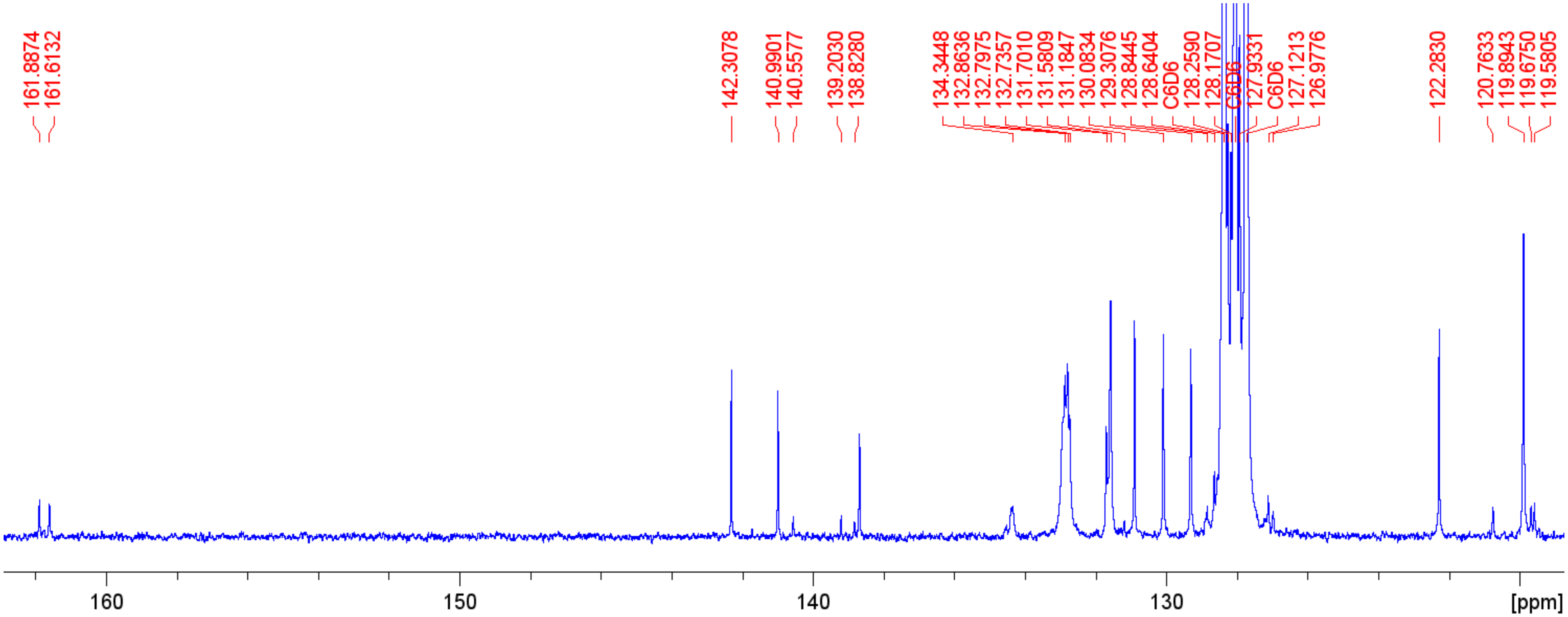

Figure S100: $^{13}C\{^{1}H\}$ NMR (75 MHz, C_6D_6) spectrum of **5** expansion on the aromatic region.

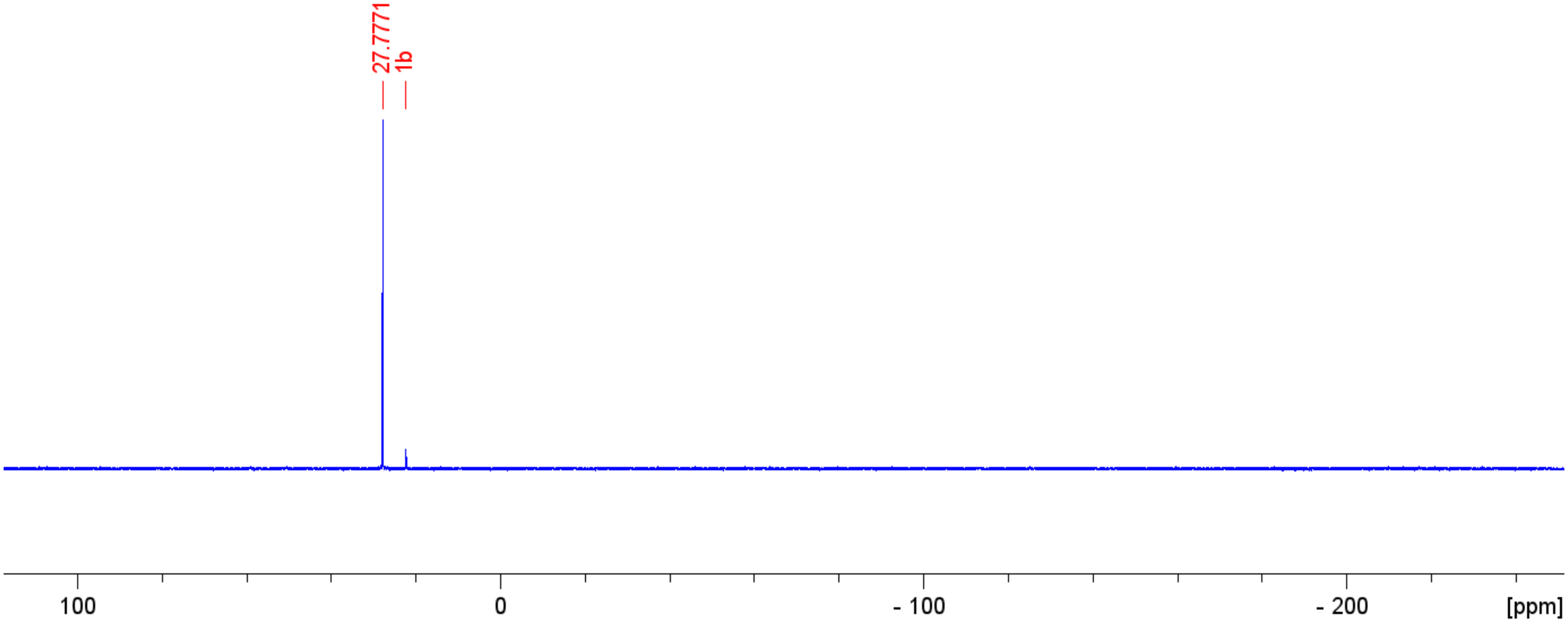

Figure S101: $^{31}P\{^{1}H\}$ NMR (121 MHz, C_6D_6) spectrum of **5**, showing contamination with **1b**.

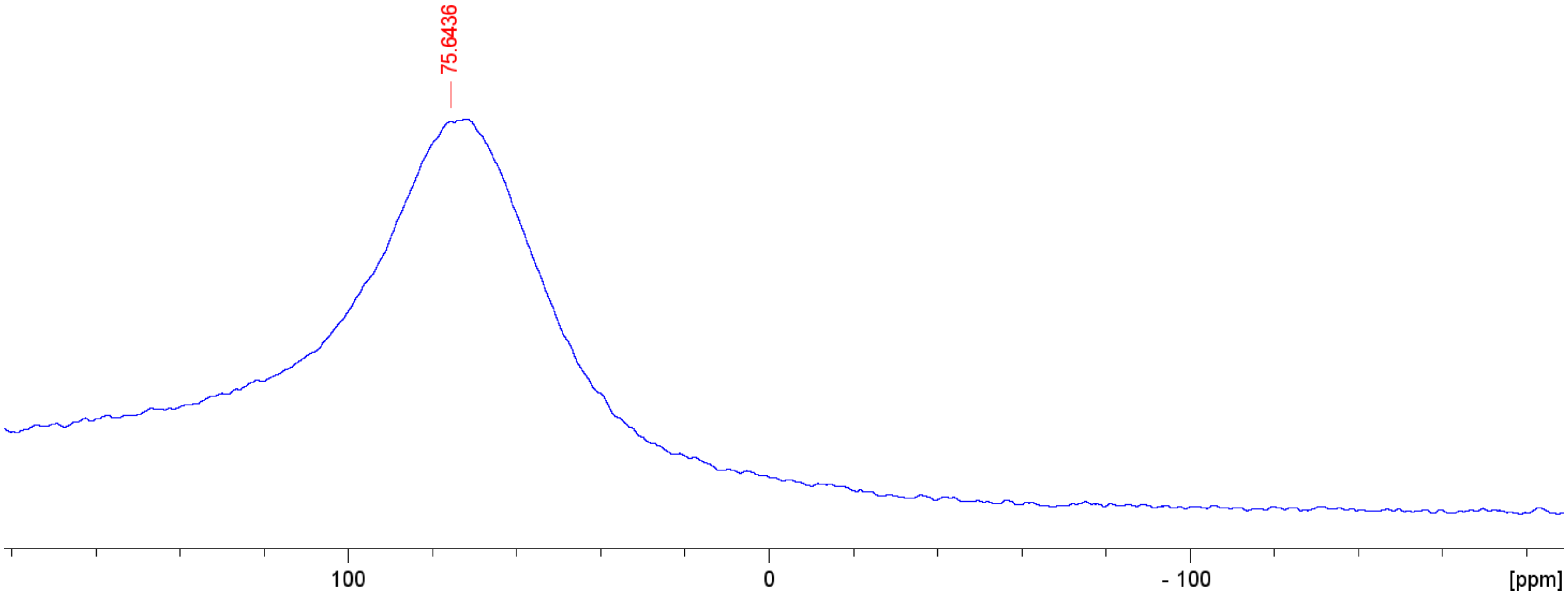

Figure S102: ^{27}Al NMR (78 MHz, C_6D_6) spectrum of **5**.

Characterization Data of 6

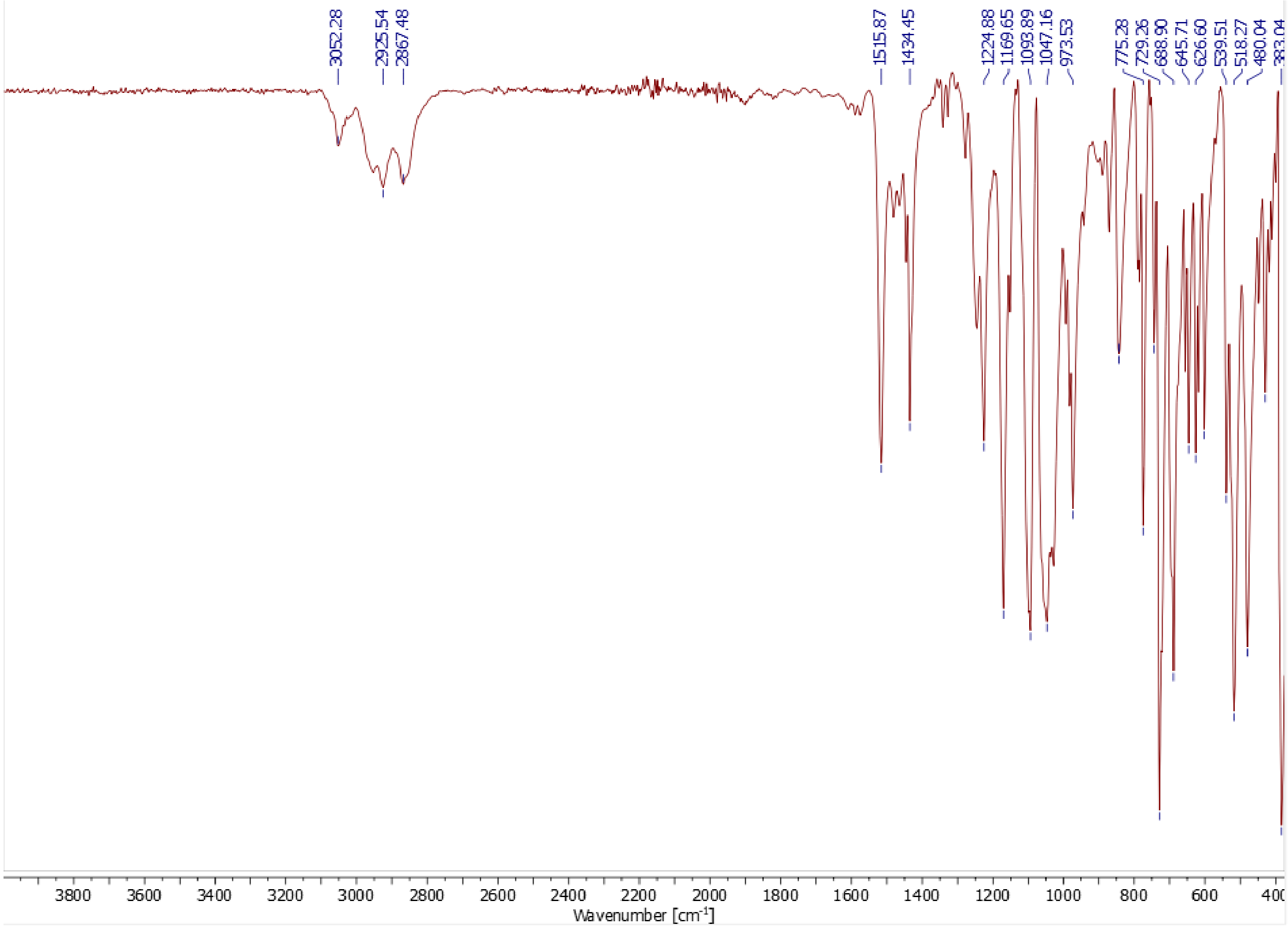

Figure S103: IR Spectrum (ATR) of **6**.

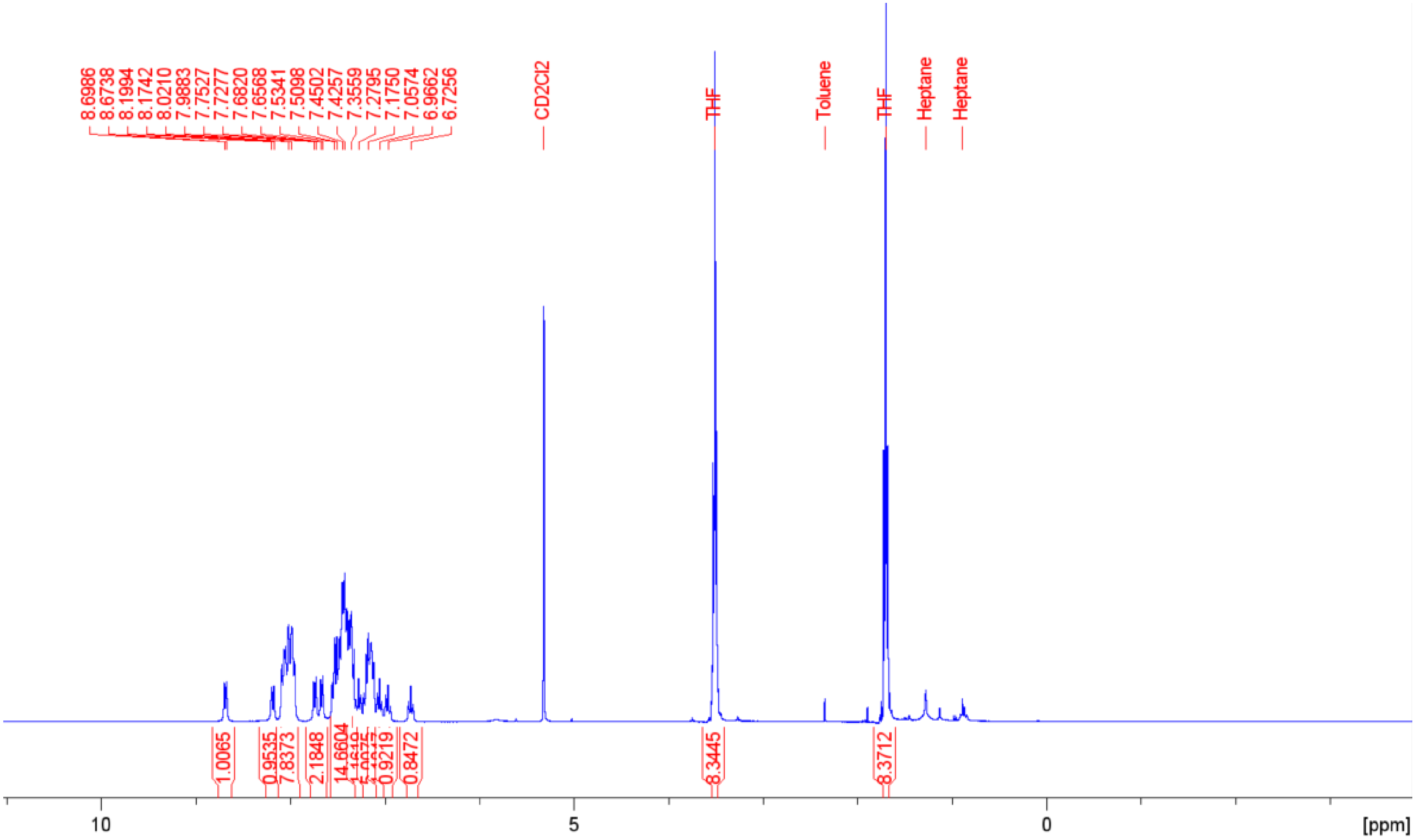

Figure S104: ^{1}H NMR (300 MHz, CD_2Cl_2) spectrum of **6**.

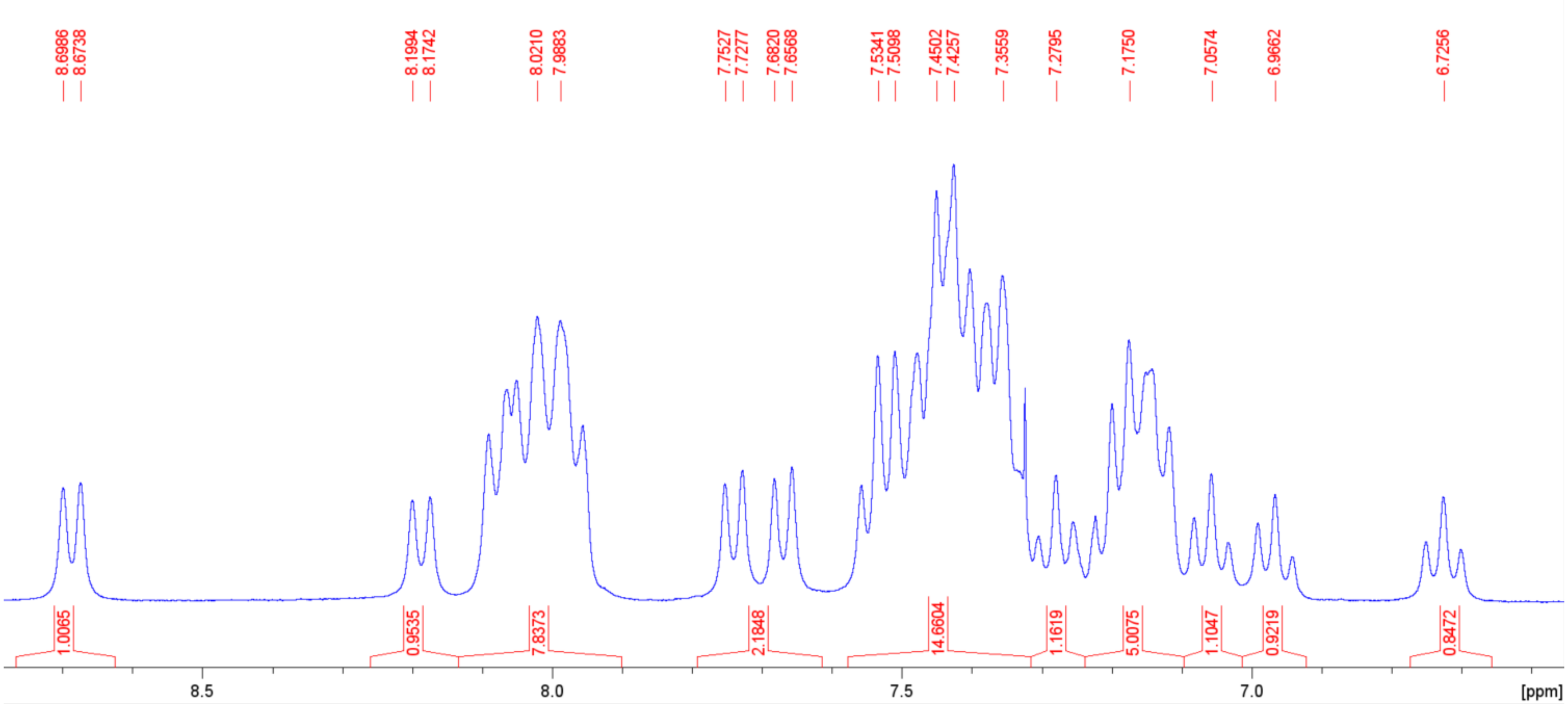

Figure S105: ^{1}H NMR (300 MHz, CD_2Cl_2) spectrum of **6**, expansion of aromatic region.

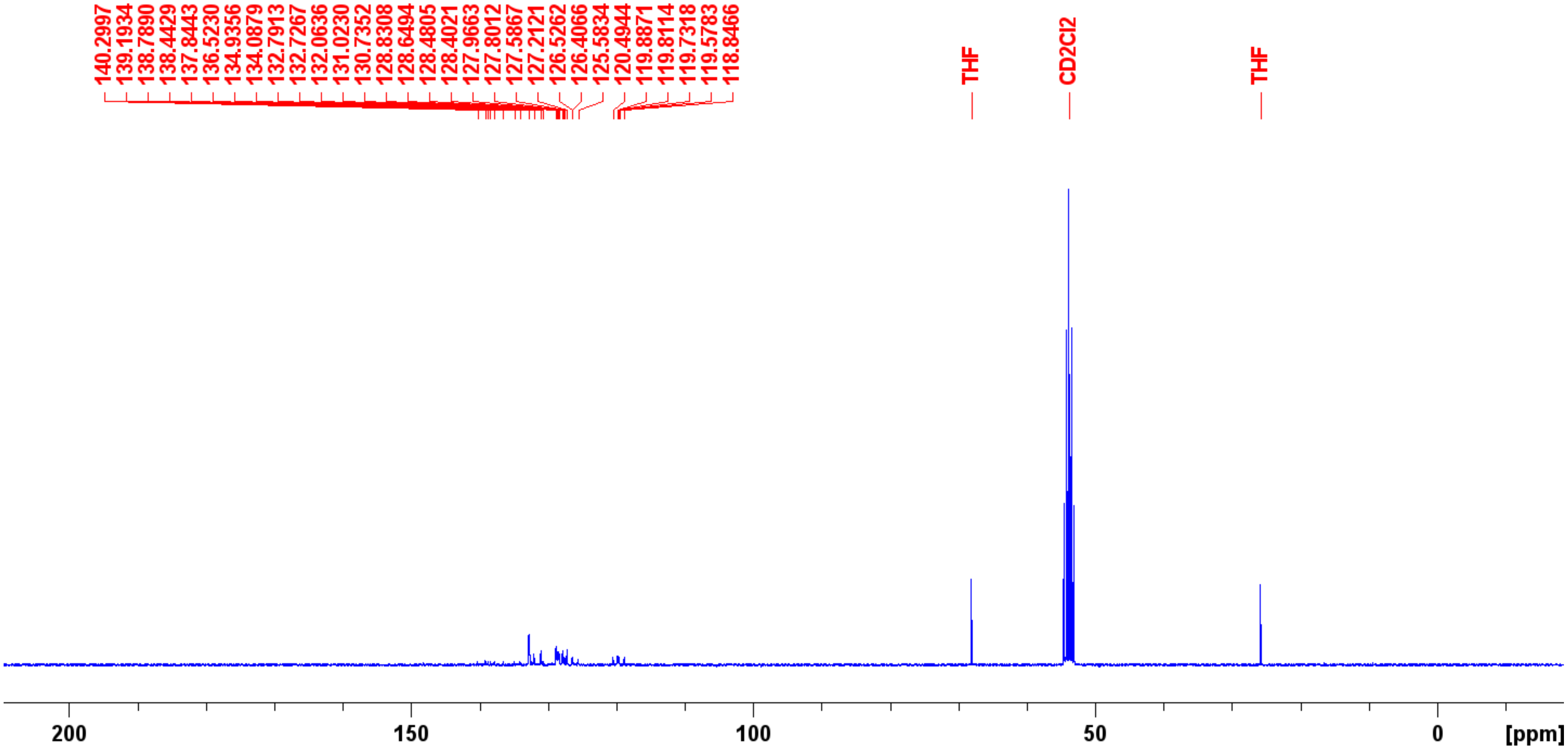

Figure S106: $^{13}C\{^1H\}$ NMR (75 MHz, CD_2Cl_2) spectrum of **6**.

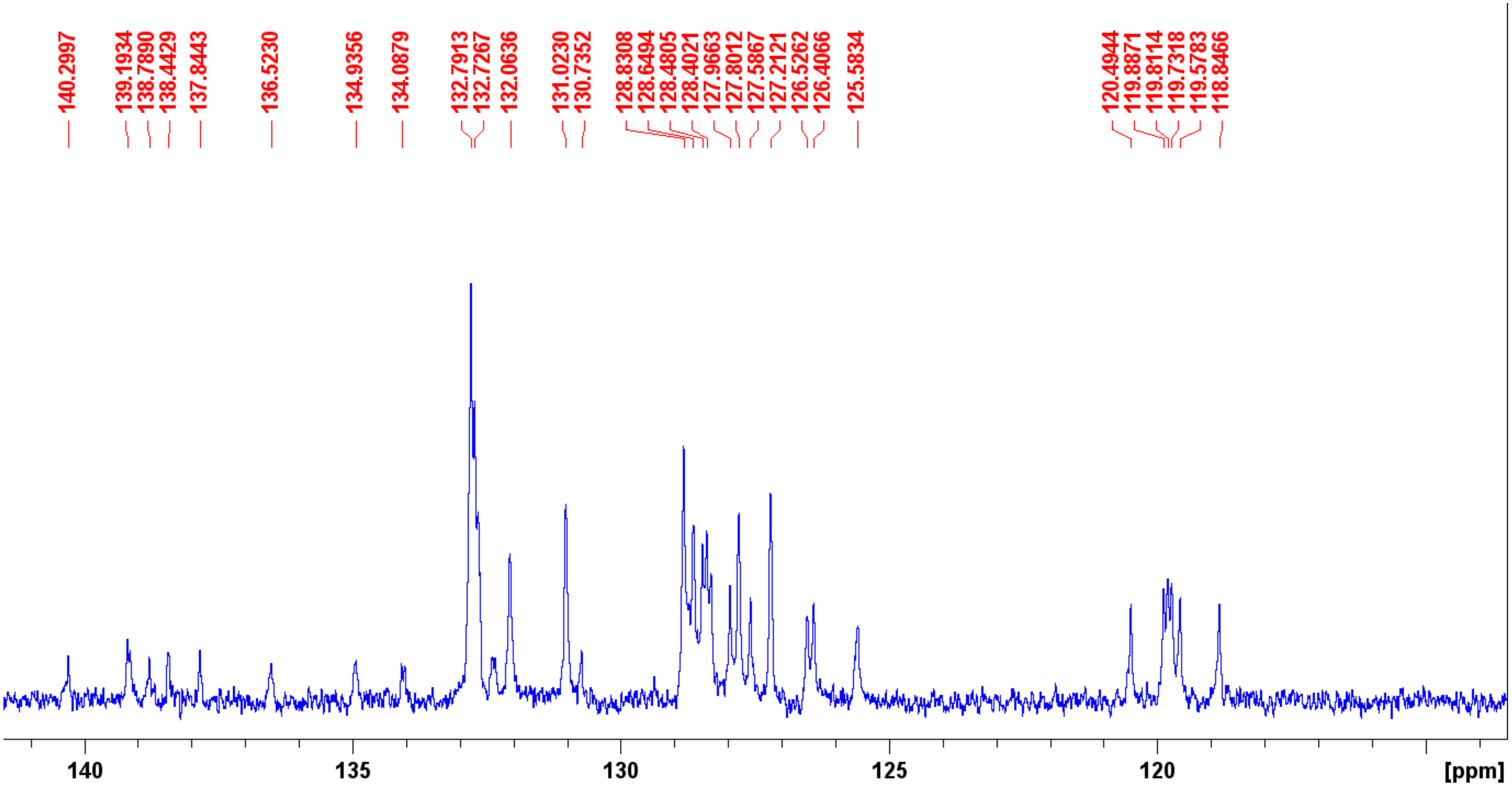

Figure S107: $^{13}C\{^1H\}$ NMR (75 MHz, CD_2Cl_2) spectrum of **6**, expansion of aromatic region.

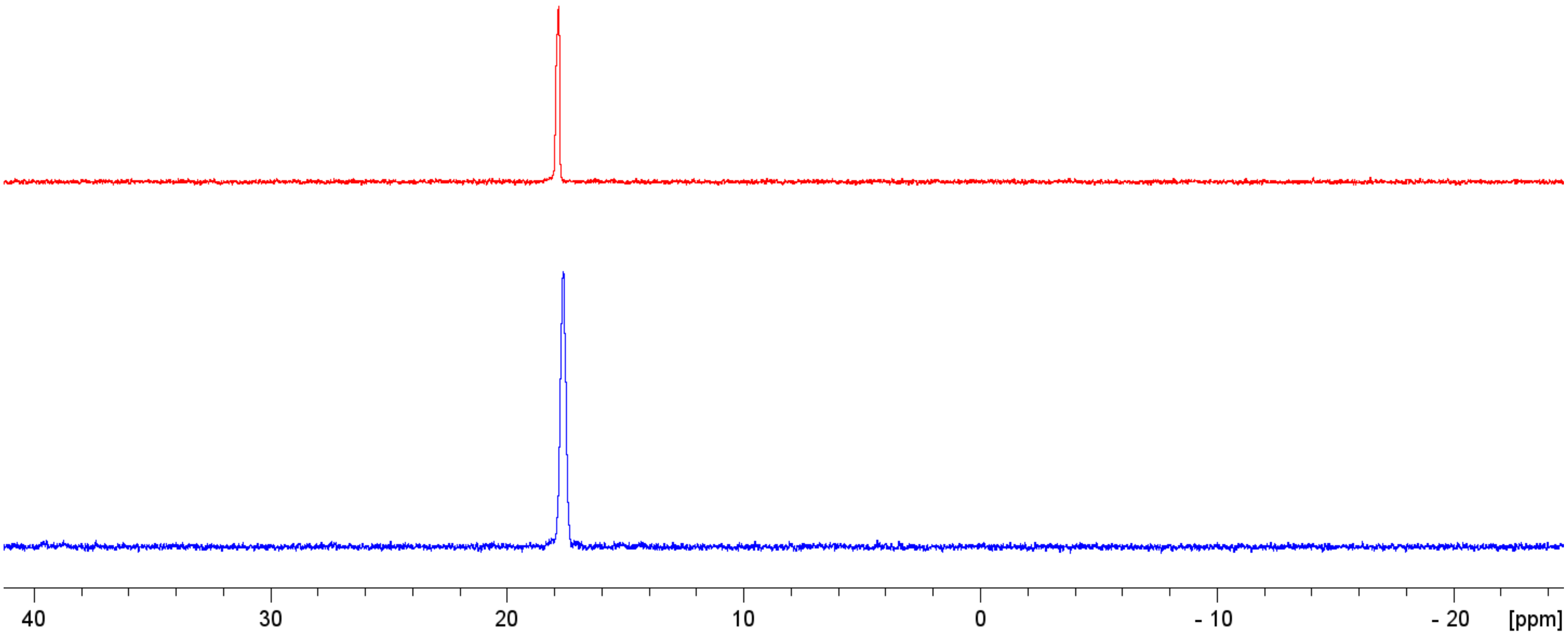

Figure S108: $^{31}P\{^{1}H\}$ NMR (121 MHz) spectrum of **6** dissolved in non-deuterated THF with a drop of C_6D_6 (top, red) or CD_2Cl_2 (bottom, blue) for a lock.

Characterization Data of Polymers

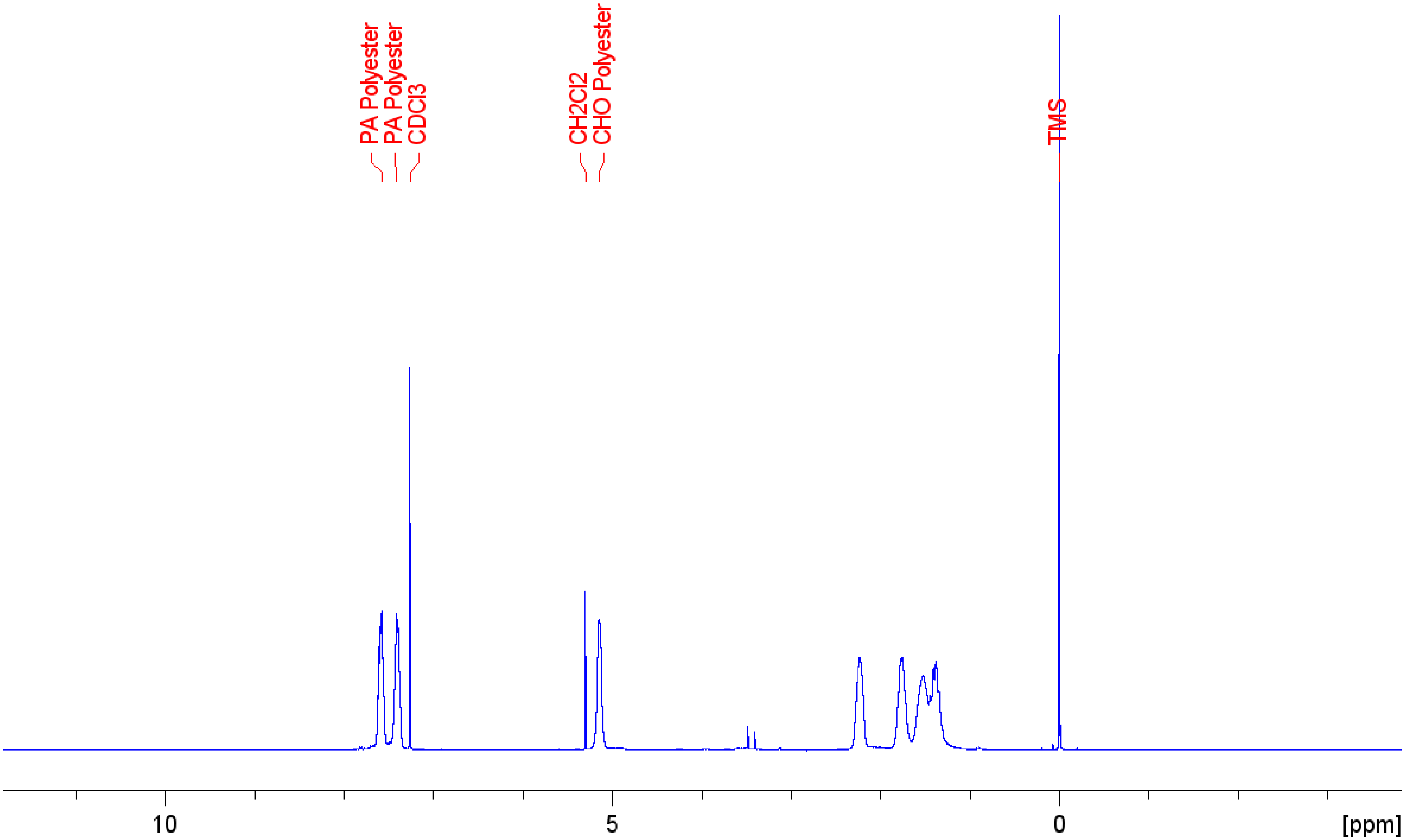

Figure S109: ^{1}H NMR (300 MHz, $CDCl_3$) spectrum of dried polymer from Table 3, entry 3 (**4** with PPNCl).

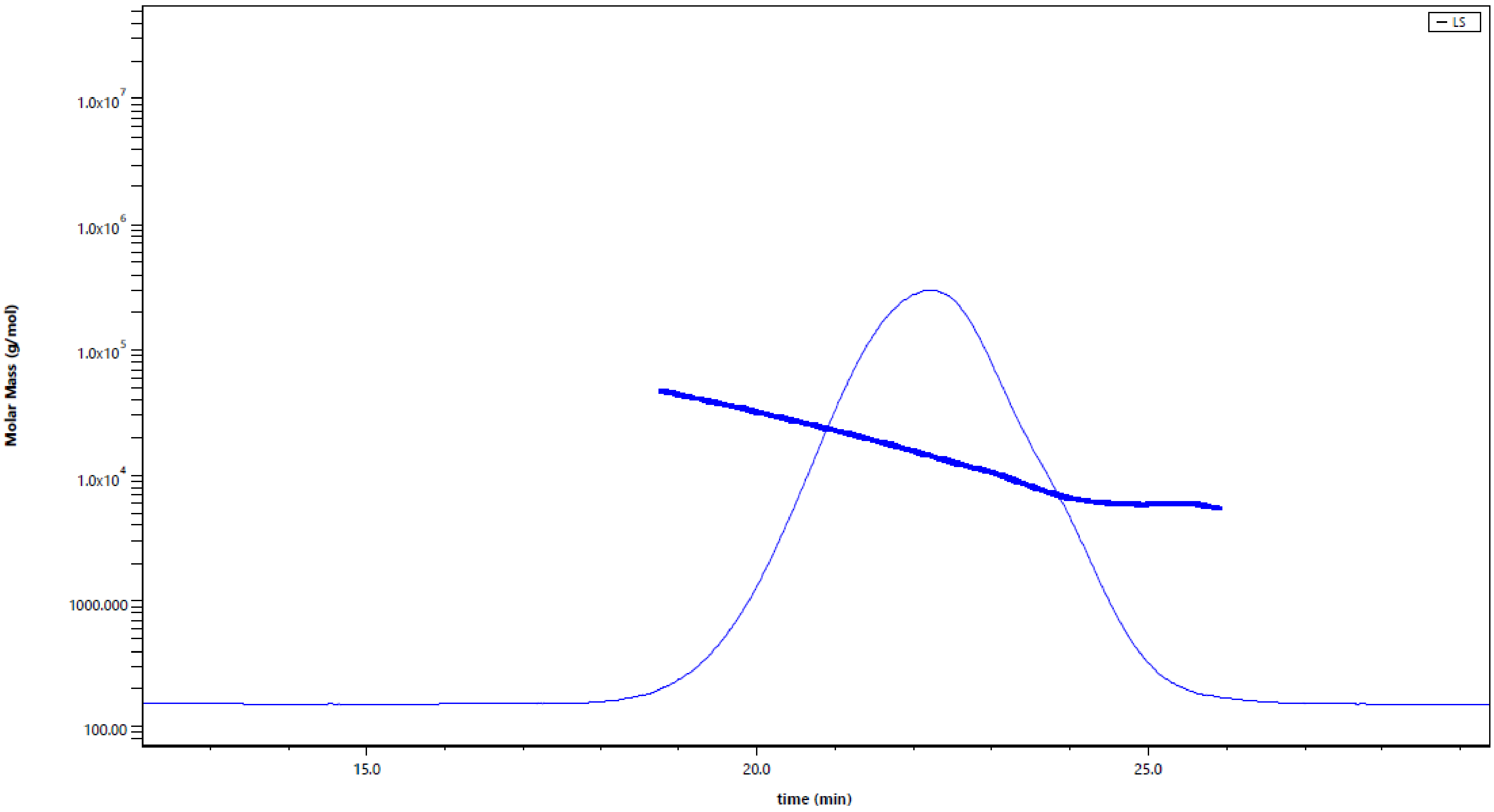

Figure S110: Light scattering GPC trace for the ROCOP of PA + CHO using **4** and PPNCl $[PA]_0:[CHO]_0:[4]_0:[PPNCl]_0$ = 100:500:1:1, 80 °C, 4 h (Table 3, entry 3).

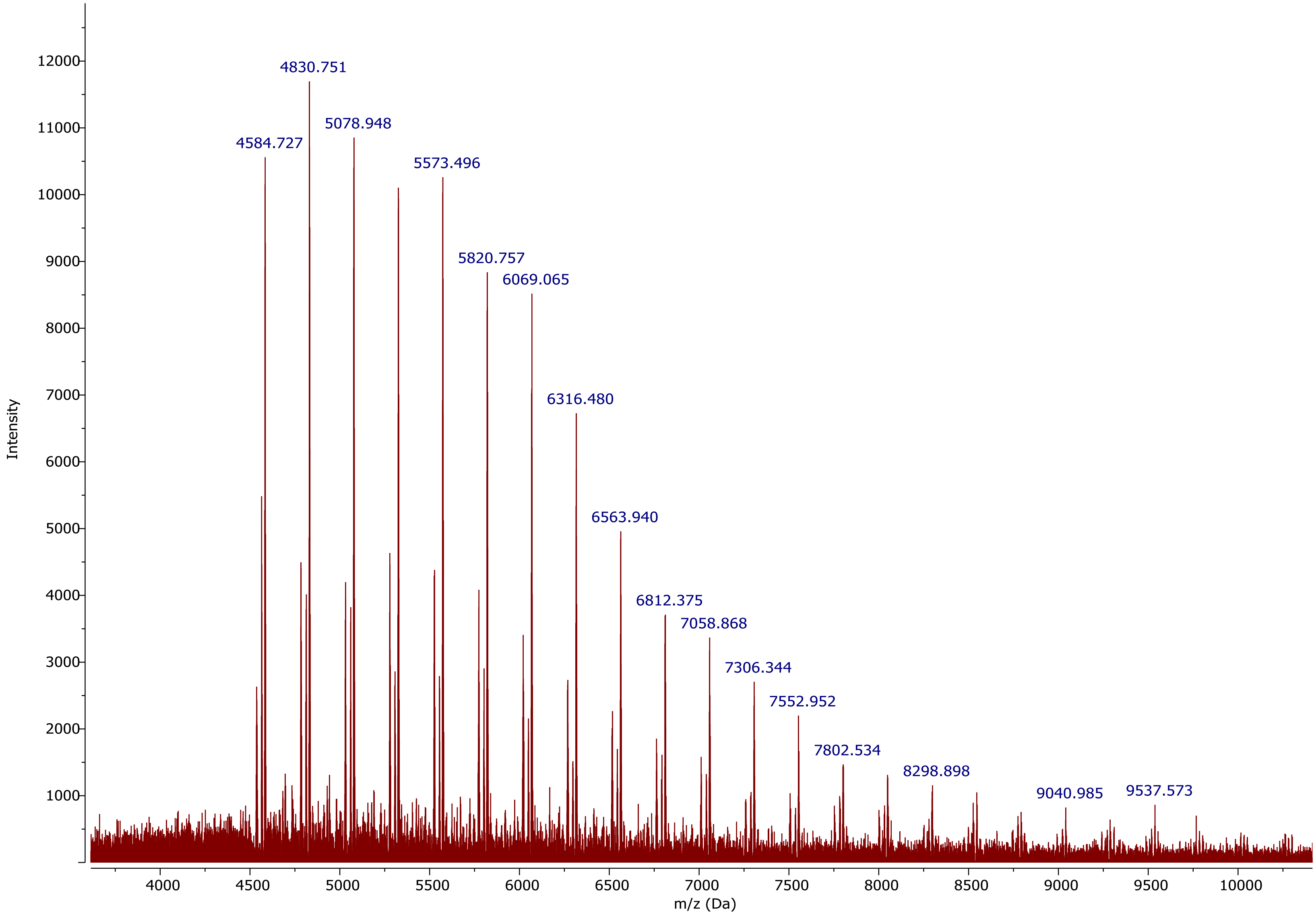

Figure S111: MALDI-TOF mass spectrum for the ROCOP of PA + CHO using **4** and PPNCl $[PA]_0:[CHO]_0:[4]_0:[PPNCl]_0$ = 100:500:1:1, 80 °C, 4 h (Table 3, Entry 3). Taken in positive reflectron mode.

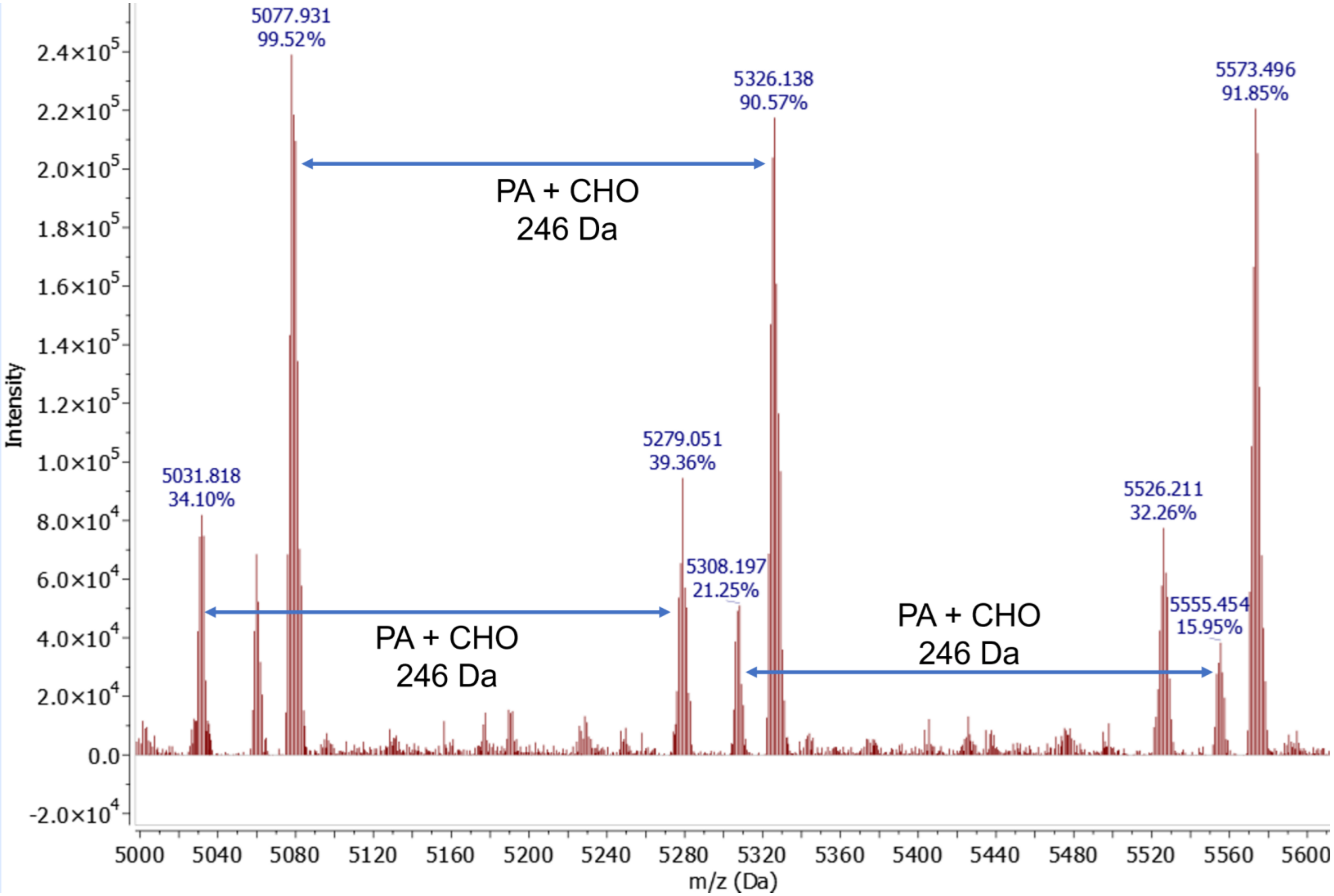

Figure S112: Expansion and annotation of MALDI-TOF mass spectrum for the ROCOP of PA + CHO using **4** and PPNCl $[PA]_0$:$[CHO]_0$:$[\mathbf{4}]_0$:$[PPNCl]_0$ = 100:500:1:1, 80 °C, 4 h (Table 3, Entry 3). Taken in positive reflectron mode.

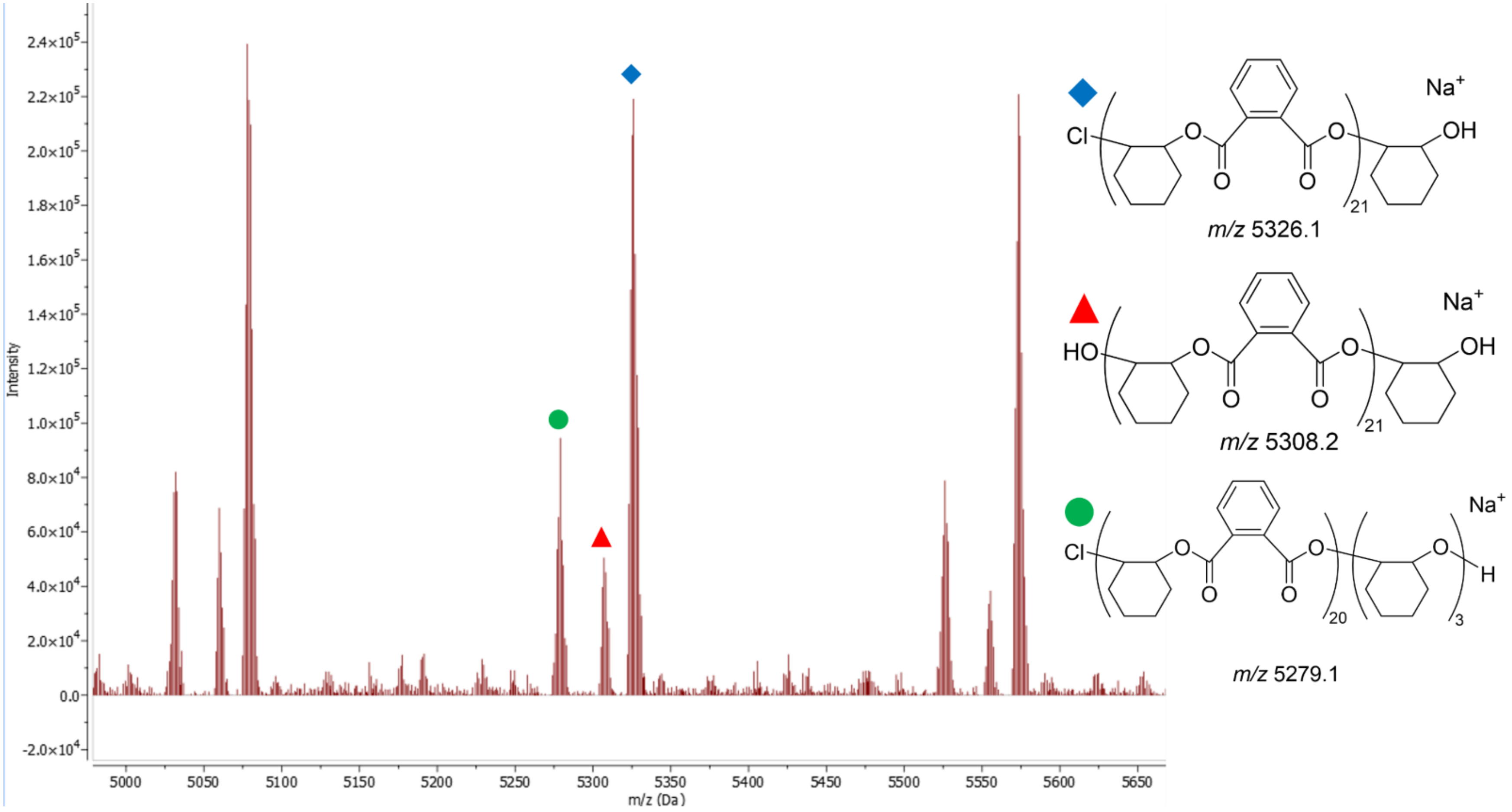

Figure S113: Expansion and polyester assignments of MALDI-TOF mass spectrum for the ROCOP of PA + CHO using **4** and PPNCl $[\text{PA}]_0$:$[\text{CHO}]_0$:$[\mathbf{4}]_0$:$[\text{PPNCl}]_0$ = 100:500:1:1, 80 °C, 4 h (Table 3, Entry 3). Taken in positive reflectron mode.

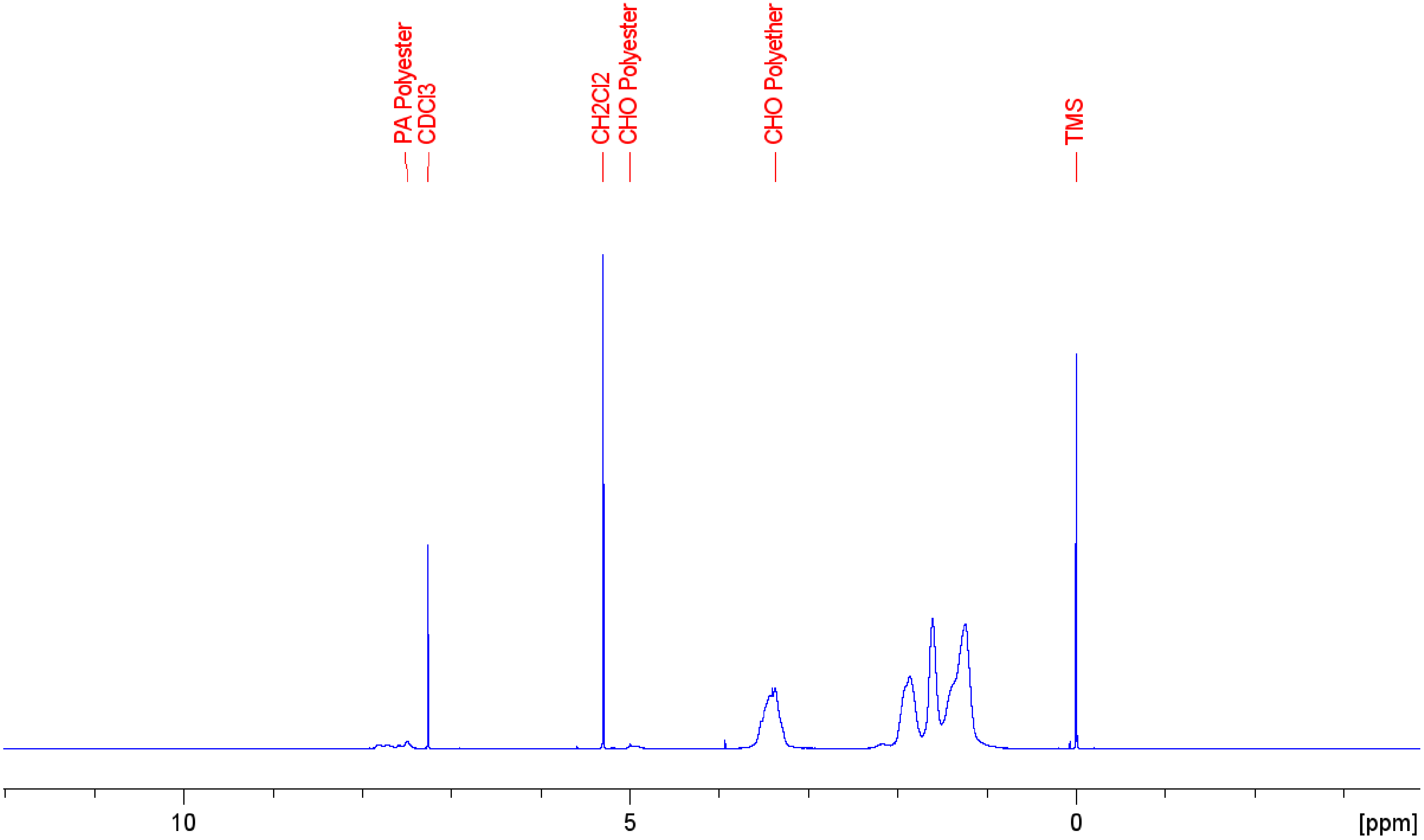

Figure S114: ^{1}H NMR (300 MHz, $CDCl_3$) spectrum of dried polymer from Table 3, entry 4 (**4** without PPNCl).

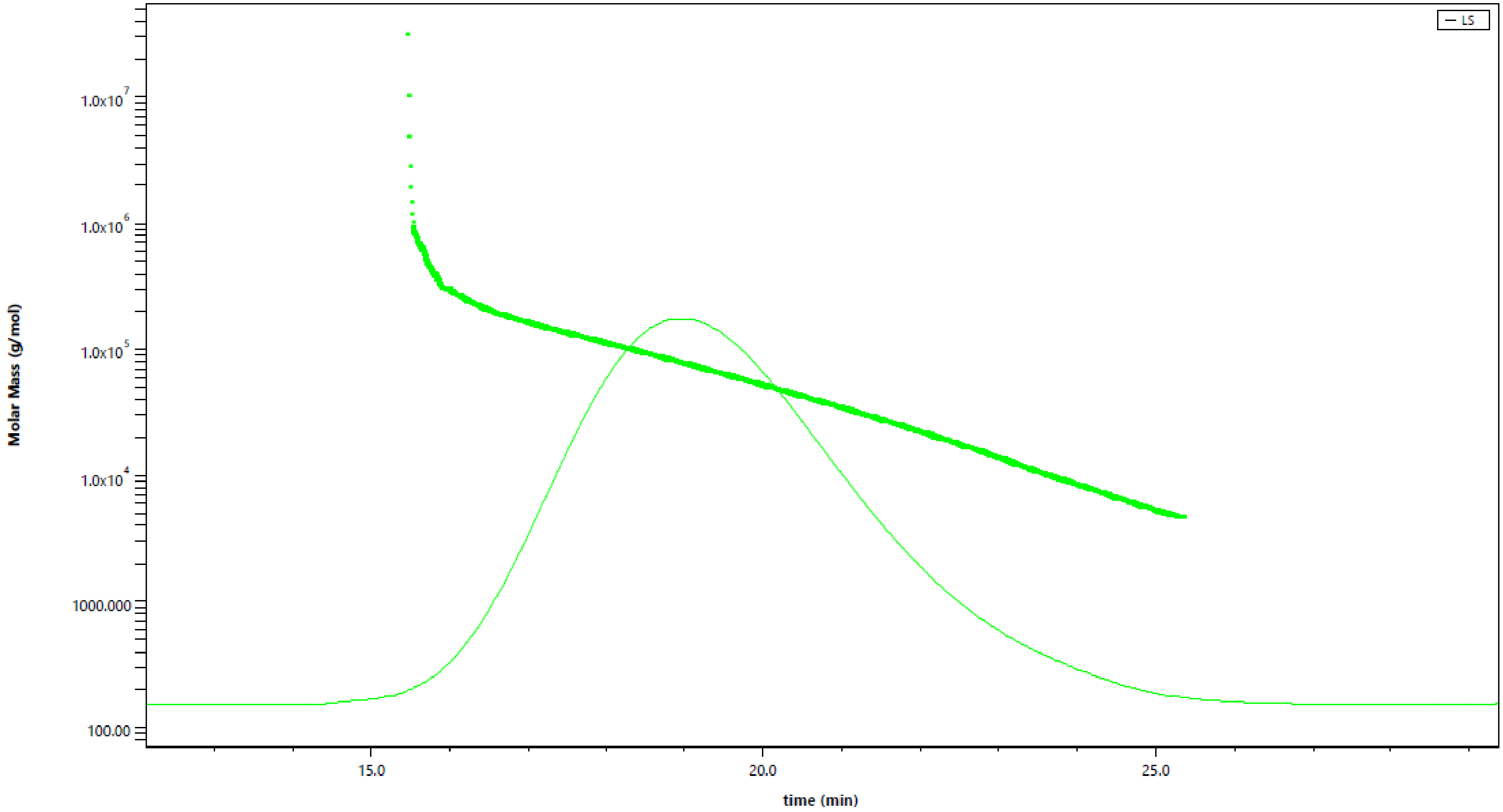

Figure S115: Light scattering GPC trace for the ROCOP of PA + CHO using **4** $[PA]_0:[CHO]_0:[4]_0$ = 100:500:1, 80 °C, 4 h (Table 3, entry 4).

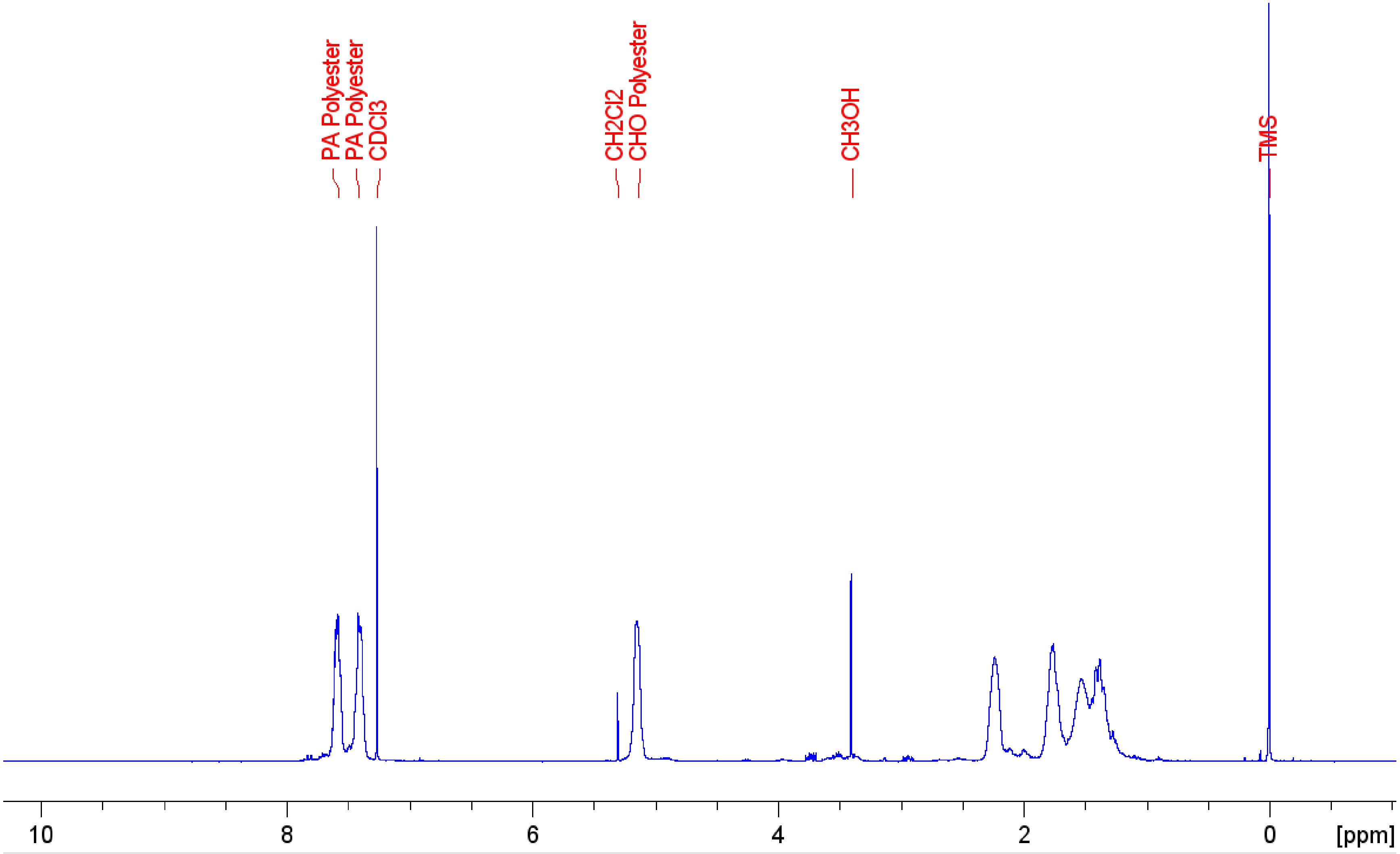

Figure S116: ^{1}H NMR (300 MHz, $CDCl_3$) spectrum of dried polymer from Table 3, entry 5 (5 with PPNCl).

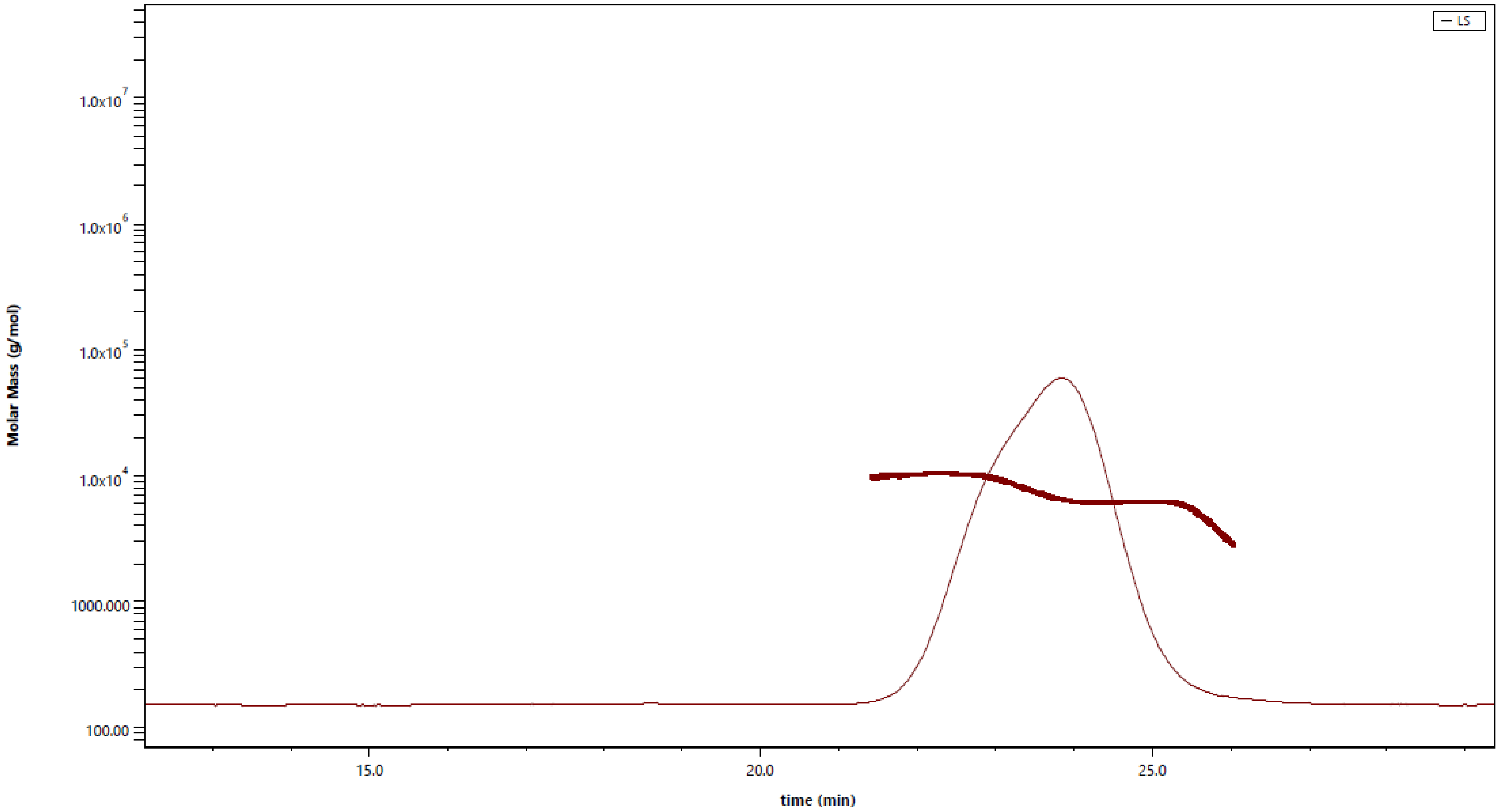

Figure S117: Light scattering GPC trace for the ROCOP of PA + CHO using **5** and PPNCl $[PA]_0:[CHO]_0:[4]_0:[PPNCl]_0$ = 100:500:1:1, 80 °C, 4 h (Table 3, entry 5).

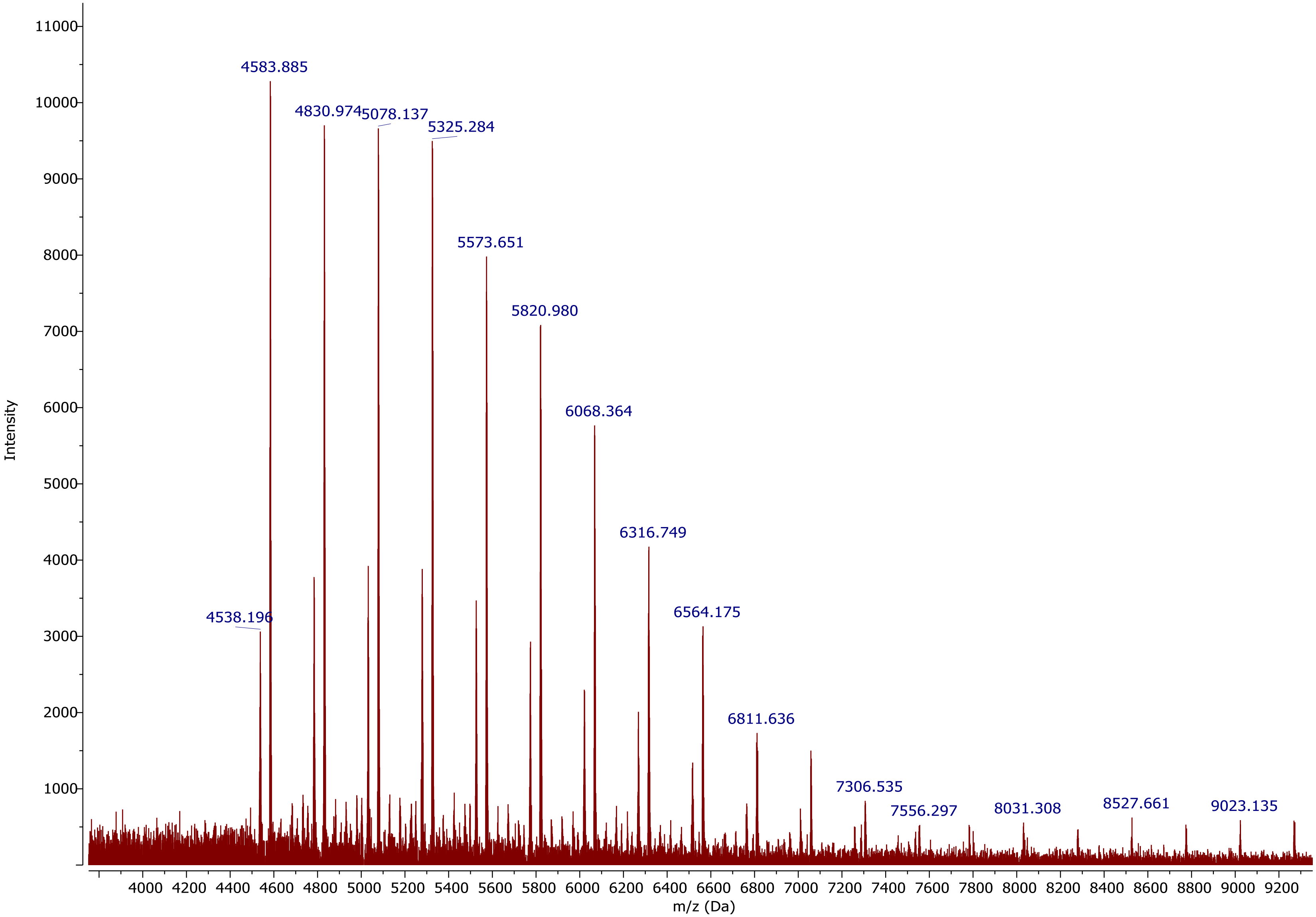

Figure S118: MALDI-TOF mass spectrum for the ROCOP of PA + CHO using **5** and PPNCl $[PA]_0:[CHO]_0:[4]_0:[PPNCl]_0$ = 100:500:1:1, 80 °C, 4 h (Table 3, Entry 5). Taken in positive reflectron mode.

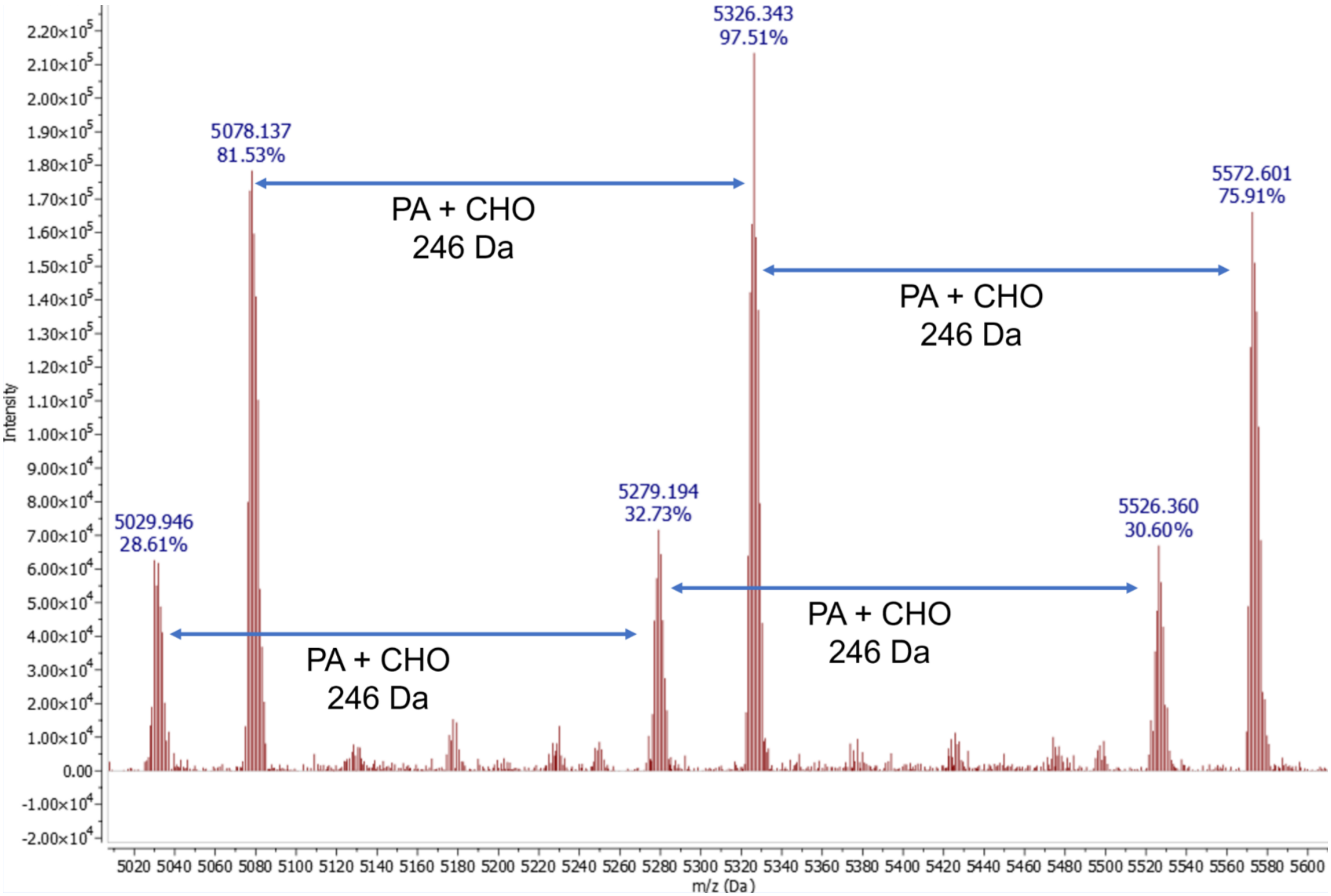

Figure S119: Expansion and annotation of MALDI-TOF mass spectrum for the ROCOP of PA + CHO using **5** and PPNCl $[PA]_0:[CHO]_0:[4]_0:[PPNCl]_0$ = 100:500:1:1, 80 °C, 4 h (Table 3, Entry 5). Taken in positive reflectron mode.

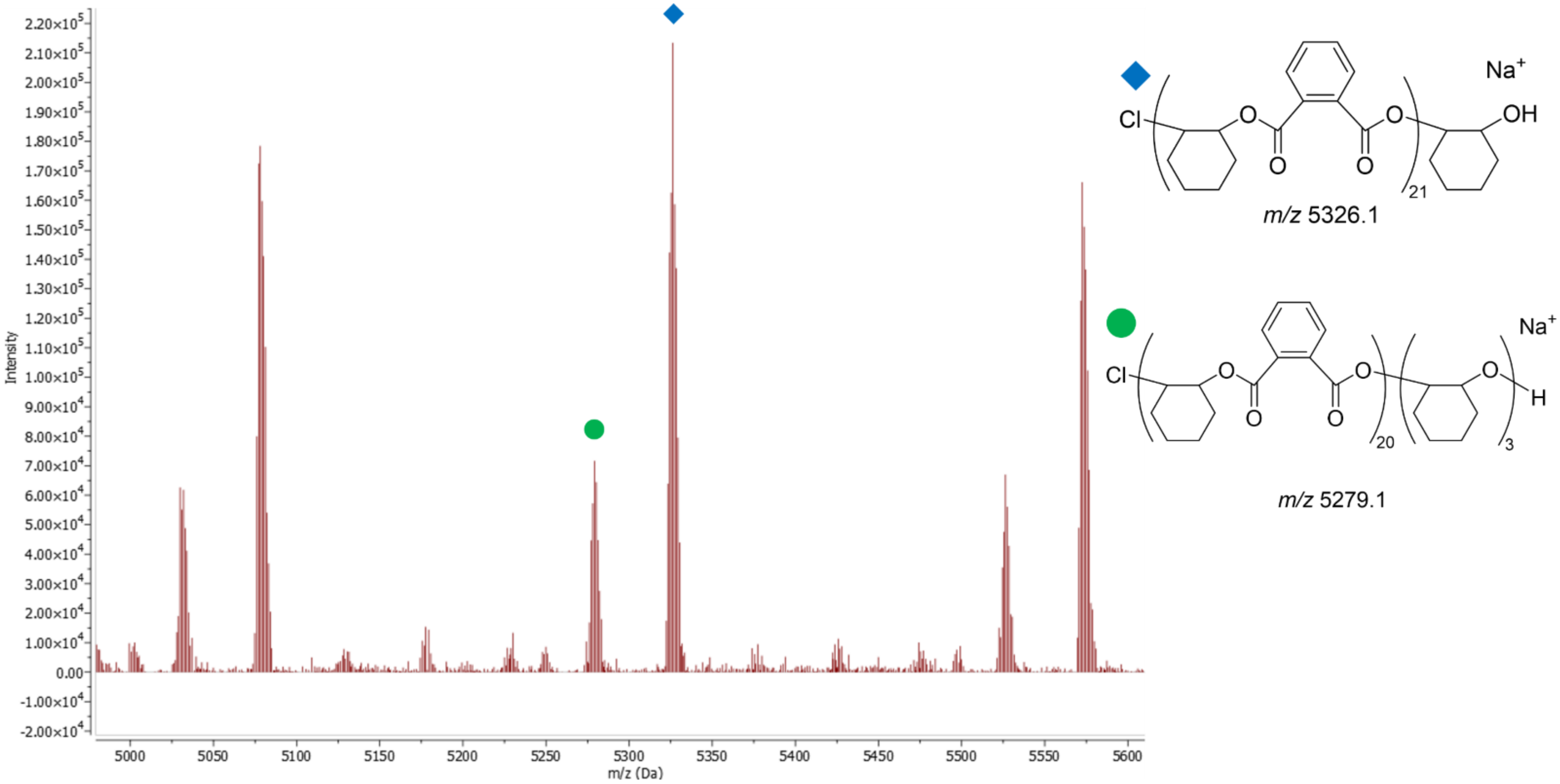

Figure S120: Expansion and polyester assignments of MALDI-TOF mass spectrum for the ROCOP of PA + CHO using **5** and PPNCl $[PA]_0:[CHO]_0:[4]_0:[PPNCl]_0$ = 100:500:1:1, 80 °C, 4 h (Table 3, Entry 5). Taken in positive reflectron mode.

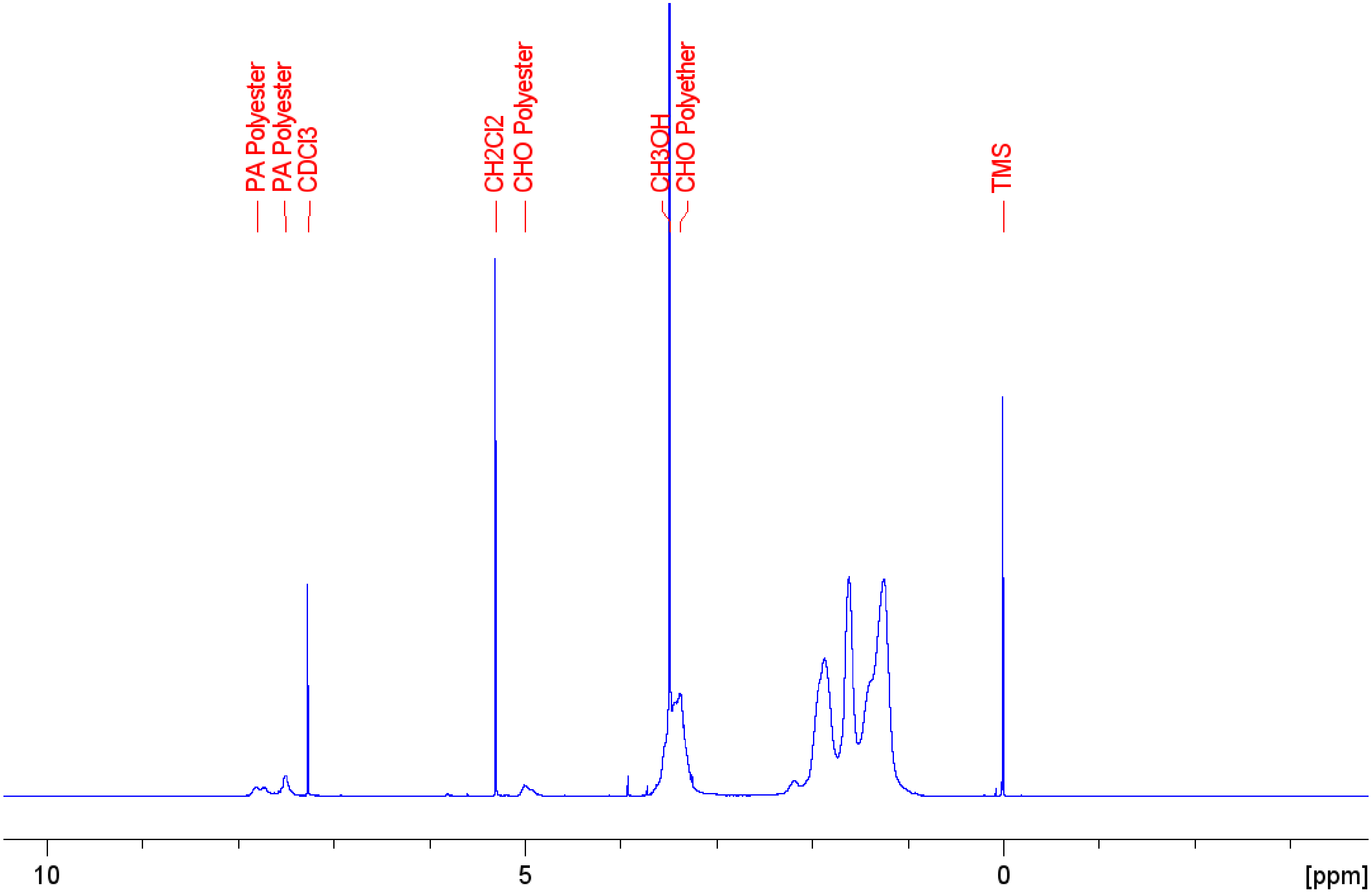

Figure S121: ^{1}H NMR (300 MHz, $CDCl_3$) spectrum of dried polymer from Table 3, entry 6 (**5** without PPNCl).

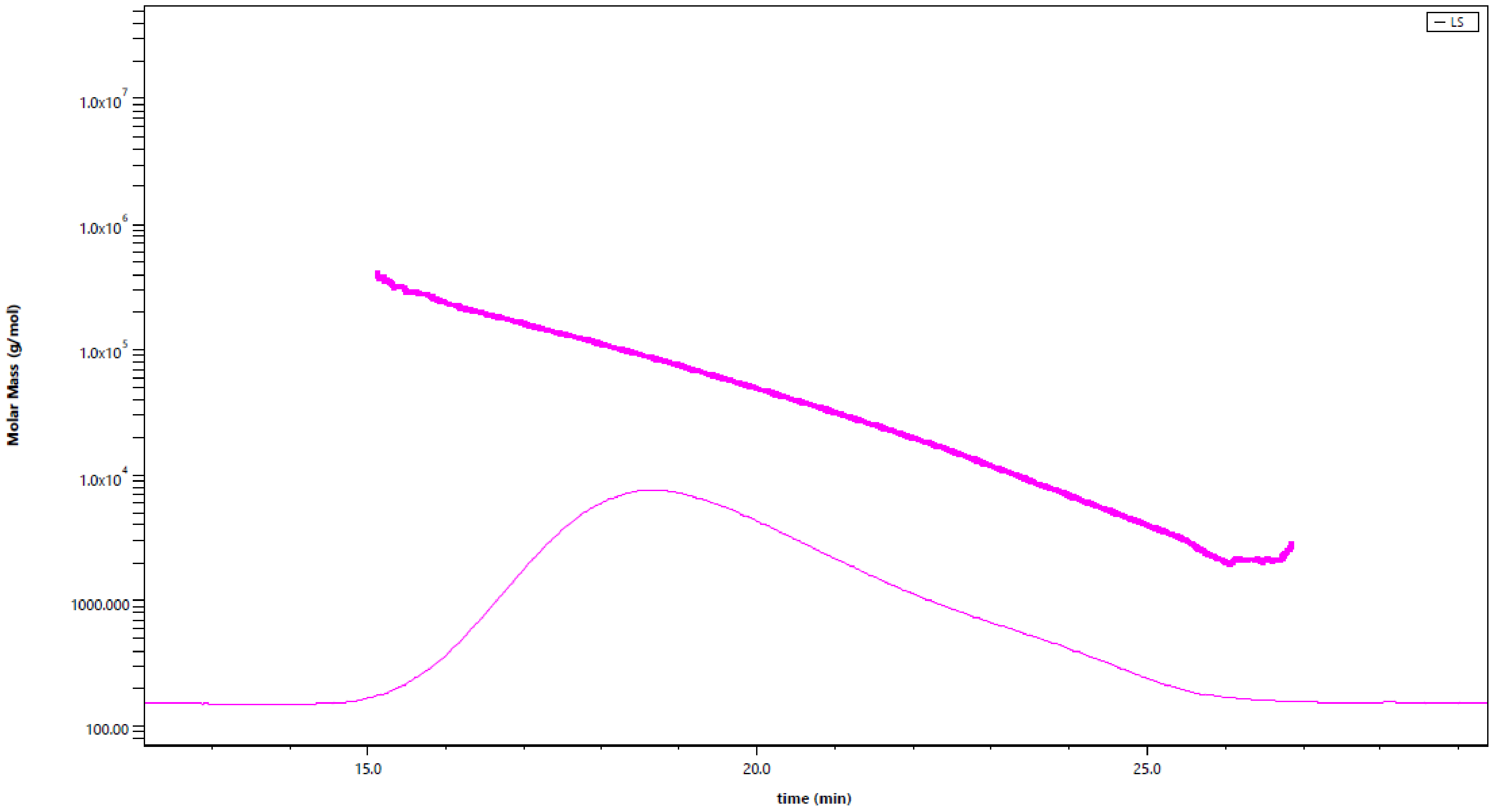

Figure S122: Light scattering GPC trace for the ROCOP of PA + CHO using **5** $[PA]_0:[CHO]_0:[4]_0 = 100:500:1$, 80 °C, 4 h (Table 3, entry 6).

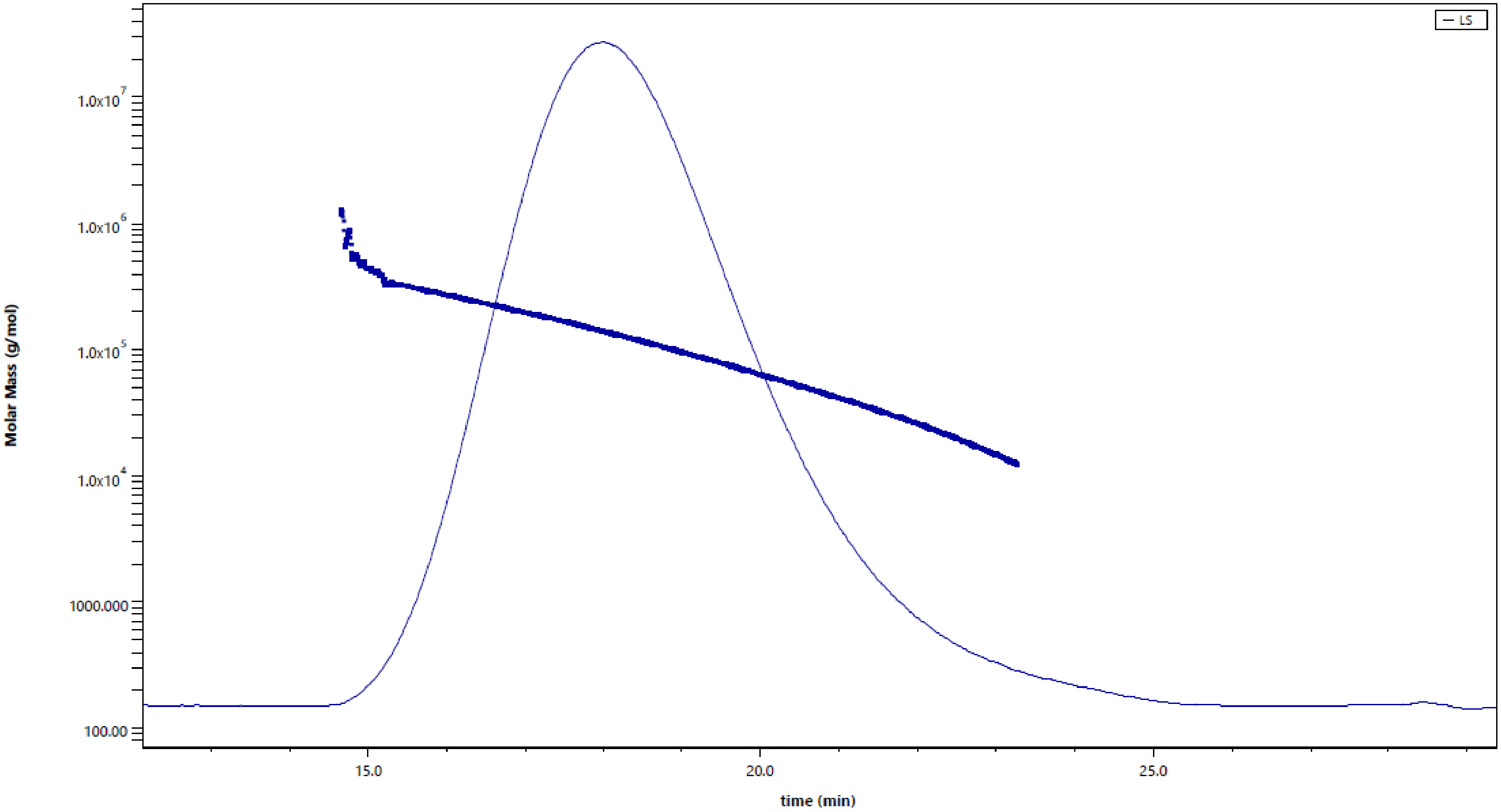

Figure S123: Light scattering GPC trace for the ROCOP of PA + CHO using **4** $[PA]_0:[CHO]_0:[4]_0$= 100:500:1, 20 °C, 4 h (Table 3, entry 8).

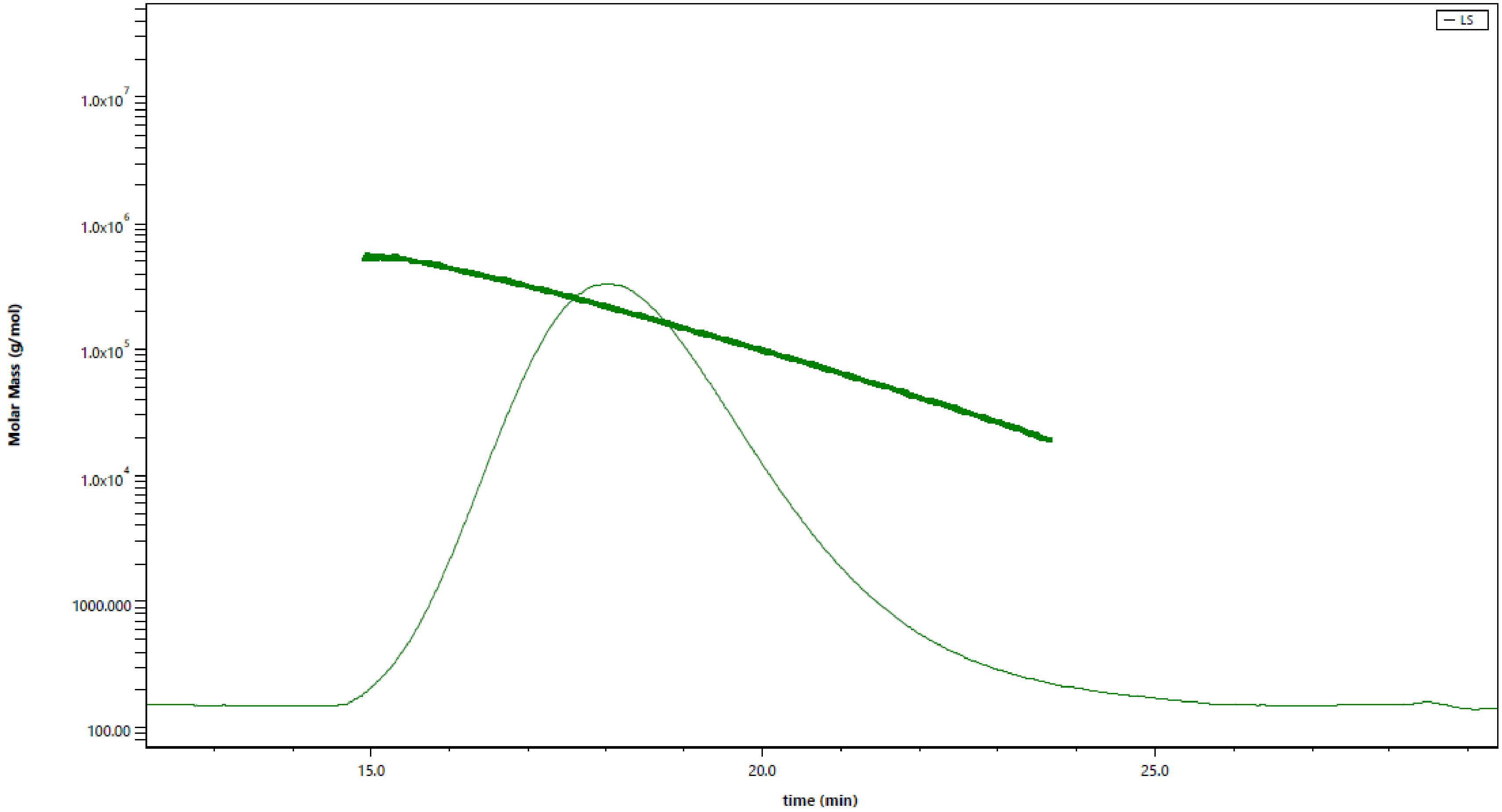

Figure S124: Light scattering GPC trace for the ROCOP of PA + CHO using **5** [PA]$_0$:[CHO]$_0$:[4]$_0$= 100:500:1, 20 °C, 4 h (Table 3, entry 10).

.

XYZ Coordinates for ESP Calculations

Atomic Coordinates (XYZ) for Compound 5

Zn	-0.163487	0.764978	-0.735516
P	-1.573892	-1.224830	1.293917
P	1.280040	-1.541536	0.893924
N	-0.150475	-1.888376	1.482456
N	-1.394487	0.328363	0.773031
N	-2.532037	1.147562	0.871075
N	1.135924	-0.734599	-0.537438
N	2.381907	-0.544243	-1.177632
C	-2.449235	-1.170798	2.863975
C	-3.407380	-2.138998	3.211918
H	-3.673847	-2.794149	2.577481
C	-3.964327	-2.136297	4.482410
H	-4.606609	-2.794731	4.721104
C	-3.582843	-1.169551	5.407107
H	-3.962217	-1.173417	6.278175
C	-2.654270	-0.201767	5.064571
H	-2.404610	0.463047	5.695596
C	-2.089437	-0.205092	3.798385
H	-1.449639	0.458330	3.566671
C	-2.534009	-2.249762	0.161797
C	-1.904117	-3.305244	-0.500197
H	-0.996482	-3.511727	-0.311179
C	-2.606954	-4.051292	-1.434705
H	-2.177553	-4.758126	-1.900385
C	-3.943626	-3.758276	-1.683755
H	-4.426898	-4.267771	-2.323782
C	-4.574503	-2.727732	-1.007772
H	-5.491671	-2.544254	-1.172882
C	-3.874624	-1.967760	-0.094613
H	-4.305474	-1.252697	0.358851
C	-2.242228	2.403790	1.051098
C	-0.960758	3.089780	1.371428
C	0.326626	2.619916	1.644692
H	0.522287	1.691907	1.588833
C	1.317301	3.527434	1.998712
H	2.196458	3.212577	2.170813
C	1.046221	4.891725	2.107313
H	1.739033	5.497001	2.344445
C	-0.246092	5.366162	1.865877
H	-0.439831	6.292072	1.951576

C	-1.240710	4.475684	1.500749
C	-2.674971	4.699291	1.271768
C	-3.423152	5.862211	1.305813
H	-3.010755	6.702419	1.468851
C	-4.798268	5.768072	1.093927
H	-5.333626	6.552482	1.127474
C	-5.398587	4.532833	0.833113
H	-6.337146	4.489213	0.690972
C	-4.642520	3.366587	0.778799
H	-5.050678	2.530764	0.584874
C	-3.280219	3.454492	1.014875
C	2.242917	-0.657501	2.134452
C	1.848618	-0.744574	3.472157
H	1.080919	-1.251471	3.709358
C	2.582999	-0.086847	4.458878
H	2.320771	-0.156963	5.369424
C	3.690978	0.667514	4.116532
H	4.179287	1.121793	4.792684
C	4.092176	0.764770	2.793374
H	4.856455	1.280832	2.564706
C	3.370610	0.102263	1.796000
H	3.644736	0.167184	0.888809
C	2.164057	-3.071870	0.555235
C	3.083758	-3.602208	1.463008
H	3.271523	-3.142755	2.273157
C	3.723507	-4.800873	1.180542
H	4.363464	-5.149915	1.790251
C	3.433698	-5.496215	0.006476
H	3.857805	-6.327466	-0.171448
C	2.522869	-4.971487	-0.901399
H	2.330224	-5.440521	-1.704817
C	1.894948	-3.761809	-0.636424
H	1.279843	-3.400131	-1.263933
C	2.334591	-0.515564	-2.471588
C	1.277871	-0.840791	-3.457881
C	-0.049929	-1.240000	-3.328826
H	-0.440708	-1.344966	-2.469543
C	-0.799096	-1.484180	-4.485391
H	-1.710635	-1.738772	-4.408653
C	-0.223420	-1.358453	-5.748415
H	-0.751238	-1.512359	-6.522966
C	1.111280	-1.011406	-5.885834
H	1.502907	-0.944573	-6.748604
C	1.867347	-0.762654	-4.752211
C	3.284850	-0.408749	-4.608658

C	4.287354	-0.264111	-5.556492
H	4.112493	-0.422901	-6.476680
C	5.559952	0.119512	-5.127139
H	6.260147	0.211573	-5.762494
C	5.818218	0.373043	-3.778279
H	6.681889	0.661093	-3.507523
C	4.812757	0.203884	-2.826385
H	4.982118	0.371713	-1.906754
C	3.560859	-0.214444	-3.251463
C	-1.209166	3.226106	-2.137056
H	-2.075499	2.771370	-2.195311
H	-1.092030	3.806651	-2.917825
H	-1.178648	3.766938	-1.320332
C	-0.091672	2.180516	-2.095072
H	0.954322	2.416560	-2.321781
H	-0.594632	1.837546	-3.006455

Atomic Coordinates (XYZ) for Compound 6

Al	-1.320825	0.088695	0.767347
P	1.533749	0.763930	1.702864
P	0.613744	2.053257	-0.619559
N	1.118052	2.076376	0.891217
N	0.464474	-0.454893	1.386342
N	0.413329	-1.377752	2.483232
N	-0.881339	1.320702	-0.680281
N	-1.181268	1.161542	-2.032751
C	1.589652	1.153517	3.458162
C	2.476948	0.482677	4.297076
H	3.105807	-0.128568	3.932010
C	2.442257	0.707182	5.663483
H	3.051015	0.252039	6.233207
C	1.529190	1.586860	6.198982
H	1.505243	1.731918	7.137450
C	0.646056	2.260374	5.373541
H	0.016286	2.866270	5.745908
C	0.680351	2.050773	4.000905
H	0.081247	2.521794	3.433572
C	3.193962	0.215182	1.257823
C	3.430455	-1.077202	0.787348
H	2.719131	-1.705491	0.745269
C	4.704705	-1.442715	0.381720
H	4.860161	-2.318189	0.047240
C	5.751977	-0.541065	0.460750

H	6.625437	-0.800898	0.192415
C	5.523413	0.738135	0.931218
H	6.242964	1.355629	0.988227
C	4.252929	1.124857	1.319706
H	4.100269	2.010171	1.628780
C	0.256922	-2.625808	2.188214
C	0.257913	-3.402882	0.927976
C	0.554868	-3.049024	-0.383499
H	0.767713	-2.149590	-0.602777
C	0.536234	-4.028439	-1.368590
H	0.739861	-3.795737	-2.266937
C	0.221835	-5.347572	-1.052534
H	0.205064	-6.002687	-1.740307
C	-0.067587	-5.719773	0.255630
H	-0.278647	-6.621480	0.467536
C	-0.041817	-4.748574	1.243860
C	-0.238465	-4.860158	2.699875
C	-0.577049	-5.941603	3.505955
H	-0.737500	-6.798218	3.127762
C	-0.675374	-5.739453	4.880526
H	-0.917259	-6.465779	5.443040
C	-0.425797	-4.493498	5.443746
H	-0.484058	-4.383749	6.385478
C	-0.090186	-3.401353	4.641174
H	0.076826	-2.547738	5.023128
C	-0.008117	-3.597580	3.273800
C	0.487271	3.763124	-1.158936
C	0.853806	4.789160	-0.291204
H	1.226248	4.580475	0.557403
C	0.676981	6.115172	-0.661021
H	0.929274	6.812150	-0.066830
C	0.133422	6.420881	-1.895832
H	-0.003240	7.328626	-2.140761
C	-0.214479	5.404208	-2.781420
H	-0.573342	5.619389	-3.634262
C	-0.036663	4.072273	-2.416756
H	-0.270321	3.376842	-3.020340
C	1.769252	1.222111	-1.740331
C	3.018524	1.804295	-1.919801
H	3.195250	2.667712	-1.564881
C	4.009300	1.124475	-2.617585
H	4.862302	1.524896	-2.738245
C	3.758731	-0.133135	-3.137612
H	4.441847	-0.598940	-3.605680
C	2.513423	-0.711116	-2.975093

H	2.337907	-1.569030	-3.343712
C	1.520270	-0.043715	-2.276893
H	0.668120	-0.447537	-2.162517
C	-2.379990	0.958819	-2.470845
C	-2.511222	0.672026	-3.916259
C	-1.519852	0.553373	-4.878295
H	-0.603197	0.653817	-4.650132
C	-1.905814	0.283202	-6.186873
H	-1.246526	0.217781	-6.867713
C	-3.250636	0.107611	-6.509282
H	-3.492660	-0.090890	-7.406355
C	-4.245177	0.217284	-5.542463
H	-5.159672	0.092154	-5.766935
C	-3.863576	0.515541	-4.236088
C	-4.647989	0.768324	-3.018191
C	-6.021753	0.871501	-2.849254
H	-6.612392	0.701126	-3.573563
C	-6.516942	1.228034	-1.602447
H	-7.454888	1.312906	-1.477164
C	-5.657795	1.462665	-0.534300
H	-6.016936	1.694374	0.314238
C	-4.275903	1.361973	-0.692570
H	-3.693709	1.528011	0.039522
C	-3.760692	1.014611	-1.940305
C	-2.240706	-1.414427	-0.083707
H	-1.574755	-1.881810	-0.818062
H	-3.143701	-1.051872	-0.588058
H	-2.518802	-2.151357	0.678404
C	-2.213379	0.953544	2.279046
H	-1.559849	1.729405	2.693959
H	-2.429831	0.206700	3.051438
H	-3.150294	1.408846	1.938302

References

(1) Ritch, J. S.; Chivers, T.; Eisler, D. J.; Tuononen, H. M. Experimental and Theoretical Investigations of Structural Isomers of Dichalcogenoimidodiphosphinate Dimers: Dichalcogenides or Spirocyclic Contact Ion Pairs? *Chem. – Eur. J.* **2007**, *13* (16), 4643–4653. https://doi.org/10.1002/chem.200700001.

(2) Ritch, J. S.; Chivers, T.; Ahmad, K.; Afzaal, M.; O'Brien, P. Synthesis, Structures, and Multinuclear NMR Spectra of Tin(II) and Lead(II) Complexes of Tellurium-Containing Imidodiphosphinate Ligands: Preparation of Two Morphologies of Phase-Pure PbTe from a Single-Source Precursor. *Inorg. Chem.* **2010**, *49* (3), 1198–1205. https://doi.org/10.1021/ic9021728.

(3) Liu, P.; McCarren, P.; Cheong, P. H.-Y.; Jamison, T. F.; Houk, K. N. Origins of Regioselectivity and Alkene-Directing Effects in Nickel-Catalyzed Reductive Couplings of Alkynes and Aldehydes. *J. Am. Chem. Soc.* **2010**, *132* (6), 2050–2057. https://doi.org/10.1021/ja909562y.

(4) Myers, E. L.; Raines, R. T. A Phosphine-Mediated Conversion of Azides into Diazo Compounds. *Angew. Chem. Int. Ed.* **2009**, *48* (13), 2359–2363. https://doi.org/10.1002/anie.200804689.

(5) Davis, P. J.; Harris, L.; Karim, A.; Thompson, A. L.; Gilpin, M.; Moloney, M. G.; Pound, M. J.; Thompson, C. Substituted Diaryldiazomethanes and Diazofluorenes: Structure, Reactivity and Stability. *Tetrahedron Lett.* **2011**, *52* (14), 1553–1556. https://doi.org/10.1016/j.tetlet.2011.01.116.

(6) APEX II (Bruker, 2008) Bruker AXS Inc., Madison, Wisconsin, USA.

(7) SAINT (Bruker, 2008) Bruker AXS Inc., Madison, Wisconsin, USA.

(8) SADABS (Bruker, 2009) Bruker AXS Inc., Madison, Wisconsin, USA.

(9) Sheldrick, G.M. (2008) *Acta Cryst*., A64, 112-122; Sheldrick, G.M. (2015) *Acta Cryst*., A71, 3-8; Sheldrick, G.M. (2015) *Acta Cryst*., C71, 3-8.

(10) Spek, A. L. (2003). J. Appl. Cryst. 36, 7-13.

(11) CrysAlisPro (Rigaku Oxford Diffraction, 2023) Rigaku Oxford Diffraction, Yarnton, England.

(12) Mercury CSD 4.3 (2008) Macrae, C.F.; Bruno, I.J.; Chisholm, J.A.; Edgington, P.R.; McCabe, P.; Pidcock, E.; Rodriguez-Monge, L.; Taylor, R.; van de Streek, J.; Wood, P.A. *J. Appl. Cryst*. 41, 466–470.